DISSERTATIONES PHYSICAE UNIVERSITATIS TARTUENSIS
58

DISSERTATIONES PHYSICAE UNIVERSITATIS TARTUENSIS
58

ANDI HEKTOR

Neutrino Physics beyond the Standard Model

TARTU UNIVERSITY
PRESS

This study was carried out at the National Institute of Chemical Physics and Biophysics, Tallinn and the University of Tartu, Estonia.

The Dissertation was admitted on May 9, 2008, in partial fulfillment of the requirements for the degree of Doctor of Philosophy in physics (particle physics), and allowed for defense by the Council of the Department of Physics, University of Tartu.

Supervisor: Dr. Martti Raidal,
National Institute of Chemical Physics and Biophysics,
Tallinn, Estonia

Opponent: Dr. Katri Huitu,
University of Helsinki, Helsinki, Finland

Defense: August 26, 2008, University of Tartu, Estonia

ISSN 1406–0647
ISBN 978–9949–11–914–1 (trükis)
ISBN 978–9949–11–915–8 (PDF)

Tartu Ülikooli Kirjastus
www.tyk.ee
Tellimus nr 275

Contents

List of related publications

This thesis consists of an introductory and linking review part, followed by three research publications [I–III]. The relevant publications are listed below.

I A. Hektor, M. Kadastik, M. Müntel, M. Raidal, and L. Rebane. *Testing neutrino masses in little Higgs models via discovery of doubly charged Higgs at LHC*. Nucl. Phys., **B787**, 198-210, 2007, [0705.1495].

II J. Ellis, A. Hektor, M. Kadastik, K. Kannike, and M. Raidal. *Running of Low-Energy Neutrino Masses, Mixing Angles and CP Violation*. Phys. Lett., **B631**, 32-41, 2005, [hep-ph/0506122].

III G. D'Ambrosio, T. Hambye, A. Hektor, M. Raidal, and A. Rossi. *Leptogenesis in the minimal supersymmetric triplet seesaw model*. Phys. Lett. **B604**, 3-4, 199–206, 2004, [hep-ph/0407312].

Other publications of the dissertant:

IV A. Hektor, Y. Kajiyama, and K. Kannike. *Muon Anomalous Magnetic Moment and Lepton Flavor Violating Tau Decay in Unparticle Physics*. Submitted to Phys. Lett. B, 2008, [0802.4015].

V F. del Aguila et al. *Collider aspects of flavour physics at high Q*. (2008), [0801.1800].

VI CMS Collaboration: G. L. Bayatian et al. *CMS physics: Technical design report*. CERN Notes: CERN-LHCC-2006-001, 2006.

VII CMS Collaboration: G. L. Bayatian et al. *CMS technical design report, volume II: Physics performance*. J. Phys. **G34**, 995–1579, 2007.

VIII B. C. Allanach et al. *Les Houches 'Physics at TeV colliders 2005' Beyond the standard model working group: Summary report*. 2006, [hep-ph/0602198].

IX A. Hektor, L. Anton, M. Kadastik, K. Skaburskas, and H. Teder, *First scientific results from the Estonian Grid* Proc. Estonian Acad. Sci. Phys. Math. **54**, 111, 2005, [physics/0411024].

X A. Hektor, M.K. Klintenberg, A. Aabloo, and J.O. Thomas. *MD simulation of the effect of a side-chain on the dynamics of the amorphous LiPF6-PEO system.* J. Mat. Chem. **13**, 2, 214–218.

XI A. Hektor, E. Kolbe, K. Langanke, and J. Toivanen. *Neutrino induced reaction rates for r process nuclei.* Phys. Rev. **C61**, 055803, 2000.

Chapter 1

Introduction

Neutrino is a particle hardly reachable in any modern experiment. Despite that, this particle seems to have a rather crucial role in the history of the Universe. Furthermore, some modern physical theories suppose that our existence is based on the effects caused by neutrinos. First, it occured when our Universe was very young, in the process called leptogenesis. A very slight asymmetry between matter and antimatter was generated in leptogenesis, which saves a small amount of baryon matter to build up stars, planets, us. Second, with the death of early stars many billion years ago, neutrino helped to produce heavier elements. Then, Nature had all the needed materials to build small planets and life on these planets.

This thesis aggregates three publications in phenomenological and experimental neutrino related physics. The work will give a general physical overview and link the topics of the publications. The thesis will start with a short introductory description of particle physics and cosmology. We will give a short overview of the present theory of particle physics, the Standard Model. In the last section we will introduce the framework of cosmology.

Next chapter, Chapter 3, will be focused on the experimental and the observational effects beyond the Standard Model. We will touch upon matter-antimatter asymmetry in the observed Universe. In the second section we will introduce some observational neutrino mass effects: oscillation effects and cosmological scale changes of matter perturbations caused by massive neutrinos. As we know, the mass of neutrino is clearly a topic of particle physics beyond the Standard Model. In the last sections we will introduce some experimental topics beyond well-established particle physics: cold dark matter and muon anomalous magnetic moment.

Chapter 4 will describe some neutrino models beyond the Standard

Model. We will start the chapter with a very brief introduction to two general extensions to new physics beyond the Standard Model: grand unified theories and supersymmetry. After that, in the second section of the chapter we will deal with a potential mechanism to generate neutrino mass. We will describe the three mechanisms for neutrino mass: type I, II and II see-saw. Also, we will discuss CP-violation in the neutrino sector and the running of neutrino parameters.

In Chapter 5 we will introduce leptogenesis. We will start with equilibrium and non-equilibrium thermal bath in the early Universe. Next, we will give a short introduction to kinematics and Boltzmann equations. Finally, having all the needed tools, we will describe a model of leptogenesis, the type I see-saw, in detail. In the last chapter we will give a summary of the thesis.

Chapter 2

The standard model of particle physics and cosmology

2.1 Introduction

In this chapter we will give a short introduction to the framework of particle physics and cosmology. It is the first step that has to be taken to enter neutrino physics beyond the current models in particle physics and cosmology.

Let us start with particle physics. The shape of the Standard Model was formed in 1960th and 1970th. Naturally, the main ideas of the model were based on the great development line of particle physics in the 20th century: quantum mechanics, quantum field theory, QED, gauge theories, renormalization, etc. The Standard Model of particle physics covers a wide range of physical phenomena in Nature. The model describes consistently the three strongest interactions in Nature, *weak*, *electromagnetic* and *strong* interactions. It unifies the weak and electromagnetic theories into a consistent electroweak theory. The model provides an excellent agreement for experimental results. At the moment accordance between the model and experiments is up to space resolution 10^{-18} m and up to energy approximately 1 TeV. No doubt, the Standard Model of particle interactions is a most accurate and consistent physics theory of the 20th century.

The mathematical description of Standard Model covers all the directly observed particles in Nature. In total the model contains 12 spin-1/2 fermions, 12 spin-1 bosons and one spin-0 boson. Only the spin-0 boson, the Higgs boson is yet to be discovered. It is the last missing building block of the Standard Model. The discovery of Higgs boson is a great challenge for the running Tevatron collider at Fermilab and a main target of the Large Hadron Collider (LHC) soon to start at CERN.

Also, we have to note that the Standard Model uncovers a clear set of experimental effects in particle physics, which are waiting for a theory beyond the Standard Model. However, it is already a story of the next chapter where we will briefly concentrate on four main puzzles in particle physics nowadays: matter-antimatter asymmetry, neutrino mass, dark matter and muon anomalous magnetic moment.

In the second section of the chapter we will introduce the Standard Model of cosmology or ΛCDM model. It is based on two great achievements of the 20th century: theory of general relativity and rapid development of wide technologies of astronomical observations. General relativity gives us a chance to describe large scale dynamics of the Universe. Different observations help to fix the parameter space of the theory. During some last decades two observational sources have dominated the field: the cosmological microwave background radiation (CMB) and large scale structure and velocity measurements. The observations have given many important hints for new physics: cold dark matter, the cosmological constant etc.

In conclusion, let us take a quick look at the mathematical side of particle physics and cosmology. We see that cosmology is very elegantly described by the short and compact Einstein equation working on the curved space-time. On the other hand, the Standard Model of particle physics has a rather long form, but it works on the flat Minkowskian space-time. It is unclear how we should unite these two sides of the theory of Nature to one unified theory. Many theories have been proposed, but we do not have one clear answer.

2.2 Standard Model of particle physics

2.2.1 Symmetries in Quantum Field Theory

The physicists have connected the electromagnetic, weak and strong interactions into a general mathematical framework. The *Standard Model* is a Quantum Field Theory in which the interactions are induced due to gauge symmetries.

The mathematical language of the model is based on *quantum field theory*, composed of the ideas from quantum mechanics and field theory. The field theory of the Standard Model uses the fields in the Minkowski space-time. Quantum mechanics describes the physical world in microscopic scale. Loosely speaking it is composed of the following mathematical objects:

- The physical state of the particle is a ket in the complex Hilbert space.
- The observable is an operator represented in the Hilbert space. The physical parameters are the eigenvalues of the operator with the probabilities represented by the scalar product of state vectors.
- The physical symmetries of the system are described by unitary operators. Thus, the state vectors are defined in the representation space of the symmetry group.
- The time evolution (dynamics) of the physical system is described by a special unitary time evolution operator.

In quantum field theory all operators and kets are functions of space-time coordinates. Usually we can follow a traditional path where the classic Lagrangian summarizes the dynamics of the fields. On the Lagrangian we can impose global and local symmetries expected of the model. The quantization procedure follows. Only in some special cases can the quantized system be solved directly. More general, the local behavior of the system can be understood by use of perturbation methods. Some important questions, like the renormalizability of the model, have to be solved. Ultimately, at the level of perturbation effects it is possible to formulate any theory as a *S-matrix theory*. However, it is shown that a set of non-perturbative effects exists, including sphalerons, monopoles etc. The S-matrix theory is insufficient to describe them.

In the field theory the space-time symmetry of the system can be global or local. In the first case the transformation is independent of the space-time coordinates and in the second case it depends on the space-time coordinates. Also, some classical level symmetries exhibited by the Lagrangian can be broken after quantization. This type of symmetry breaking is called *anomaly*.

Thus, a physical particle is described as an *irreducible representation* of the global symmetry group G. In the Standard Model the group G is the Poincare group P as the theory should have a covariant form of special relativity.

Unfortunately Poincare group has a rather complicated structure. The group is a 10-dimensional nontrivial noncompact Lie group: 4 parameters are the noncompact parameters for translation and 6 parameters are the compact parameters: 3 parameters for space rotations and 3 for boosts.

The Poincare group is the semidirect product of the Lorentz group L and the translation group T:

$$P = T \triangleleft L,$$

which derives from the multiplication law of the elements. If we write an element of the Poincare group as (Λ, a) so that the group translation is presented by the following equation:

$$x^{\mu} \rightarrow x'^{\nu} = \Lambda^{\nu}_{\mu} x^{\mu} + a^{\nu},$$

where Λ is a Lorentz transformation and a^{ν} is a translation, then the multiplication law is given by

$$(\Lambda_1, a_1)(\Lambda_2, a_2) = (\Lambda_1\Lambda_2, \Lambda_1 a_2 + a_1).$$

The equation presents a semidirect product of subgroups. The structure of the Poincare group is complicated due to the following facts:

- the Poincare group has the Abelian translation subgroup, so the group is nontrivial,
- the Poincare group involves 3 discrete elements: C-, P- and T-reflection
- the topological structure of the manifold of the Lorentz group is complicated

It is definitely a nontrivial task to construct the representations of the Poincare group. The only relief comes from the global or local compactness of the subgroups. The Lie algebra of any compact Lie group can be decomposed as a direct sum of an Abelian Lie algebra and some number of simple algebras.

Fortunately, only a subset of representations has a physical meaning. It can be shown that the physical representations of the Poincare group are only (positive energy) unitary irreducible representations. In 1939 Wigner presented a complete classification of all the unitary irreducible representations of the Poincare group [1]. The construction of a representation can be indexed by the *Casimir operators* P^2 and w^2 of the group. The operators are connected to the physical properties of the system:

1. P^2 is *mass* squared, nonnegative number related to the translation subgroup

2. w^2 is *spin* squared, integer or half-integer related to the Lorentz subgroup

The construction of the representations can be done by covering groups with trivial topology. Also, the final representations are constructed using known representations of the subgroups via the *generation* procedure.

The gauge symmetries are needed in the Standard Model to describe the interactions between particles. The modern Standard Model is a *Yang-Mills theory* based on the electroweak symmetry group $SU(2)_L \otimes U(1)_Y$ by Glashow, Salami and Weinberg [2–4] and the strong $SU(3)_c$ group of quantum electrodynamics (QCD) by Gell-Mann et al [5–8]. In conclusion, the symmetry group of the model is the direct product

$$SU(3)_c \otimes SU(2)_L \otimes U(1)_Y. \tag{2.1}$$

Also, on the level of S-matrix no way exists to mix the global Poincare and local gauge symmetries into one symmetry group. The path is restricted by the Coleman-Mandula no-go theorem [9]. It states that every quantum field theory that has a mass gap and satisfies certain technical assumptions about its S-matrix with non-trivial interactions can only have a symmetry Lie algebra which is always a tensor product of the Poincare group and an internal group. With no mass gap the theory has more freedom. For example, the algebra could be a tensor product of the conformal algebra with an internal Lie algebra. Moreover, in quantum electrodynamics it is possible to construct conserved vector and tensor charges (as there is no mass gap). Interestingly, the *supersymmetry* discussed later in this work may be considered as a possible "loophole" of the Coleman-Mandula theorem. It contains additional generators, *supercharges*, that are not scalars but spinors. The anticommutator of the generator of the supercharge yields a translation in spacetime. The reason of the loophole is that supersymmetry is a Lie superalgebra, not a Lie algebra. The corresponding theorem for supersymmetric theories with a mass gap is the Haag-Lopuszanski-Sohnius theorem [10].

In the next subsection we are going to summarize the current understanding about the elementary particles and intercations (except gravitation) of the Standard Model. It is convenient to describe all the known elementary particles in two stages: the elementary fermions and the elementary bosons in the model. The fermions of the model are three generations of spin-1/2 leptons and quarks. The spin-1 bosons of the model are carriers of electromagnetic, weak and strong interactions. Before the *electroweak spontaneous symmetry breaking* (EWSB) the model has only matter (1/2-spin) and gauge fields (spin-1). All the fields are massless before EWSB.

2.2.2 Standard Model below EWSB

Fields of the Standard Model

Before the introduction of gauge symmetries let us start with the fermion content of the Standard Model. All the fermions in the model have spin 1/2. The Dirac wave equation describes a free spin-1/2 particle with positive and negative energy states. All the fermion fields have to follow the representations of the gauge fields. Their fields are multiplets of the representation of the gauge symmetry. For example, quarks are the triplets under $SU(3)_c$, they "feel" the strong interaction, and all leptons are color singlets as they do not interact strongly.

Also, we can split an energy eigenstate to left-handed and right-handed components,

$$f_{L,R} = \frac{1 \mp \gamma_5}{2} f. \tag{2.2}$$

The physical meaning of the procedure is clear. The Dirac spinor (as a state description of spin-1/2 particle) has two degrees of freedom for both helicity states. The helicity states are mixed only in the case of massive fermions by the mass term

$$-m\bar{f}f = -m(\bar{f}_R f_L + \bar{f}_L f_R). \tag{2.3}$$

As the fermions in the Standard Model are massless before EWSB the left-handed and right-handed states are independent fields. First, let us focus our attention to weak interaction and write the left-handed doublets of $SU(2)_L$ of electron, muon and tau generation:

$$\begin{pmatrix} \nu_e \\ e \end{pmatrix}_L, \qquad \begin{pmatrix} \nu_\mu \\ \mu \end{pmatrix}_L, \qquad \begin{pmatrix} \nu_\tau \\ \tau \end{pmatrix}_L, \tag{2.4}$$

and for quarks:

$$\begin{pmatrix} u \\ d' \end{pmatrix}_L, \qquad \begin{pmatrix} c \\ s' \end{pmatrix}_L, \qquad \begin{pmatrix} t \\ b' \end{pmatrix}_L. \tag{2.5}$$

When we start to write down to the right-handed doublets the Nature has a little suprise for us: there are no right-handed neutrinos! A series of experiments in the 1950s led to the suggestion that the weak interaction violates reflection (or parity, P) symmetry, the reason for the missing of right-handed neutrinos. In 1956 C. S. Wu et al detected a correlation between the spin of a polarized Co^{60} nucleus and the direction of the emitted β particle:

$$\mathrm{Co}^{60} \to \mathrm{Xe}^{60} + e + \nu_e.$$

It means clear P violation: parity inversion leaves the spin of the nucleus unchanged

$$P : \vec{J} \to \vec{J},$$

while the direction of electron is reversed

$$P : \vec{p_e} \to \vec{p_e}.$$

The correlation of $\vec{J} \cdot \vec{p_e}$ is P-violation. It was the first experiment where a symmetry strongly believed in was violated. In the same way, C-symmetry is maximally violated in the case of weak interaction.

Violation of P-symmetry is very clearly presented in high energy processes. As the mass of fermions is negligible in high energy processes fermions are left- or right-handed. It is experimentally well-proved that only left-handed fermions (right-handed antifermions) participate in weak interaction processes. P-violation is the reason we see no right-handed neutrinos not left-handed antineutrinos in experiments. Neutrino has no electric or color charge, so it can couple with other matter only weakly (to say nothing about gravitation). As only left-handed neutrinos and right-handed antineutrinos have weak interaction and neutrinos do not have electric or color charge then right-handed neutrinos and left-handed antineutrinos are called *sterile*. In the Standard Model no reason exists to include sterile neutrinos as they are not observable. However, later in this work we will discuss gravitational effects of dark matter and oscillation effects and sterile neutrinos can have an important role in that case.

In conclusion, when we start to write down the right-handed states we have only the right-handed lepton isosinglets with no neutrinos included:

$$e_R, \qquad \mu_R, \qquad \tau_R. \tag{2.6}$$

Also, for quarks we have the pairs of isosinglets:

$$u_R, d_R; \qquad c_R, s_R; \qquad t_R, b_R. \tag{2.7}$$

For convenience we will occasionally number the generations with the index $i = 1, 2, 3$ below. In general, the number of the generations is an

5

open question in particle physics. Definitely, it has no final answer in the Standard Model. However, we have no direct experimental evidence for any generations beyond the third one. Some slight theoretical hints exist in the Standard Model (e.g. the cancellation of *quantum anomalies*) that the current number of generations should be final. Experimentally, a fourth generation with a light neutrino (mass less than half of Z boson mass) has been ruled out by measurements of the decay widths of the Z boson. It will be described in more detail in the next chapter. Also, the high precision measurements in the electroweak sector and the observations in cosmology place strong restrictions on the fourth generation [11–13].

We will use a short notation below, where l_L marks the left-handed lepton isodoublets, l_R the right-handed lepton isosinglets, q_L the left-handed quark isodoublets and u_R and d_R marks the right-handed quark isosinglets.

In conclusion we have three generations of left- and right-handed *chiral* fermion fields. The left-handed fermions are weak isodoublets (as they participate in electroweak interaction) and the right-handed fermions are weak isosinglets (as they do not participate in electroweak interaction). Using the properties of the representation of the Lie algebra we can develop from the generators of $SU(2)$ and $U(1)$ a relation

$$Y = 2(Q - T_3), \tag{2.8}$$

where Q is elementary electric charge, Y is the *hypercharge*, the component of the generator of $U(1)$, and T_3 is the third component of the $SU(2)$ generators, so called *weak isospin*. $T_3 = \pm\frac{1}{2}$ for left-handed isodoublets and $T_3 = 0$ for right-handed isosinglets. Here, short notation is useful:

$$l_L \sim (2, -1),\ l_R \sim (1, -2); \tag{2.9}$$

$$q_L \sim (2, 1/3),\ u_R \sim (1, 4/3),\ d_R \sim (1, -2/3); \tag{2.10}$$

where the first number marks the order of the multiplet and the second one is the hypercharge. The upper row presents leptons (l) and the lower row presents quarks (q, u, d).

Only quarks participate in strong interactions: quarks are triplets under $SU(3)_c$ and leptons are color singlets under $SU(3)_c$. Also, if we like we can add a number for the representation of strong interaction to the notation above. Then it will read

$$l_L \sim (2, -1, 1),\ l_R \sim (1, -2, 1); \tag{2.11}$$

$$q_L \sim (2, 1/3, 3),\ u_R \sim (1, 4/3, 3),\ d_R \sim (1, -2/3, 3). \tag{2.12}$$

Let us start the second part of the story of the Standard Model, the description of the gauge fields mediating interactions between fermions. We know that there are four bosons to carry electroweak interaction and eight bosons to carry strong interaction. Electroweak interaction is strongly coupled to the mechanism of the mass generation of the model. For that reason we focus our attention mainly on the electroweak sector of the current story. However, it should be mentioned here, only the complete Standard Model gauge theory based on the group $SU(3)_c \otimes SU(2)_L \otimes U(1)_Y$ is free of quantum anomalies. Only an anomaly free theory is *renormalizable*. The anomaly cancellation in the model involves complete generations of leptons and quarks, e.g. ν, e, u, d for the first generation. Therefore, the Standard Model makes sense with only the full set of leptons or quarks. However, on the level of the classical Lagrange density we may deal with the symmetries separately.

We know that there are four electroweak gauge bosons in Nature,

$$\gamma, Z^0, W^\pm. \tag{2.13}$$

Using the Yang-Mills technique the correspondence between the generators and boson fields has been proposed. It is reasonable to connect single electromagnetic boson to the Abelian symmetry group $U(1)$ and three weak bosons to $SU(2)$. The electroweak symmetry group is then the product $SU(2)_L \otimes U(1)_Y$. The field B_μ corresponds directly to the generator Y of $U(1)_Y$. Three W_3^i fields corresponds to the generators T_i of $SU(2)_L$. From the Lie theory we know that the commutation relations between the generators T_i are

$$[T^i, T^j] = i\epsilon^{ijk} T_k, \tag{2.14}$$

where T_i are $T_i = \frac{1}{2}\sigma_i$ and electroweak indices $i, j, k = 1, 2, 3$. Here σ_i are the Pauli matrices. The $U(1)_Y$ group is Abelian, so it is commutative.

The physical gauge fields are linear combinations of the generator fields B_μ and W_μ^i, which for Z_μ^0 and γ_μ is

$$\begin{pmatrix} \gamma_\mu \\ Z_\mu^0 \end{pmatrix} = \begin{pmatrix} \cos\Theta_W & \sin\Theta_W \\ -\sin\Theta_W & \cos\Theta_W \end{pmatrix} \begin{pmatrix} B_\mu \\ W_\mu^3 \end{pmatrix}, \tag{2.15}$$

and for $W_\mu^\pm$

$$W_\mu^\pm = W_\mu^1 \pm i W_\mu^2, \tag{2.16}$$

where Θ_W is the *Weinberg* or *weak mixing angle.*

In the case of $SU(3)_c$ the octet of generators exists corresponding to the gauge fields G^a_μ, $a = 1, 2, ..., 8$, the *gluon* gauge fields. The commutation rules are

$$[T^a, T^b] = if^{abc}T_c, \tag{2.17}$$

$$Tr(T^aT^b) = \frac{1}{2}\delta_{ab}, \tag{2.18}$$

where f^{abc} are the structure constants of $SU(3)_c$ and color indices $a, b, c = 1, 2, ...8$.

Dynamics of the Standard Model fields

The Standard Model is a Yang-Mills theory, so the matter fields are coupled to the gauge fields through the *covariant derivative*

$$D_\mu \equiv \partial_\mu - ig_sT_aG^a_\mu - ig_wT_iW^i_\mu - i\frac{1}{2}g_eYB_\mu, \tag{2.19}$$

where g_s, g_w and g_e are the coupling constants of strong, weak and electromagnetic interactions, respectively. We notice here that every coupling constant is related to its own symmetry group: g_e to $U(1)_Y$, g_w to $SU_L(2)$ and g_s to $SU(3)_c$. We will deal with the topic in more detail in the fourth chapter. We will describe the unification of the Standard Model symmetry groups to a bigger symmetry group with just one coupling constant in the framework of *Grand Unified Theories* (GUT).

Now we are ready to write down the Lagrangian of the Standard Model before EWSB. The Lagrangian has only massless fields and in total it has the form

$$\begin{aligned}\mathcal{L}_{SM} = -\frac{1}{4}G^a_{\mu\nu}G^{\mu\nu}_a - \frac{1}{4}W^a_{\mu\nu}W^{\mu\nu}_a - \frac{1}{4}B_{\mu\nu}W^{\mu\nu} + \\ \bar{l}_{Li}iD_\mu\gamma^\mu l_{Li} + \bar{l}_{Ri}iD_\mu\gamma^\mu l_{Ri} + \\ \bar{q}_{Li}iD_\mu\gamma^\mu q_{Li} + \bar{u}_{Ri}iD_\mu\gamma^\mu u_{Ri} + \bar{d}_{Ri}iD_\mu\gamma^\mu d_{Ri}.\end{aligned} \tag{2.20}$$

It is possible to show that the Lagrangian is invariant under the local gauge transformations of $SU(3)_c \otimes SU(2)_L \otimes U(1)_Y$.

Unfortunately, the symmetry $SU(2)_L \otimes U(1)_Y$ is clearly violated if we add the fermion mass term,

$$-m_f\bar{\psi}\psi = -m_f(\bar{\psi}_R\psi_L + \bar{\psi}_L\psi_R), \tag{2.21}$$

to the Standard Model Lagrangian by hand. Since ψ_R is isosinglet and ψ_L is isodoublet it is impossible to connect them directly as it is done in the mass term (2.21). Also, it is impossible to add the mass term of the electroweak bosons without violation of the local gauge symmetry. Interestingly, despite the fact that gluons are massless and strong sector is described by *vector theory* (both chiralities of all quarks appear and couple the same way in the strong theory), it is possible to add mass term of gluons (and quarks) in the gauge invariant way for $SU(3)_c$.

Thus, we need a clever mechanism to generate masses for the weak gauge bosons and fermions in the gauge invariant way. The Anderson-Higgs mechanism can give masses to the fermions and weak gauge bosons. In the Standard Model it is connected to the electroweak sector, so it is referred to as EWSB.

2.2.3 Spontaneous electroweak symmetry breaking

Generation of boson mass

The main idea of the EWSB is simple (and ingenious): we should add a scalar field with a specific form of the potential to the Lagrangian. In the interactions with other fields of the Lagrangian the scalar field can "generate" the mass terms of the field.

Let us consider a simple example, the Higgs mechanism for a field with the Abelian $U(1)$ symmetry. The Lagrangian of the field have been chosen

$$\mathcal{L}_{\text{boson}} = -\frac{1}{4} F_{\mu\nu} F^{\mu\nu}, \tag{2.22}$$

where $F_{\mu\nu} = \partial_\mu A_\nu - \partial_\nu A_\mu$. It is a massless field and, for example, it can describe a free photon.

Now, we include the complex scalar field to the Lagrangian with the interaction term between vector and scalar field. The interaction is done through covariant derivative

$$D_\mu = \partial_\mu - ieA_\mu, \tag{2.23}$$

and the Lagrangian is

$$\mathcal{L} = \mathcal{L}_{\text{boson}} + D_\mu \phi^* D^\mu \phi - V(\phi). \tag{2.24}$$

where $V(\phi)$ is defined as

$$V(\phi) = \mu^2 \phi^* \phi + \lambda (\phi^* \phi)^2 = \mu^2 |\phi|^2 + \lambda |\phi|^4. \tag{2.25}$$

In the case of $\mu^2 > 0$ and $\lambda > 0$ (which it has to be, otherwise the potential is not bounded below) it is the description of the scalar (spin-0) complex field with the mass μ^2 and self-coupling with the intensity λ. Also, the potential in the Lagrangian is invariant under the global $U(1)$ symmetry $\phi \to \phi' = e^{i\alpha}\phi$.

The case of $\mu^2 < 0$ is more interesting. Then the minimum shifts from $\phi \equiv \phi_1 + i\phi_2 = 0$ to $\phi = \upsilon e^{i\theta}$, where θ is real, which means for $\phi_{1,2}$

$$\phi_1^2 + \phi_2^2 = \upsilon^2, \tag{2.26}$$

where

$$\upsilon^2 \equiv -\frac{\mu^2}{\lambda} > 0. \tag{2.27}$$

The parameter υ is called *vacuum expectation value* or *vev* in short.

Thus, one can choose a minimum, which is the violation of the symmetry of possible solutions. To clarify the meaning of the violation let us split $\phi(x)$ to the real functions $\eta(x)$ and $\xi(x)$,

$$\phi(x) = \frac{1}{\sqrt{2}}(\upsilon + \eta + i\xi), \tag{2.28}$$

where $\eta(x) = \xi(x) = 0$ at the minimum of $V(\phi)$. Before we put the equation (2.28) to the Lagrangian we introduce the *unitary gauge*

$$\phi(x) \to e^{-i\xi(x)\upsilon}\phi(x) \text{ and } A_\mu \to \frac{1}{e\upsilon}\delta_\mu\xi(x). \tag{2.29}$$

As with any gauge the physical meaning of the fields have been conserved. The feature of the gauge is that we "move" the field $\xi(x)$ to the longitudinal component of the gauge field $A(x)$. The Lagrangian now has the following form

$$\mathcal{L} = \frac{1}{2}\partial_\mu\eta\partial^\mu\eta - \upsilon^2\lambda\eta^2 - \frac{1}{4}F_{\mu\nu}F^{\mu\nu} + \frac{1}{2}e^2\upsilon^2 A_\mu A^\mu + \\ \frac{1}{2}e^2 A_\mu A^\mu(2\upsilon\eta + \eta^2) + \frac{1}{4}\upsilon^4\lambda - \lambda\upsilon\eta^3 - \frac{1}{4}\lambda\eta^4. \tag{2.30}$$

To summarize, in the example the photon field with two degrees of freedom has absorbed the would-be boson $\xi(x)$, a so called *Goldstone boson*, with one degree of freedom and become a massive boson field with three degrees of freedom. As we see the initial $U(1)$ gauge symmetry disappeared it is said to be spontaneously broken. So, in the case of the Higgs mechanism "the gauge transformation *ate* the Goldstone boson".

Now, to construct EWSB for the electroweak sector of the Standard Model, let us summarize properties of the physical electroweak bosons:

- Photon, γ: massless boson (spin-1), carrier of electromagnetic interaction. It is an orthogonal superposition of the W^3 and B fields in the Standard Model.
- W and Z: massive bosons ($m_{\mathrm{W}} = 80.4$ [14–16] and $m_{rmZ} = 91.2$ GeV [17]), the carriers of weak interaction. $W^{\pm}$ are two orthogonal superpositions of fields W^1 and W^2. Z^0 boson is orthogonal superposition of the W^3 and B fields.

Based on the experience of the simple example above we should need three degrees of freedom for the EWSB scalar field to give masses to weak bosons. It is easy to see from the isodoublet structure of the weak sector of the Standard Model that the only possibility to combine all the masses is a complex $SU(2)$ doublet of scalar fields ϕ,

$$\Phi = \begin{pmatrix} \phi^+ \\ \phi^0 \end{pmatrix} = \frac{1}{\sqrt{2}} \begin{pmatrix} \phi_1 + i\phi_2 \\ \phi_3 + i\phi_4 \end{pmatrix}, \tag{2.31}$$

where ϕ^+ and ϕ^0 are the complex fields with four degrees of freedom ϕ_i altogether. So, three degrees of the freedom should be eaten by the massive weak bosons. One degree of freedom is left for the Higgs boson.

The relevant part of the Lagrangian for the Higgs doublet is

$$\mathcal{L} = (D^{\mu}\Phi)^{\dagger}(D_{\mu}\Phi) - V(\Phi), \tag{2.32}$$

where

$$V(\Phi) = \mu^2 \Phi^{\dagger}\Phi + \lambda(\Phi^{\dagger}\Phi)^2. \tag{2.33}$$

As it is presented above in the case of $\mu^2 < 0$ the potential has a minimum,

$$\Phi^{\dagger}\Phi = -\frac{\mu^2}{2\lambda} = \frac{\upsilon^2}{2}. \tag{2.34}$$

If we combine the last equation above and the $U(1)$ (charge conservation) symmetry, the convenient choice of the solution is

$$\phi_1 = \phi_2 = \phi_4 = 0. \tag{2.35}$$

The neutral component ϕ_3 of the doublet acquires a nonzero vev,

$$\langle \Phi \rangle \equiv \langle 0|\Phi|0 \rangle = \frac{1}{\sqrt{2}} \begin{pmatrix} 0 \\ \upsilon \end{pmatrix}, \tag{2.36}$$

where

$$\upsilon^2 = -\frac{\mu^2}{\lambda}. \tag{2.37}$$

Let us start to remove the unnecessary degrees of freedom. We use the fact that only ϕ_3 acquires a nonzero vev and use the unitary gauge. We propose the parametrization

$$\Phi(x) = \frac{1}{\sqrt{2}} e^{\frac{i}{v}\theta_a \sigma^2} \left(\begin{array}{c} 0 \\ v + h(x) \end{array} \right), \tag{2.38}$$

where $a = 1, 2, 3$. We are able to eliminate the exponent using $e^{-\frac{i}{v}\theta_a \sigma^2}$. Now the gauged Φ has the simple form

$$\Phi(x) = \frac{1}{\sqrt{2}} \left(\begin{array}{c} 0 \\ v + h(x) \end{array} \right). \tag{2.39}$$

The kinetic term $(D^\mu \Phi)^\dagger (D_\mu \Phi)$ can be expanded, using the gauged Φ, as

$$\begin{aligned} (D^\mu \Phi)^\dagger (D_\mu \Phi) = & \frac{g_2^2 v^2}{8} (W_1^\mu + i W_2^\mu)(W_\mu^1 - i W_\mu^2) \\ & + \frac{v^2}{8} \left(g_2 W_3^\mu - g_1 Y_H B^\mu \right)^2 + \frac{1}{2} (\partial^\mu h)^2 + ... \end{aligned} \tag{2.40}$$

The covariant derivative includes all the needed mass terms. The first mass term in the equation (2.40) above is the mass of $W^\pm$ as

$$W_\mu^\pm = \frac{1}{\sqrt{2}} (W_\mu^1 \mp W_\mu^2), \tag{2.41}$$

and so the mass of $W^\pm$ is

$$M_W = \frac{1}{2} v g_2. \tag{2.42}$$

The mass relation allows to fix the vev in terms of the experimental mass of $W^\pm$ and the Fermi constant G_F,

$$M_W^2 = \frac{1}{4} v^2 g_2^2 = \frac{\sqrt{2} g_2^2}{8 G_F}, \tag{2.43}$$

from where the vev is

$$v = (\sqrt{2} G_F)^{-1/2} \simeq 246 \text{ GeV}, \tag{2.44}$$

and

$$G_F = \frac{\sqrt{2}}{8} \left(\frac{g_2}{M_W} \right)^2 \simeq 1.16639 \times 10^5 \text{ GeV}^2. \tag{2.45}$$

The second mass term in (2.40) promises to fix the mass of W_3^μ and B^μ. The photon field A_μ has to be massless, so the only possibility to get massless field from the second term is the signalization, see the Weinberg mixing from (2.15)

$$Z_\mu = \frac{1}{\sqrt{g_1^2 + g_2^2}}(g_2 W_\mu^3 - g_1 G_\mu), \tag{2.46}$$

$$A_\mu = \frac{1}{\sqrt{g_1^2 + g_2^2}}(g_2 W_\mu^3 + g_1 G_\mu), \tag{2.47}$$

thus the mass of Z is

$$M_Z = \frac{v}{2}\sqrt{g_1^2 + g_2^2}. \tag{2.48}$$

In summary, EWSB spontaneously breaks the symmetry

$$SU(2)_L \otimes U(1)_Y \rightarrow U(1)_Q. \tag{2.49}$$

In the languages of the generators we lose three generators of $SU(2)_L$ from four initial generators of $SU(2)_L \otimes U(1)_Y$ and three Goldstone bosons arise. The arisen Goldstone bosons are absorbed by the $W^\pm$ and Z fields as the longitudinal (massive!) components. The remaining symmetry $U(1)_Q$ guarantees that the photon field of electromagnetic interaction will be massless.

Generation of fermion mass

The Higgs doublet Φ gives us a simple chance to construct mass terms for the Standard Model fermion fields. We can easily unite left-hand doublets to right-hand singlets using the Higgs doublet. If we do not want to violate hypercharge, the only possibility is

$$\mathcal{L} = -\lambda_l \bar{l}_L \Phi l_R - \lambda_d \bar{q}_L \Phi d_R - \lambda_u \bar{q}_L \tilde{\Phi} u_R - h.c., \tag{2.50}$$

where the *h.c.* marks all the members hermitically conjugated and $\tilde{\Phi}$ is

$$\tilde{\Phi} = i\sigma_2 \Phi^* = \begin{pmatrix} \phi^{0*} \\ -\phi^- \end{pmatrix} = \frac{1}{\sqrt{2}} \begin{pmatrix} v + h(x) \\ 0 \end{pmatrix}. \tag{2.51}$$

The form of Φ above is needed for conservation of the hypercharge. If we include $\tilde{\Phi}$ to the Lagrangian (2.50) the hypercharge is conserved: $-1/3 - 1 + 4/3 = 0$.

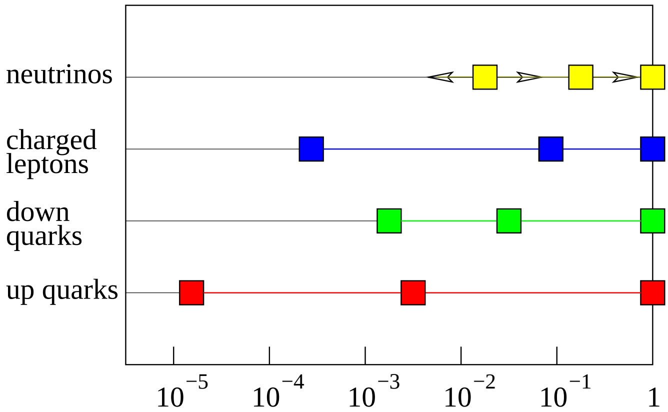

Figure 2.1: The mass of the heaviest fermion of a given type is depicted as one unit and the mass scale is logarithmic. As we can see, the scale and the scale type is unique for every sector. The upper sector has the biggest difference, but quite equal differences in the logarithmic scale. The down and charged lepton sectors have different hierarchy, the differences vary and they have opposite structure. The figure is adapted from [18].

The fermion masses from the Lagrangian (2.50) are

$$m_{e_i} = \frac{\lambda_{e_i}}{\sqrt{2}}, \tag{2.52}$$

$$m_{u_i} = \frac{\lambda_{u_i}}{\sqrt{2}}, \tag{2.53}$$

$$m_{d_i} = \frac{\lambda_{d_i}}{\sqrt{2}}, \tag{2.54}$$

where the index i counts the generations. Each massive particle in the Standard Model has its own Yukawa coupling constant λ with Higgs fields which, together with vev determine the mass of the particle. Figure 2.1 gives a picture about the mass scale and hence the strengths of the Yukawa couplings. The different mass structure of every sector in the figure gives an insight why it is difficult to connect the mass (and Yukawa) structure to a more general theory beyond the Standard Model.

It is very important to notice that all the generations of neutrino remain precisely massless in the EWSB of the Standard Model. We will deal with the topic of neutrino masses later in this work.

Name of the field	$SU(3)_c \otimes SU(2)_L \otimes U(1)_Y$
W	$(1,3,0)$
B	$(1,1,0)$
g	$(8,1,0)$
$L_L = (\nu, l)_L^T$	$(1,2,-1)$
e_R	$(1,1,2)$
$Q_L = (u,d)_L^T$	$(3,2,1/3)$
u_R	$(\bar{3},1,-4/3)$
d_R	$(\bar{3},1,2/3)$
H	$(1,2,1)$

Table 2.1: Boson, fermion and scalar multiplets of the Standard Model. In the first set of rows there are the gauge bosons of electroweak and strong sector. In the second and third sets are the lepton and quark fields accordingly. The last row H denotes the Higgs scalar field.

2.2.4 Standard Model summarized

In the Standard Model the local gauge interactions are described by $SU(3)_c \otimes SU(2)_L \otimes U(1)_Y$. There are three (experimentally known) families of quarks and leptons. One family consists of states $\{Q_L, u_R, d_R; L_L, e_R\}$, where the label L marks left-handed isodoublet and the label R marks right-handed isosinglet, $\{Q, u, d\}$ is the quark sector and $\{L, e\}$ is the lepton sector. It is a chiral theory as there is asymmetry between left-handed and right-handed fields. The fields transform under $SU(3)_c \otimes SU(2)_L \otimes U(1)_Y$ as Table 2.2.4 shows.

In the Standard Model only the local symmetries are imposed. The global symmetries of the Standard Model are *accidental*: baryon number B and lepton flavour numbers L_e, L_μ and L_τ. It is useful to define the total lepton number

$$L = L_e + L_\mu + L_\tau. \tag{2.55}$$

Accidental means that the symmetries are not imposed on the Lagrangian. The accidental symmetries are there due to the field content of the Standard Model and by the requirement of renormalizability. In summary, the following accidental global symmetry arises (at the perturbative level) in the Standard Model:

$$U(1)_B \otimes U(1)_e \otimes U(1)_\mu \otimes U(1)_\tau, \tag{2.56}$$

where B notes the baryon number and e, μ and τ the lepton numbers.

The SM has 19 arbitrary parameters. Only experimental data determine the value of the parameters. There are three arbitrary gauge couplings: g_1, g_2 and g_3, where g_1 and g_2 are the $SU(2)_L$ and $U(1)_Y$ couplings and g_3 is the $SU(3)_c$ coupling. In addition, there are 9 Yukawa parameters associated with the 9 charged fermion masses, and 4 mixing angles in the quark CKM matrix. Two parameters, v and λ, are connected directly to the Higgs potential, the first is the Higgs vev and the second is its quartic self-coupling. Also, a free QCD parameter θ exists.

As mentioned the neutrinos remain massless in the Standard Model. However, experimental data from the oscillation experiments provide convincing evidence for neutrino masses. Thus, we urgently need a theory beyond the Standard Model. If neutrino is a *Dirac particle* then 7 free parameters are needed to describe the oscillation data: 3 masses, 3 mixing angles and one CP phase for the *MNS mixing matrix.* If neutrino is a *Majorana particle* then two more parameters are needed: 2 additional phases should be included in the MNS matrix. We will deal with the neutrino sector more carefully in the next chapters as it is a topic beyond the Standard Model.

The Standard Model cannot give answers for a number of questions, some of which are following:

- Why is the local gauge interaction group $SU(3)_c \otimes SU(2)_L \otimes U(1)_Y$ (and thus there are three couplings)?
- Why are there three generations of fermions?
- What is the origin of the mass spectrum of fermions?
- Why is electric charge quantized as it is presented in the quark and lepton sector of the Standard Model?
- What is the mechanism to protect the Higgs boson mass against the quadratically divergent contributions from very high energy physics?

A bunch of experimental effects disturbs the picture of the Standard Model. One is the mechanism of neutrino mass which need an urgent solution. In the next chapter we will describe some experimental problems in more detail.

2.3 Standard Model of cosmology

2.3.1 Motivations

The standard framework of cosmology is based on four main assumptions based on strong observational and experimental evidences.

1. The Universe is nonstatic and it is expanding in the current epoch of its history.

2. The *cosmological principle* postulates that the Universe appears to be homogeneous and isotropic on large scales. Mathematically, the geometry of our Universe is described by the Friedmann-Robertson-Walker (FRW) line element.

3. Cosmological objects are moving along timelike geodesics that do not intersect except at a singular point in the finite or infinite past or future. Mathematically, the matter content of the Universe can be described as *ideal fluid*.

4. The theory of *general relativity* describes of the dynamics of the Universe.

Thus we need four components to build a cosmological model: the metrica of the Universe (e.g. FRW metrics), the equation describing the dynamics of the Universe (e.g. the general relativity), the inital conditions for the dynamics (e.g. the Big Bang) and the equation of state of matter (e.g. ideal fluid).

The astronomical observations suggest that our Universe is expanding. The dependence between cosmological distance and velocity of the expansion, *Hubble's law*, was first formulated by Edwin Hubble and Milton Humason in 1929 after nearly a decade of observations [19]. Specifically, the law states that velocity of the expansion is proportional to distance. The formulation of the Hubble's law is very simple

$$v = H_0 D = H(t_0) D, \tag{2.57}$$

where v is the cosmological velocity of the object (measured by the redshift of the object), H_0 is the *Hubble constant*, $H(t)$ is the Hubble parameter in time, t_0 marks the present time epoch and D is the distance between us and the distant object in the approximated rest frames. Typically, v is measured in km/s and D in Mpc. In cosmology and astronomy it is more convenient to think in the terms related to the Doppler effect of electromagnetic radiation. In the expanding Universe it means redshift, usually marked as z. In the unrelativistic case the redshift is the following

$$z = \frac{\nu_{\text{emit}} - \nu_{\text{obs}}}{\nu_{\text{obs}}} \simeq \frac{v_{12}}{c}, \tag{2.58}$$

where ν_{emit} is the frequency of the emitted light, ν_{obs} is the observed frequency, v_{12} difference of the velocity between the observer and the emitter and c marks the speed of light (we write it out here for clarity). For the general case in cosmological scale the value of redshift z follows from the metric of the Universe, which we will define below, and the condition of light-like signal, $ds^2 = 0$, where ds is space-time interval. The current value of H_0 is $71^{+1}_{-2} \frac{\text{km}}{\text{s Mpc}}$ combined from the data of *cosmic microwave background radiation* (CMB) measured by the WMAP3 project and the observations of the Supernova Legacy Survey (SNLS) [20].

If we simply reverse the expansion of the Universe we notice that it should start some time ago from the violent explosion-like event called the *Big Bang*. Gamow and his collaborators proposed a possibility that the abundances of the elements had a cosmological origin in the 1940s [21]. The initial distribution of the elements was fixed in the early stage of the Universe when it was very hot and dense, enough to allow for the nucleosynthesis processing of hydrogen to heavier elements. The process of the nucleosynthesis is called the *Big Bang Nucleosynthesis* (BBN). Also, as the Universe was cooling down, there had to be a moment when ionized plasma (nuclei and electrons) recombined to neutral gas and the gas content became to be transparent for radiation. The recombination left a magnificent data signature for us: it was recorded in CMB mentioned above. In other words, CMB is the last snapshot of the surface of recombining plasma at the recombination temperature, $T \cong 10^3$. Due to the high redshift of the surface, $z = 1100$, the radiation temperature is only $T = 2.725 \pm 0.002$ K nowadays [22]. Also, the early state processes of the Universe have left some other marks in the current epoch of the Universe. We will describe it in the following paragraphs and subsections.

The *cosmological principle*, which means homogeneity and isotropy of the Universe, is based on numerous different cosmological observations. Mainly, the assumption follows from three sets of the observation counted below.

- The observed expansion of the Universe (the Hubble's law) does not depend on the direction and distance. The property has been verified with high precision.

- Homogeneity of the Universe follows from BBN at the very high level of accuracy. BBN was highly sensitive to temperature and other conditions in the early Universe. The theory of nucleosynthesis predicts the relative abundance of the elements with approximately 75% of hydrogen, 24% of helium and a small fraction of some light elements such as deuterium, helium and lithium. The equality of the consentrations everywhere in the observed Universe is confirmed by observations at very high accuracy.

- Isotropy of the Universe follows most accurately from CMB. The root mean square of the isotropy fluctuations is at a very low level, at temperature $T = 1.8 \cdot 10^{-5}$ K [22].

This list is clearly not exhaustive. Far too many nice reviews and textbooks are dedicated to the topic to list them here. For example, in the context of particle physics a short and up-to-date review is given regularly by Particle Data Group [11].

2.3.2 Dynamics of the Universe

The observed homogeneity and isotropy enable us to describe the overall geometry and evolution in terms of two cosmological parameters accounting for the spatial curvature and the overall expansion (or contraction) of the Universe. The quantities appear in the most general expression for a space-time metric, known as the *FRW metric*,

$$ds^2 = dt^2 - R^2(t)\left[\frac{dr^2}{1-kr^2} + r^2\left(d\theta^2 + \sin^2\theta d\varphi^2\right)\right]. \tag{2.59}$$

The curvature parameter k can be chosen to be discrete number by scaling the radial coordinate r and it can have the values -1, 0 and 1. $R(t)$ is the cosmological scale factor which determines proper distances in terms of the co-moving coordinates. We notice that the metric has a maximally symmetric 3D subspace of a 4D space-time. The curvature parameter k determines the spatial geometry of the Universe: $k = -1$ corresponds to hyperbolic, $k = 0$ to Euclidean and $k = 1$ to spherical geometry.

Sometimes it is convenient to define a *dimensionless scale factor*,

$$a(t) = \frac{R(t)}{R_0}, \tag{2.60}$$

where $R_0 = R(t_0)$ is the scale factor at the present epoch t_0. Also, we can define *conformal time*

$$d\eta = \frac{dt}{a(t)}. \tag{2.61}$$

Now we can calculate the relation between the redshift z and the scale factor $R(t)$. The redshift is defined as $z \equiv (\Lambda_{\rm obs} - \Lambda_{\rm emit})/\Lambda_{\rm emit}$, where $\Lambda_{\rm obs}$ is the observed wavelength and $\Lambda_{\rm emit}$ is the emitted wavelength. In the expansion,

$$\Lambda_{\rm emit} = \frac{R(t)}{R_0}\Lambda_{\rm obs}, \tag{2.62}$$

and therefore

$$z = \frac{R_2}{R_1} - 1. \tag{2.63}$$

The large scale dynamics of the Universe is described by the general relativity. The total action is composed of the gravitational Einstein-Hilbert action $I_{\rm EH}$ and the matter action $I_{\rm M}$,

$$I_{\rm tot} = I_{\rm EH} + I_{\rm M} = \int d^4x\sqrt{-g}\left(\frac{R}{16\pi G_{\rm N}} - \frac{\Lambda}{8\pi G_{\rm N}} + \mathcal{L}_{\rm M}\right), \tag{2.64}$$

where $g = \det(\lambda_{\mu\nu})$ is the determinant of a spacetime Lorentz metric $\lambda_{\mu\nu}$, R is the Ricci scalar, Λ is cosmological constant, $G_{\rm N}$ is the Newtonian gravitation constant and $\mathcal{L}_{\rm M}$ is the Lagrangian of matter. We have freedom to associate the cosmological constant Λ either with the gravitational action or the matter action as we have no experimental evidence for the mechanism behind the constant. The Einstein equations derived from the total action are

$$R_{\mu\nu} - \frac{1}{2}g_{\mu\nu}R = 8\pi G_{\rm N}T_{\mu\nu} - g_{\mu\nu}\Lambda, \tag{2.65}$$

where we have added the cosmological constant to the matter side of the equation.

If the FRW line element (2.59) describes the geometry of the Universe and the ideal (isotropic and homogeneous) fluid describes matter content of the Universe,

$$T_{\mu\nu} = pg_{\mu\nu} + (p+\rho)u_\mu u_\nu, \tag{2.66}$$

the general Einstein equations reduce to ordinary differential equations. In the equation, p is isotropic pressure, ρ is the total energy density and $u = (1,0,0,0)$ is the 4-velocity for the isotropic fluid in co-moving coordinates. The *Friedmann-Lemaitre equations* (FL) present the solution of the differential equations in the case of the perfect fluid source,

$$\left(\frac{\dot{R}}{R}\right)^2 = \frac{8\pi G_{\rm N}}{3}\rho - \frac{k}{R^2} + \frac{1}{3}\Lambda, \tag{2.67}$$

and now

$$\frac{\ddot{R}}{R} = \frac{\Lambda}{3} - \frac{4\pi G_{\rm N}}{3}(\rho - 3p), \tag{2.68}$$

where the Hubble parameter $H(t) \equiv \dot{R}/R$. We can use the equations (2.67) and (2.68) or the conservation of the energy-momentum $T^{\mu\nu}_{;\mu} = 0$ to develop a very convenient relation

$$\dot{\rho} = 3H(t)(\rho + p). \tag{2.69}$$

Eq. (2.67) shows that the behavior of the Universe is determined by the curvature constant k. Also, we can derive a simple equation for the time development of the density

$$\rho = \rho_0 a^{-3(w+1)}, \tag{2.70}$$

where the constant w connects the pressure and density of the ideal fluid, $p = w\rho$. Some of the most important values of w are classified as the following cases:

- *radiation* (relativistic matter):

$$w = 1/3 \Rightarrow p = \frac{1}{3}\rho \Rightarrow \rho = \rho_0 a^{-4}, \tag{2.71}$$

- *ideal dust* (pressureless perfect fluid):

$$w = 0 \Rightarrow p = 0 \Rightarrow \rho = \rho_0 a^{-3}, \tag{2.72}$$

- *stiff fluid* (very viscous fluid):

$$w = 1 \Rightarrow p = \rho \Rightarrow \rho = \rho_0 a^{-6}, \tag{2.73}$$

- *"cosmological constant"* connected to the matter content, e.g. see Eq. (2.65):

$$w = -1 \Rightarrow p = -\rho \Rightarrow \rho = \rho_0 = \text{const.} \tag{2.74}$$

It is useful and comfortable to define several other measurable cosmological parameters. The *scaled Hubble parameter* h is defined by

$$H \equiv 100h \text{ km s}^{-1} \text{ Mpc}^{-1}, \tag{2.75}$$

and the reversed Hubble parameter which is connected to the age of the Universe and its causal radius

$$H^{-1} = 9.78h^{-1} \text{ Gyr} = 2998h^{-1} \text{ Mpc}. \tag{2.76}$$

One can define the *critical density* ρ_c from the equation (2.67) such that $k = 0$ and $\Lambda = 0$

$$\rho_c = \frac{3H^2}{8\pi G_N} = 1.88 \cdot 10^{-26} h^2 \text{ kg m}^{-3} = 1.05 \cdot 10^{-5} h^2 \text{ GeV cm}^{-3}. \tag{2.77}$$

For example, let us calculate the critical density ρ_c in the terms of the proton mass. The mass of proton is $\sim$1 GeV, so the critical density is in the magnitude of 10 protons (or hydrogen atoms) per cubic meter.

Also, it is very useful define the *cosmological density parameter* by

$$\Omega_{\text{tot}} = \rho_{\text{tot}}/\rho_{\text{c}}, \tag{2.78}$$

where $\rho_{\text{tot}} = \rho + \rho_\Lambda$ is the density of the Universe. One can reformulate the Friedmann equation (2.67)

$$\frac{k}{R^2} = H^2(\Omega_{\text{tot}} - 1). \tag{2.79}$$

It is very useful to divide the total density into some "subdensities" with different behavior in time. For example, one can separate the density of ideal dust Ω_{mat}, the density of radiation Ω_{rad} and the density of vacuum $\Omega_\Lambda = \Lambda/3H^2$ related to the cosmological constant Λ. So, the Fridmann equation can be presented by

$$\frac{k}{R_0^2} = H^2(t)(\Omega_{\text{mat}}(t) + \Omega_{\text{rad}}(t) + \Omega_\Lambda(t) - 1). \tag{2.80}$$

The different behavior of the subcomponents will be discussed in detail in Subsection 2.3.4.

As mentioned, the curvature k determines the geometry of the Universe. The defined density parameter Ω_{tot} is clearly related to k. The relation can be summarized in three cases:

- $\Omega_{\text{tot}} < 1 \Leftrightarrow k = -1$, the Universe is open (or it has compact hyperbolic geometry),
- $\Omega_{\text{tot}} > 1 \Leftrightarrow k = 1$, the Universe is closed,
- $\Omega_{\text{tot}} = 1 \Leftrightarrow k = 0$, the Universe is flat.

If we imagine possible values of the unstable density parameter Ω then the case $\Omega = 1 \Leftrightarrow k = 0$ seems to be very fine-tuned. Thus it was a big puzzlement for physicists when the observations showed that the value of k is very close to zero. We will deal with the problem in the subsections below.

We know the time development of the density from Eq. (2.71-2.74). Is it possible to develop the time evolution of the $R(t)$? If we neglect the curvature k and cosmological constant Λ terms in the Friedmann equation 2.67, it is easy to integrate the equation to obtain the time evolution of $R(t)$,

$$R(t) \propto t^{\frac{2}{3(1+w)}}. \tag{2.81}$$

In principle, it is possible to distinguish between three important special cases of the matter action of the Universe. They are *radiation-dominated*, *matter-dominated* and *vacuum-dominated* Universe. We will write out the evaluation equations of $R(t)$ and analyze them case by case below. The curvature paramater has been taken to be zero, $k = 0$.

- Radiation-dominated Universe, $w = 1/3$,

  $$\rho \propto R^{-4}, \qquad R \propto t^{1/2}, \qquad H \propto \frac{8}{9}t^{-1}. \tag{2.82}$$

  In the early epoch the Universe was very hot, at the energy far above the mass of the known particle species. It means that the content was clearly relativistic. So, the development of the scale factor was radiation driven.

- Matter-dominated Universe, $w = 0$,

  $$\rho \propto R^{-3}, \qquad R \propto t^{2/3}, \qquad H \propto \frac{2}{3}t^{-1}. \tag{2.83}$$

  At relatively late times when the Universe has cooled at the energy far below the mass of the heavy stable particles, non-relativistic matter eventually has started to dominate over radiation in the energy density.

- Vacuum-dominated Universe, $w = -1$,

$$\rho = const, \qquad R \propto e^{\sqrt{\frac{\Lambda}{3}}t}, \qquad H \propto \sqrt{\frac{\Lambda}{3}} = \mathrm{const}. \tag{2.84}$$

  The vacuum energy driven evolution can dramatically influence the history and future of the Universe. The exponent behavior of the vacuum driven scalar factor can always "win" the power functions in the cases of initial radiation and matter domination. Also, $H = \mathrm{const}$ only if $\Lambda = \mathrm{const}$ in time.

In general, we have to pay attention to the fact that w is not a constant in the history of the Universe.

Also, if we do not fix k at zero, then the vacuum dominated Universe follows the *de Sitter solution*, corresponding to

$$a(t) \sim \begin{cases} \sinh\left(\sqrt{\frac{\Lambda}{3}}t\right), & k = -1, \\ e^{\sqrt{\frac{\Lambda}{3}}t}, & k = 0, \\ \cosh\left(\sqrt{\frac{\Lambda}{3}}t\right), & k = 1. \end{cases} \tag{2.85}$$

2.3.3 Horizons of the Universe

If the age of the Universe is finite then the distance between causally connected areas has a maximum finite value. For example, a photon can travel only a finite distance in the current age of the Universe. As the propagation of causality is limited by the velocity of light it is the maximum distance that the causal signal can pass during the age of the Universe.

The called *particle horizon* $d_{\mathrm{ph}} = \eta c$, where $c = 1$ is the speed of light and η is conformal time, determines the size of the region that an observer can see in principle at a finite time t,

$$d_{\mathrm{ph}}(t) = \int_0^t \frac{dt'}{a(t')} = R(t) \int_0^t \frac{dt'}{R(t')}. \tag{2.86}$$

For example, if we consider a general case valid for radiation and matter content,

$$R \sim t^q,\ 0 < q < 1, \tag{2.87}$$

then the particle horizon is

$$d_{\mathrm{ph}} = \frac{q}{1-q} H^{-1} \propto t. \tag{2.88}$$

Also, the *event horizon* delimits the part of the Universe from which we can receive information. Let us suppose that the time history is limited by $t_{\max}$ for events taking place at the moment t, then the event horizon is

$$d_{eh}(t) = R(t) \int_t^{t_{\max}} \frac{dt'}{R(t')}. \tag{2.89}$$

For the already mentioned case which is valid for radiation and matter content, $R \sim t^q$, $0 < q < 1$, there is no event horizon $d_{\rm eh} \propto t \to \infty$ since $t_{\max} \to \infty$. Interestingly, for vacuum driven case, $R \sim e^{Ht}$, $H = const$, the event horizon is a constant $d_{\rm eh} = H^{-1}$ and an observer can receive information no farther away than H^{-1}. Let us summarize it as follows:

- for the matter and radiation driven Universe:

$$d_{\rm eh} \to \infty \text{ if } t \to \infty, \tag{2.90}$$

- for the vacuum driven Universe:

$$d_{\rm eh} = \text{const if } t \to \infty. \tag{2.91}$$

Physical distance L between two particles in an expanding Universe can be written as

$$L = R(t) L_{\rm c}, \tag{2.92}$$

where the co-moving distance $L_{\rm c}$ is measured in *co-moving coordinates* and it is constant in time in the case of freely moving particles. Also, we notice that cosmological "particle" (freely) moving along geodesics was an assumption of the cosmology mentioned above. If the distance L between the particles is larger than horizon $L > d_{\rm ph}$ they are not causally connected.

2.3.4 Components of the Universe

The density of the Universe can be divided into different components following the dynamical behavior of them. We already presented some cases:

- *radiation* (relativistic matter), $w = 1/3$;
- *ideal dust* (pressureless perfect fluid), $w = 0$;
- *"cosmological constant"* connected to the matter content, $w = -1$.

Thus, the total density $\Omega_{\rm tot}$ can be defined as the sum of three density components $\Omega_{\rm tot} = \Omega_{\rm rad} + \Omega_{\rm mat} + \Omega_\Lambda$.

The radiation density $\Omega_{\rm rad}$ is very small fraction of the total density in the present Universe. However, some epochs of the early Universe were totally radiation dominated.

The member $\Omega_{\rm mat}$ is rather complicated. A fraction of $\Omega_{\rm mat}$ can be approximated as *ideal dust*. The dust approximation works only in very large scale. For example, a cosmic gas cloud which has thermodynamical pressure and temperature can not be approximated as ideal dust. Thus, the matter density can include different components with different temperature and pressure, only the extreme $T = p = 0$ is ideal dust.

Numerous different observations have shown that the matter density $\Omega_{\rm mat}$ has at least two different subcomponents: the density of baryonic matter $\Omega_{\rm b}$ and the density of cold dark matter $\Omega_{\rm CDM}$. Baryonic matter interacts strongly and thus it behaves as gas. CMB, the dynamics and collisions of the galaxies show the existence of CDM. The temperature of CDM has to be low to enables the growth of density fluctuations to form stars and galaxies. In the context of particle physics it should consist of very weakly interacting particles.

Also, $\Omega_{\rm mat}$ can have the component of *hot dark matter* (HDM). For example, (relict) cosmological neutrinos from the early Universe can be one component of HDM. Cosmological observations have shown that the fraction of HDM is quite small in the total density.

In principle, the vacuum density Ω_Λ can present a gravitation related constant in the Einstein equations (2.65). However, the matter side of the equation can contain a mysterious content of the Universe, the *dark energy* (DE). It should be constant (or at least very close to constant) in spatial and time scale. Also, as it has negative pressure, the stability of DE is a question. DE may become dark matter when buffeted by baryonic particles and it is described as a dynamical field. The type of field is referred to as *quintessence*. In principle, quintessence can vary in spatial and time scale. For example, to prevent instability it must have a very long Compton wavelength, meaning it has to be very light.

2.3.5 The main cosmological parameters

The measurements of CMB by the WMAP project during the first year (2003) of the experiment improved our cosmological knowledge significantly [23]. By the end of third year of the WMAP experiment it had gathered a magnificent dataset which makes it a most valuable scientific experiment in human history. Thus, all the following values of the cosmological parameters are based on the WMAP3 report [20]. Naturally, the values have been improved by the results from the other experiments cited below.

In the case of the flat universe, the combination of WMAP and the Supernovae Legacy Survey (SNLS) data [24] yields a significant constraint on the equation of state of the dark energy,

$$w = -0.97^{+0.07}_{-0.09}. \tag{2.93}$$

If we assume that $w = -1$ the deviations from the critical density, $\Omega_{\mathrm{k}} = \Omega_{\mathrm{tot}} - 1$, are small. The combination of WMAP and the SNLS data imply

$$\Omega_{\mathrm{k}} = -0.015^{+0.020}_{-0.016}. \tag{2.94}$$

The combination of WMAP three year data and the Hubble Space Telescope (HST) Key Project [25] constraint on H_0 implies

$$\Omega_{\mathrm{k}} = -0.010^{+0.016}_{-0.009}. \tag{2.95}$$

The vacuum density from the same experiments is

$$\Omega_{\Lambda} = 0.72 \pm 0.04. \tag{2.96}$$

The combined result from WMAP and the Sloan Digital Sky Survey (SDSS) luminous red galaxy (LRG) [26] survey gives the matter density

$$\Omega_{\mathrm{mat}} = 0.267^{+0.018}_{-0.025}. \tag{2.97}$$

The same combination of the measurements gives the baryonic density

$$\Omega_{\mathrm{b}} = 0.0444^{+0.0042}_{-0.0035}. \tag{2.98}$$

If we fix flatness at $k = 0$ the combination of WMAP and other astronomical data (large scale structure and supernova data) yield a constraint on the neutrino masses (at 95% CL),

$$\sum m_{\nu} < 0.68 \text{ eV}. \tag{2.99}$$

2.3.6 Problems of the Big Bang model

Problem of horizon, isotropy and homogeneity

We are able to evaluate the growth of particle horizon compared to the growth of length scale $R(t)$ quantitatively. Let $d'_{\mathrm{ph}}(t_0)$ mark the value of $d_{\mathrm{ph}}(t_r)$ measured at the current epoch t_0, where t_{r} is the time of the recombination. The value of $d'_{\mathrm{ph}}(t_0)$ can be calculated using the equation (2.92),

$$d'_{\mathrm{ph}}(t_r) = \frac{R(t_0)}{R(t_{\mathrm{r}})} d_{\mathrm{ph}}(t_{\mathrm{r}}). \tag{2.100}$$

On the other hand the particle horizon of the current can be developed from (2.88),

$$d_{\mathrm{ph}}(t_0) = \frac{H(t_0)}{H(t_{\mathrm{r}})} d_{\mathrm{ph}}(t_{\mathrm{r}}). \tag{2.101}$$

We are able now to write down the ratio of $d_{\mathrm{ph}}(t_0)$ and $d'_{\mathrm{ph}}(t_{\mathrm{r}})$,

$$N = \frac{d_{\mathrm{ph}}(t_0)}{d'_{\mathrm{ph}}(t_{\mathrm{r}})} = \frac{H(t_0)}{H(t_{\mathrm{r}})} \frac{R(t_{\mathrm{r}})}{R(t_0)} = \frac{\dot{R}(t_{\mathrm{r}})}{\dot{R}(t_0)}, \tag{2.102}$$

where we used the definition $H(t) = R(t)/\dot{R}(t)$. The value of $R(t_r)$ is fixed as $t_r = \mathrm{const}$ in the case. Now we can develop two different versions using equations (2.82-2.84):

- Radiation and matter dominant Universe

  $$R(t_0) \propto t^q \Rightarrow \dot{R} \propto t^{q-1} \Rightarrow N \propto \frac{1}{t^{q-1}} \propto t^{1-q}, \tag{2.103}$$

  where the matter and radiation state equations bound q as $0 < q < 1$. The last condition means that the exponent of t is positive, $1-q > 0$, and N is growing in time. So, in the matter or radiation dominated Universe a causal region engages new and new areas which have not had any causal contact before.

- Vacuum dominant Universe

  $$R(t_0) \propto e^{\sqrt{\frac{\Lambda}{3}}t} \Rightarrow \dot{R} \propto \frac{\Lambda}{3} e^{\sqrt{\frac{\Lambda}{3}}t} \Rightarrow N \propto e^{-\sqrt{\frac{\Lambda}{3}}t}. \tag{2.104}$$

  The equation shows that N decreases in time in the vacuum dominated Universe. So, in the vacuum dominated Universe the causal regions fall apart into causally unconnected areas.

If we follow the classical Big Bang model, the Universe was radiation dominated in the early stages. Thus, the particle horizon compared to the length scale developed as shown in the first case above:

$$N \propto \frac{1}{t^{q-1}} \propto t^{1-q}, \tag{2.105}$$

where $0 < q < 1$. If the equation is valid throughout the history of the early Universe, the question arises: how is a very homogeneous and isotropic Universe possible? For example, we can calculate the ratio N of the Universe at the recombination time and nowadays. It is more convenient to use the temperature scale for the history of the Universe instead of the time scale of the history. We know the current temperature of the Universe very accurately from the CMB measurements [20, 22]. Also, we can estimate the temperature at the recombination as we know the physics of the recombination well. The expansion of the Universe after the recombination is matter dominated ($q = 2/3$) and it is an adiabatic process

$$T(t)a(t)^{\gamma} \propto S = \text{const}, \tag{2.106}$$

where S is entropy and $\gamma \cong 1$ is a constant related to the number of degrees of freedom for matter. So, using the equations (2.106) and (2.83) we can write

$$\frac{R(t_0)}{R(t_r)} = \frac{T(t_r)}{T(t_0)} = \left(\frac{t_0}{t_r}\right)^{\frac{2}{3}} \Rightarrow \frac{t_0}{t_r} = \left(\frac{T(t_r)}{T(t_0)}\right)^{\frac{3}{2}}. \tag{2.107}$$

If we set the ratio t_0/t_r to the expression (2.103) we get

$$N = \left(\frac{t_0}{t_r}\right)^{\frac{1}{3}} = \left(\frac{T(t_r)}{T(t_0)}\right)^{\frac{1}{2}}. \tag{2.108}$$

Finally, using the known values of temperature, $T(t_r) \approx 3000K$ and $T(t_0) \approx$ 2.7 K, we find the value of N

$$N = \left(\frac{3000}{2.7}\right)^{\frac{1}{2}} \approx 30, \tag{2.109}$$

and the corresponding surface (N^2) and volume elements (N^3) are

$$N^2 = \frac{3000}{2.7} \approx 10^3, \tag{2.110}$$

$$N^3 = \left(\frac{3000}{2.7}\right)^{\frac{3}{2}} \approx 10^5. \tag{2.111}$$

If we compare the values to the observation data of CMB, LSS and other experiments we see that the observed Universe is very homogeneous and isotropic. For example, as it is already mentioned above, the root mean square of the isotropy fluctuations of CMB is very small, about $\Delta T = 1.8 \cdot 10^{-5}$ K [22]. How are the homogeneity and isotropy possible as no thermodynamical smoothing mechanism can work between the noncausal regions? Might it be that a physical mechanism exists which produces a very smooth Universe? It seems to be the opposite. Quantum fluctuations which can "work" between the noncausal regions in the very early quantum scale Universe can only produce inhomogeneities. Also, gravitation can only magnify the inhomogeneities in the early stage.

During the 1970s the question puzzled and frustrated the cosmologists. A paradigm change was needed to solve the question in 1980s, but it is a topic of next subsection.

Problem of flatness

As it is shown above the density ρ and density parameter $\Omega = \rho/\rho_c$ evolve in time. Let us reformulate the equation (2.79)

$$\frac{k}{R^2} = H^2(\Omega_{\text{tot}} - 1), \tag{2.112}$$

for the density Ω as

$$\Omega - 1 = k\dot{R}^{-2}(t). \tag{2.113}$$

We can take the time evolution of $R(t)$ from the equations (2.82-2.84) for the matter, radiation and vacuum dominated Universe:

- *radiation dominated Universe*

$$\Omega - 1 = k\dot{R}^{-2}(t) \propto t, \tag{2.114}$$

- *matter dominated Universe*

$$\Omega - 1 = k\dot{R}^{-2}(t) \propto t^{\frac{2}{3}}, \tag{2.115}$$

- *vacuum dominated Universe*

$$\Omega - 1 = k\dot{R}^{-2}(t) \propto e^{-2\sqrt{\frac{\Lambda}{3}}t}, \tag{2.116}$$

In the two first cases $\Omega = 1$ is an unstable stationary point. So, even a small fluctuation of $\Omega = 1$ causes a continuous departure from unit in time. On the other hand, as it is marked above in Eq. (2.94) and Eq. (2.95) the measurements show that Ω is very close to one. We have a serious problem: the Universe is very advanced in years, approximately 10^{18} s, but Ω is very close to one even nowadays. It means Ω had to be extremely fine-tuned in the young Universe. For example, at the time of the nucleosynthesis, $t \sim 1$ s, Ω had to be fine-tuned at the level of

$$|\Omega - 1| \lesssim 10^{-17}, \tag{2.117}$$

to get the present value of Ω. If we go back to the Planck time, $t \sim 10^{-43}$, the fine-tuning is enormous,

$$|\Omega - 1| \lesssim 10^{-60}. \tag{2.118}$$

Problem of exotic relics

Particle physics predicts that many "exotic" particles/defects could have been produced in the early hot Universe. There can be different mechanism behind the production: phase transitions, topological effects etc. For example, the GUT theories can propose monopoles, strings and other kind of topological objects which have not yet been observed in Nature. The most well-known of such particles is the magnetic monopole, a stable "knot" of magnetic field. Monopoles are expected to be produced at high temperatures and they should have persisted to the present epoch [27]. On the other hand, no experiments have found a magnetic monopole [11]. Also, other mechanisms exist in the different models which could have produced weird stable topological objects in the early hot Universe.

Other problems

The questions above puzzled the physicists from the birth of the Big Bang model to the 80s. However, three questions above do not finish the list of unsolved problems. Number of other problems arise in the Big Bang model. The set of questions are connected with particle physics: what lies behind CDM, the vacuum energy problem etc. As we do not know the physics beyond the electroweak symmetry breaking scale it is difficult to propose any answer. Also, one of the main question, the question of the initial singularity, seems to vex the physicists constantly.

2.3.7 Inflation and the ΛCDM model

In 1980 a paper with the title "The Inflationary Universe: A Possible Solution to the Horizon and Flatness Problems" was published by Alan Guth [28]. During the years that followed Andrei Linde, Andreas Albrecht and Paul Steinhardt complemented the theory and gave the theory its modern form [29, 30]. The mechanism called *inflation* can solve the problems of the horizon and flatness. Also, it can give a solution for undiscovered exotic relics.

The main idea of the inflation could already be seen in the last subsection, where we described the problems of the Big Bang model, and it is the vacuum dominated Universe. Let us check all the problems in the case of the inflation: problem of horizon, isotropy and homogeneity, problem of flatness, problem of exotic relics. Let us consider the horizon problem first. We showed the parameter N increase in the case of matter or radiation

$$N \propto t^{\alpha}, \tag{2.119}$$

where α is 1 or 2/3 accordingly. So, any causal region engages new non-causal areas in the matter and the radiation dominated Universe. On the other hand, the only know possibility to explain homogeneity and isotropy is to assume that the causal contact and smoothing have been there somehow before the radiation or matter domination. However, if we study the case of vacuum dominated development of the Universe we see that it can be the solution! For the vacuum domination the parameter N is

$$N \propto e^{-\sqrt{\frac{\Lambda}{3}}t}. \tag{2.120}$$

So, N decreases exponentially, which means that the causally connected regions before the inflation are spread out exponentially during the inflation. After the inflation period when the radiation and then matter start to dominate, we can see the smoothed (before the inflation period) regions enter our visible Universe.

Now, let us check the flatness problem in the case of vacuum domination. The density parameter Ω behaves exactly like needed,

$$\Omega - 1 = k\dot{R}^{-2}(t) \propto e^{-2\sqrt{\frac{\Lambda}{3}}t}, \tag{2.121}$$

so the parameter is getting exponentially closer and closer to 1.

Finally, the exotic content problem works out as easily. As the scale factor R increases exponentially during the inflation,

$$R(t) \propto e^{\sqrt{\frac{\Lambda}{3}}t}, \tag{2.122}$$

all the exotic particles and other phenomena, that originated from the period before the inflation, are spread out. If the inflation is long enough, the probability to observe any exotics becomes to very small. For example, it is possible that accidentally, in our visible part of the Universe there is one exotic particle present.

Thus, the solution seems to be rather simple. However, historically the understanding of the mechanism needed a change in the paradigm. The proposed cosmological constant in the side of gravitation in the Lagrangian,

$$I_{\text{tot}} = I_{EH} + I_M = \int d^4x\sqrt{-g}\left(\frac{R}{16\pi G_N} - \frac{\Lambda}{8\pi G_N} + \mathcal{L}_M\right), \qquad (2.123)$$

seemed artificial to physicists. Also, the constant in the matter side seemed to be unnatural as the physical mechanism behind of the state equation $p = -\rho$ was not well understood.

2.3.8 ΛCDM as the standard model of cosmology

ΛCDM is the most widely accepted cosmological model nowadays. ΛCDM is a Big Bang model which includes some additions. Let us count the most important additions:

- The inflation to explain the flatness, homogeneity, isotropy and non-observability of some exotic matter (magnetic monopoles etc).
- The model has the Λ term in the Einstein equations. The constant allows the current accelerating expansion of the Universe. The cosmological constant can be described in term of Ω_Λ, the fraction of the critical density of cosmological constant. Currently, its value is $\Omega_\Lambda \simeq 0.74$.
- The model includes CDM: cold, non-baryonic and collisionless matter. This component makes up 0.22 of the critical density of the current Universe. Baryonic matter makes up the remaining 0.04. Electrons, photons, neutrinos and other light particles form a minor fraction of the total density.
- The model assumes a nearly scale-invariant spectrum of primordial perturbations.
- Also, the model assumes no observable topology, so the universe should be much larger than the observable particle horizon. Two last predictions are strongly connected to the primordial inflation.

However, the ΛCDM model is far from being a complete model of the Universe. The model says nothing about the fundamental physical origin of dark matter, cosmological constant and the mechanism behind the inflation. As we can see, all the questions listed are (or might be) strongly related to particle physics. Most urgently, CDM is a clear missing building block in particle physics and it clearly directs us beyond the Standard Model. Also, dark energy can find an answer in particle physics. Particle physics behind inflation is a mystery, but there are many suggestions, which are able to connect it to SUSY models, for example.

Chapter 3

Evidence of physics beyond the Standard Model

3.1 Introduction

The present chapter is focused on the experimental effects not described by the Standard Model of particle physics. We will list some most burning questions in experimental particle physics and observational cosmology which do not fit in the Standard Model: matter-antimatter asymmetry in the observed Universe, neutrino mass, cold dark matter candidates and muon anomalous magnetic moment.

3.2 Matter-antimatter asymmetry

If we follow the beautiful idea of symmetric laws of Nature and an equilibrium state of the Universe then matter and anti-matter should be balanced very accurately. The reason is obvious, if the Universe cools down at the annihilation temperature of leptonic and baryonic matter then all matter should annihilate and the Universe should be filled mostly by photons nowadays. However, we are lucky to exist, as in our Universe we can see clear asymmetry, matter domination over anti-matter.

First, to measure the asymmetry we use the fact that background photons originate from the annihilation. We define *a parameter of asymmetry*:

$$\eta' = \frac{n_B - n_{\bar{B}}}{n_\gamma}, \tag{3.1}$$

where n_B is the total number of baryons, $n_{\bar{B}}$ is the total number of antibaryons and n_γ is the total number of photons. Equivalently, we can use averaged spatial densities of baryons, antibaryons and photons. The photon density can be measured from CBR in quite high accuracy.

Measuring baryonic density is much more tricky. First, we can measure radiation from baryonic matter, for example, light from stars, X-rays from cosmic gas clouds etc. Unfortunately, baryonic matter can easily remain hidden to observation. For example, one can imagine small dark compact objects (e.g. brown dwarfs, neutron stars, black holes) or ionized gas clouds which can easily escape our observations. Fortunately, nowadays we have reasonable theories about star and galaxy evolution and we can develop some bounds for the amount of invisible baryonic matter. In addition, we can develop some limits to combine gravitational lensing and other cosmological data to propose the amount of baryonic matter. To calculate density of baryonic matter we have to average the observed baryonic mass over the large volumes in megaparsec scale. It adds a new possible source of error through the measurements of cosmological distances. However, the astronomers have done great improvements in the methodology of the measurements of cosmological distance. Alternatively, Big Bang nucleosynthesis gives an accurate value of η'. So, in summary, the combined value of η' is 6.0965 ± 0.2055 at 68% CL [20].

As it is described in Chapter 2, photonic density is behaving in time differently than baryonic density and the defined η' is not constant in time. It is more convenient to define a constant measure of the asymmetry, where the density of entropy is used

$$\eta = \frac{n_B - n_{\bar{B}}}{s}, \tag{3.2}$$

$$s = \alpha(T^3) n_\gamma. \tag{3.3}$$

The value of function $\alpha(T^3)$ is at 7.04 in the present Universe and the value of asymmetry parameter is between $2.6 \cdot 10^{-10} < \eta < 6.2 \cdot 10^{-10}$ [20].

Can we create that asymmetry in a natural way in particle physics and cosmology? First, to create the asymmetry from a supposed initial condition of equilibrium (or at least very close to equilibrium), three so called *Sakharov conditions* must be satisfied:

- CP- or P-symmetry violation,
- baryon number B violation,
- non-equilibrium processes in the cosmological history of the Universe.

The period of the generation of baryonic matter is called *baryogenesis*. We will analyze the conditions step by step below.

3.2.1 CP-violation

We described in Section 2.2 the C- and P-symmetries are violated maximally in the Nature. Physicists were surprised when in 1964, J. Cronin and V. Fitch provided clear evidence in kaon decays that the combined symmetry of C and P, CP-symmetry, can be broken too. Unlike maximal P- and C-violation, CP-violation is a very small effect in weak interaction processes. The CP-violation measurements have shown that possible violation phase is far too small in quark sector and clearly too small in weak sector to explain the baryon-antibaryon asymmetry in the observed Universe. The experimental results in lepton sector suggest that CP-violation phase can be reasonably large in neutrino mixing matrix to guarantee sufficient value of CP-violation through so called *leptogenesis* [31].

For a mathematical note, a theorem derives the preservation of CPT-symmetry for all of physical phenomena assuming the correctness of basic quantum laws. Specifically, the CPT theorem states that any Lorentz invariant local quantum field theory with a hermitian Hamiltonian must have CPT-symmetry. The CPT theorem appeared in the work of J. Schwinger in 1951 and later, more explicitly, in the work of G. Lüders and W. Pauli and independently by J. S. Bell.

3.2.2 Baryon number violation

To follow the Sakharov conditions for baryogenesis, Nature has to violate baryon number conservation. In the present stage of experimental particle physics we have no evidence of particle interactions where baryon number is strongly enought violated.

At first glance the property of B conservation is unnatural in the Standard Model. For example, in QCD of the Standard Model a term of B violation is able to arise very naturally in the Lagrangian:

$$L = -\frac{1}{4} tr F_{\mu\nu} F^{\mu\nu} - \frac{1}{32\pi^2} n_f g^2 \theta F_{\mu\nu} \tilde{F}^{\mu\nu} + \bar{\psi}(i\gamma^\mu D_\mu - m e^{i\theta'} \gamma^5)\psi, \quad (3.4)$$

where F is the gluon field tensor, g is the strong coupling constant and ψ is the quark field. For a nonzero QCD θ-angle and the chiral quark mass phase θ' one expects the CP-symmetry to be violated. In the strong sector the effect would be reasonably strong compared to the effect of weak interaction. Despite that no violation has been discovered in the strong sector. The zero value of the phase is an example of fine-tuning. A solution that has been proposed by Peccei and Quinn [32]. The solution proposes θ as a dynamical field, the related symmetry is broken and a new scalar particle arises called *axion* and it has a tiny mass due to breaking.

Alternatively to direct baryogenesis, a wide community of physicists has accepted the idea that baryogenesis appears through leptogenesis [31]. Leptogenesis is based on the effects of neutrino physics and it offers a quite minimal mechanism for the generation of asymmetry between leptons and antileptons. The Standard Model is able to provide a mechanism to create baryon asymmetry from lepton asymmetry above the energy scale of 1 TeV. *Sphalerons*, non-perturbative topological configurations of gauge fields in the Standard Model can convert leptons into baryons and vice versa. Therefore, baryon asymmetry can arise from lepton asymmetry through sphaleron effects.

3.2.3 Non-equilibrium processes

The last Sakharov condition states that non-equilibrium processes are needed to fortify the matter-antimatter asymmetry. As we know from cosmology, the Universe, at least most of time in its history, has been very close to thermal equilibrium. For example, the spectrum of the CMB is the most perfect blackbody spectrum available in Nature. It means that the Universe had to be very close to thermal equilibrium in the recombination, 10^5 years after the Big Bang. Also, The BBN data provide evidence that the Universe was very close to thermal equilibrium 2-3 minutes after the Big Bang. On the other hand, a non-equilibrium stage is clearly needed for baryogenesis.

Let us present a simple example which can easily carry out the core of the main idea. One can suppose there exists a massive particle which has two decay channels, one to fermion and boson and one to antifermion and boson. The following diagrams represent the "chemical chain" of the processes:

$$N \underset{k_f}{\overset{k_b}{\rightleftharpoons}} \ell + \bar{H}, \tag{3.5}$$

$$N \underset{\bar{k_b}}{\overset{\bar{k_b}}{\rightleftharpoons}} \bar{\ell} + H. \tag{3.6}$$

Here k marks the reaction rate constants, k_f is the forward reaction rate and k_b is the backward reaction rate. From the point of view of thermodynamics the reaction rate k can depend on some parameters: the cross-section of the process σ, temperature T and the mass of decay products. So, for right side components $\ell + \bar{H}$ or $\bar{\ell} + H$, the back reaction rate is the function $k_b = k(\sigma_b, T, m_\ell, m_H)$. The right side of the process is a particle decay, therefore it is temperature independent, $k_b = k(\sigma)$.

A good simplification from chemical kinetics is

$$k_b(\sigma_b, T, m_\ell, m_H) = a(\sigma_b) \cdot b(T, m_\ell, m_H). \tag{3.7}$$

The same simplification can be written for the forward process from the particle N decay width

$$k_f(\sigma_f, m_N) = a(\sigma_f) \cdot f(m_N). \tag{3.8}$$

From validity of the Lorentz and CPT symmetry follows for the cross-sections $\sigma_f = \sigma_b = \sigma$ and $\bar{\sigma_f} = \bar{\sigma_b} = \bar{\sigma}$. As the environment is in thermodynamical equilibrium, $T = \text{const}$. Also, we expect that $m_\ell = m_{\bar{\ell}}$ and $m_Y = m_{\bar{Y}}$. From CP-violation biased for matter follows $\sigma > \bar{\sigma}$, which means that for the reaction rates $k > \bar{k}$.

Now, let us approximate the concentrations for ℓ and $\tilde{\ell}$. We apply the equation of chemical consentrations for the matter chain

$$\frac{[\ell][\bar{H}]}{[N]} = \frac{k_f}{k_b} = \frac{\sigma \cdot f(m_N)}{\sigma \cdot b(T, m_\ell, m_H)} = \frac{f(m_N)}{b(T, m_\ell, m_H)} \tag{3.9}$$

and for the antimatter chain

$$\frac{[\bar{\ell}][H]}{[N]} = \frac{\bar{k_f}}{\bar{k_b}} = \frac{\bar{\sigma} \cdot f(m_N}{\bar{\sigma} \cdot b(T, m_\ell, m_H)} = \frac{f(m_N)}{b(T, m_\ell, m_H)}, \tag{3.10}$$

where $[i]$ marks the concentration of the corresponding particle type i. So, on the current approximation level we see that the total number of matter particles and antimatter particles are equal in the case of thermodynamical equilibrium.

How can the asymmetry be provided if we do not violate Lorentz and CPT symmetry? It can be done if we have a situation of thermodynamical nonequilibrium. In cosmology it can be done when the expansion (and cooling) of the Universe ruins thermodynamical equilibrium as it was described in the last section of Chapter 2. The reaction rate which generates baryon asymmetry must be less than the rate of expansion of the Universe. In this situation the particles and their antiparticles are not able to achieve thermal equilibrium due to rapid expansion which decreases the annihilation rate of particle-antiparticle pairs.

3.3 Neutrino mass

Until the 1990s the idea of massless neutrino was widely accepted in physics community. Thus, in the Standard Model all the generations of neutrino were included as massless fields. Despite that, already in the 60s the Homestake experiment had shown evidences of electron neutrino deficit in the flow of solar neutrinos until the 70s. The problem puzzled the scientists through many decades; it even had a name, the *solar neutrino problem.* As the nuclear production of solar neutrinos depends very sensitively on the core temperature of the Sun there was a window to vary some parameters in the standard solar model. So, it was difficult to give the final answer for the question of neutrino masses. However, the standard solar model and oscillation experiments tighten the bounds for the neutrino masses year by year.

In the 90s numerous neutrino experiments were started to study different kind of neutrino processes:

- *oscillation experiments*: the new solar and atmospheric neutrino experiments (GALLEX, HOMESTAKEIODINE, Kamiokande followed by Super-Kamiokande, SAGE etc); the nuclear reactor neutrino (CHOOZ, KamLAND, Palo Verde etc) and accelerator neutrino (K2K, LSND, NOMAD etc) experiments started,
- *direct neutrino mass experiments*: mainly β-decay electron energy spectroscopy experiments,
- *double β-decay experiments*: germanium double β-decay experiments,

At same time the standard solar model had been tightened to the limit where it was impossible to explain the lack of solar neutrinos by playing with the parameters of the model. So, in the beginning of the new millennium it was clear that there have to be neutrino oscillations. Nowadays a number of new experiments are starting focused on more specific topics: mainly short- and long-baseline accelerator experiments to specify oscillation parameters; more accurate direct mass and double β-decay experiments and, finally, neutrino astronomy and geology experiments. The last ones are demonstrations of a huge step in the experimental technology in neutrino physics. Neutrino astronomy can open a new exiting window studying supernova and probably core processes in the Galaxy. Some reviews with long lists of neutrino experiments can be found from [33].

Adding massive fields for neutrinos to the basic framework is not complicated. As neutrino is an uncharged particle there are two ways to add them to the model: through "standard" Dirac mechanism or through "non-standard" Majorana mechanism. Probably, the beginning double β-decay experiments can give answer about the neutrino type: is it the Dirac or Majorana type. A detailed description will follow in the next chapter.

The idea of neutrino oscillations was proposed by Bruno Pontecorvo in 1957. The idea has an analogy with a phenomena observed in neutral kaon systems. The quantitative theory was developed by Pontecorvo in 1967 and, one year later, when the solar neutrino deficit was first observed, it was followed by the famous paper "Neutrino astronomy and lepton charge" by Gribov and Pontecorvo published in 1969. Neutrino oscillation is a simple quantum mechanical mechanism to explain flavor changes between the particles with different flavor.

Neutrino oscillations are explained as a mismatch between the flavor and mass eigenstates of neutrinos. In the case of neutrino with mass, there are three (or more) neutrino mass eigenstates, ν_i, that are the analogues of the charged-lepton mass eigenstates, ℓ_i. Let i denote pure mass states and α below denote flavor states. If leptons mix, for example, the W boson couples to a charged lepton and a neutrino can couple any charged-lepton mass eigenstate ℓ_α to any neutrino mass eigenstate ν_i. Leptonic W^+ decay can yield a particular ℓ_α with any ν_i. The amplitude for the combination $\ell_\alpha^+ + \nu_i$ is $U_{\alpha i}^*$. The relationship between the eigenstates is given by the simple linear equation as

$$|\nu_\alpha\rangle = \sum_i U_{\alpha i}^* \, |\nu_i\rangle \, , \tag{3.11}$$

$$|\nu_i\rangle = \sum_\alpha U_{\alpha i} \, |\nu_\alpha\rangle \, . \tag{3.12}$$

$U_{\alpha i}$ is the *Maki-Nakagawa-Sakata* or *MNS matrix* (also called *lepton mixing matrix*). In the quark sector the CKM matrix presents similar mixing between flavor and mass eigenstates.

A simple plain-wave solution describes the propagation of the mass states of a neutrino in free space

$$|\nu_i(t)\rangle = e^{-ip\cdot x} \, |\nu_i(0)\rangle \, , \tag{3.13}$$

where t is the time interval from the start of the propagation, $p = (E, \vec{p})$ is the 4-momentum of the particle and $x = (t, \vec{x})$ is the 4-coordinate from the current position of the particle relative to its starting position. For experimental neutrinos we may always use the ultrarelativistic limit $|\vec{p}| =$

$p \gg m$. Dropping the phase factors and using a simplification $t \sim L$, where L is the travel distance, we approximate

$$|\nu_i(L_t)\rangle = e^{-i\frac{m^2}{2E}L} |\nu_i(L_0)\rangle . \tag{3.14}$$

The approximation works well for the experimental cases. The typical experimentally "visible" region for neutrinos is above MeV energy, for example

- nuclear (solar or reactor) neutrinos, in MeV scale
- accelerator neutrinos, up to TeV scale
- possible cosmical high energy neutrinos, up to PeV and EeV scale

In the region between keV to MeV no intensive sources of neutrinos are known. Very low energy cosmological background neutrinos are unreachable for direct experimental studies nowadays. (Some indirect studies are proposed, for example, the absorption line in the energetic neutrino flow due to the background neutrinos at Z-resonance [34]. A longer analysis of the different possibilities is presented in [35]). At the MeV scale neutrinos have already clearly reached ultrarelativistic limit: if their mass is on the order of 1 eV and energy is on the order of MeV then the Lorentz factor is 10^6 and our approximation should work well.

We see in Eq. (3.14) that the different mass states propagate at different speeds. The transition probability $\nu_\alpha \to \nu_\beta$, where a neutrino with an initial flavor α translates to a later observed flavor β, can be calculated from the equation

$$P_{\alpha\to\beta} = |\langle\nu_\alpha(L_0)|\nu_\beta(L_t)\rangle|^2 = \left|\sum_i U^*_{\alpha i} U_{\beta i} e^{-i\frac{m^2}{2E}L}\right|^2 . \tag{3.15}$$

If neutrinos travel through matter, their interactions can modify their propagation and the equation above has to be modified. The interplay between neutrino transit oscillations and passable matter accounts for a particular flavor change behavior and it is known as the Mikheyev-Smirnov-Wolfenstein (MSW) effect [36, 37].

In the next step we are interested the structure of the MNS matrix. First, what is the dimension of the matrix? It would be natural to propose 3×3 matrix as there are three flavor generations in the Nature. However, in general there is no clear reason why more than 3 neutrinos cannot be presented in Nature. At the moment, the W and Z experiments have shown that only three types of neutrino (which correspond to the three generations in Nature) participate in the processes of weak interaction. So, if there are additional neutrinos in Nature, they are sterile. Nowadays only a slight experimental window exists for a possibility that a sterile mass eigenstate (or eigenstates) is present [38]. As the sterile neutrino does not couple through weak interaction it is reachable only in the oscillation experiments and/or in the observable gravitational effect in cosmology. In the close future the MiniBooNE and some proposed future experiments should give a final enough answer to the question. In the next subsection we will present a longer discussion for the number of neutrino types.

In the following discussions we will assume three flavor generations and no sterile neutrino. Then the MNS matrix is a 3×3 unitary matrix. In general parametrization of $(U_{\alpha i})$ is up to us, but a convenient version is the following:

$$(U_{\alpha i}) = \begin{pmatrix} c_{12}c_{13} & s_{12}c_{13} & s_{13}e^{-i\delta} \\ s_{12}c_{23} - c_{12}s_{23}s_{13}e^{i\delta} & c_{12}c_{23} - s_{12}s_{23}s_{13}e^{i\delta} & s_{23}c_{13} \\ s_{12}s_{23} - c_{12}c_{23}s_{13}e^{i\delta} & c_{12}s_{23} - s_{12}c_{23}s_{13}e^{i\delta} & c_{23}c_{13} \end{pmatrix} \times U_M, \tag{3.16}$$

where U_M is

$$U_M = \mathrm{diag}(e^{\frac{1}{2}i\alpha_1}, e^{\frac{1}{2}i\alpha_2}, 1). \tag{3.17}$$

Historically, ν_1 and ν_2 are called the *solar pair*, where $m_1 > m_2$ and the *isolated mass state*, ν_3, is either lighter or heavier than the solar pair, $m_1 \sim m_2 \ll m_3$ or $m_1 \sim m_2 \gg m_3$. Figure 3.1 and 3.2 present the experimental structure of the mass differences. $c_{ij} = \cos\theta_{ij}$ and $s_{ij} = \sin\theta_{ij}$, where θ_{ij} are mixing angles and ij marks the combinations: 12, 23 and 13. The parameters δ, α_1 and α_2 are CP violation phases. In the case of no CP violation the parameters are zero. The α phases are presented only in case of Majorana neutrinos; they are known as *the Majorana phases.* Together with the three neutrino masses, in total there are seven flavor parameters in the neutrino sector in the case of Dirac and nine parameters in the case of Majorana. Apart from α, which has no quark analogues as quarks are charged, the parametrization of the MNS matrix is identical to the quark mixing matrix.

Having now parametrized the mixing matrix we could try to simplify Eq. (3.15). Fortunately, in a typical experimental case it is sufficient to approximate a 2×2 mixing matrix. For example, in the transition $\nu_\mu \to \nu_\tau$ of atmospheric mixing the electron neutrino plays almost no role in this case. It is also valid in the solar case of $\nu_e \to \nu_x$, where ν_x is a superposition

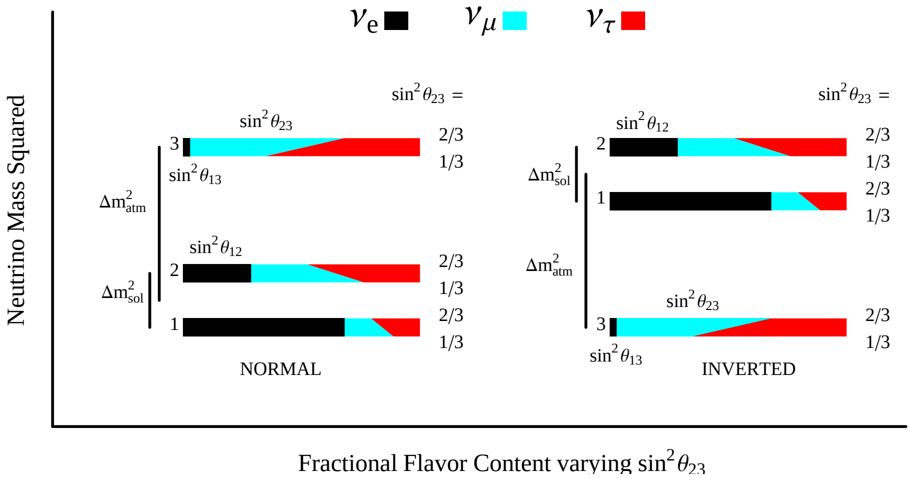

Figure 3.1: The probability range of finding the flavor α in the i-th mass eigenstate. It is shown for the two different mass hierarchies if $\sin^2\theta_{23}$ varies over its allowed range at the 90% C.L. The bottom of the bars is for the minimum allowed value of $\sin^2\theta_{23} = 1/3$ and the top of the bars is for the maximum value of $\sin^2\theta_{23} = 2/3$. The other mixing parameters are held fixed, $\sin^2\theta_{12} = 0.30$, $\sin^2\theta_{13} = 0.03$ and $\delta = \pi/2$. The figure is adapted from [39].

state of ν_μ and ν_τ. Two incidents favor us: two of the mass states are very close in mass compared to the third one (see Figure 3.1 and 3.2) and the mixing angle θ_{13} is very small. The simplified probability is

$$P_{\alpha\to\beta,\alpha\neq\beta} = \sin^2(2\theta)\sin^2(\frac{\Delta m^2 L}{4E}), \tag{3.18}$$

where the unitary U is parametrized as

$$U = \begin{pmatrix} \cos\theta & \sin\theta \\ -\sin\theta & \cos\theta \end{pmatrix}. \tag{3.19}$$

In the next subsections we will finalize the first story of neutrinos with the experimental bounds of the physical neutrino properties. We will present some following bounds in the state of year 2007: number of light neutrino species and bounds of neutrino masses from different experiments and observations.

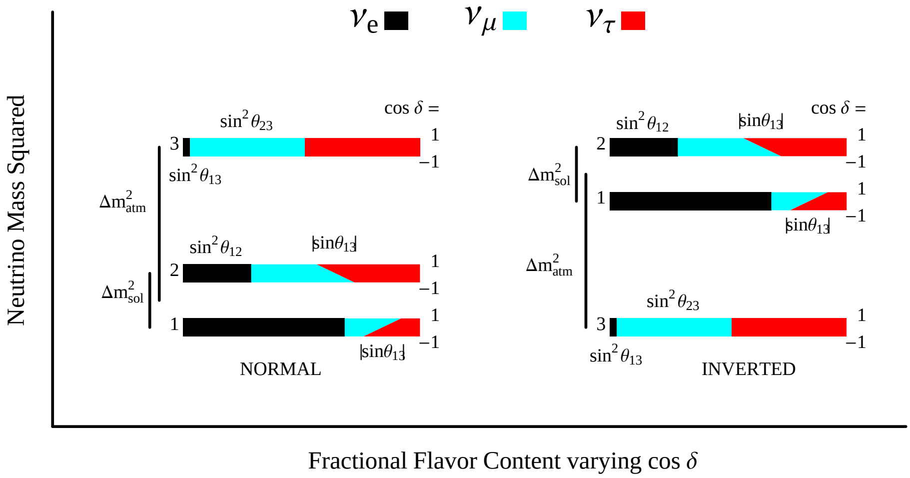

Figure 3.2: The probability range of finding the flavor α in the i-th mass eigenstate if the CP-violating phase δ is varied. The minimum allowed value of $\cos\delta = -1$ is shown in the bottom of the bars and the maximum value of $\cos\delta = 1$ is shown in the top of the bars. The other mixing parameters are held fixed, $\sin^2\theta_{12} = 0.30$, $\sin^2\theta_{13} = 0.03$ and $\sin^2\theta_{23} = 0.50$. The maximum to minimum variation of the fractional flavor content of μ or τ in mass eigenstates 1 or 2 is very close to $\sin\theta_{13}$. The only non-sensitive parameter in the picture is the sign of $\sin\delta$. The figure is adapted from [39].

3.3.1 Number of light neutrino species

The most precise measurements of the number of light weakly interactive neutrino types come from studies of width of Z boson production at the e^+e^- colliders. The data presented here originates from the collective report of the ALEPH, DELPHI, L3, OPAL, SLD Collaborations, the LEP Electroweak Working Group and the SLD Electroweak and Heavy Flavor Groups from the summer of 2006 [40].

The lightness of neutrino is defined to be less than half of Z mass. The number of light neutrino types, N_ν, can be calculated from the total width of Z, Γ_Z,

$$\Gamma_Z = \Gamma_{\rm inv} + \Gamma_{\rm had} + \sum_{\ell=e,\mu,\tau} \Gamma_{\ell^+\ell^-}, \tag{3.20}$$

where Γ_{inv} is the invisible width of Z, Γ_{had} is the hadronic fraction of the width and the last sum marks the fraction of charged leptons. The number of light neutrino types comes from the partial widths

$$\Gamma_{\text{inv}} = N_\nu \Gamma_{\nu\bar{\nu}}, \tag{3.21}$$

where assuming only the Standard Model particles contribute in the invisible width.

In practice the ratio $\Gamma_{inv}/\Gamma_{\ell\ell}$ is experimentally determined with higher precision than Γ_{inv}. In addition, the Standard Model prediction of $\Gamma_{\nu\bar{\nu}}/\Gamma_{\ell\ell}$ is more independent from the unknown Standard Model parameters. So, in order to reduce the model dependence, the more independent combination can be used

$$N_\nu = \frac{\Gamma_{\text{inv}}}{\Gamma_{\ell\ell}} \frac{\Gamma_{\ell\ell}}{\Gamma_{\nu\bar{\nu}}}, \tag{3.22}$$

where the Standard Model value of $\Gamma_{\ell\ell}\Gamma_{\nu\bar{\nu}} = 1.99125 \pm 0.00083$. The uncertainty arises mostly from variation of the experimental uncertainty of top quark mass, $m_t = 178.0 \pm 4.3$ GeV, and because of the unknown Higgs mass, in the case the bonds 100 GeV $< m_H <$ 1000 GeV are assumed. The value of $\Gamma_{inv}/\Gamma_{\ell\ell} = 5.943 \pm 0.016$. Here the lepton universality is assumed. Finally, the according number of the neutrino types is

$$N_\nu = 2.9840 \pm 0.0082. \tag{3.23}$$

It is also possible that the number of massive neutrino states is larger than the number of flavor neutrinos. At the moment the sterile neutrino species can be observed only in the cosmological observations or oscillation experiments. The results of the Liquid Scintillator Neutrino Detector (LSND) have shown some evidence of a sterile type neutrino [41]. LSND measured the appearance of electron antineutrinos in a muon antineutrino beam. The new MiniBooNE experiment is currently testing the results of LSND [42]. In April 2007 the MiniBooNE collaboration published the first results [38]. The analysis of the MiniBooNE collaboration is performed within a two neutrino appearance-only $\nu_\mu \to \nu_e$ oscillation model which uses ν_μ events to constrain the predicted ν_e rate. Only than oscillations between these two species have been observed and no effects of sterile neutrino have been found in the case. So, in this work, we will mainly consider the three-neutrino case.

Also, the cosmological data predicts the number of neutrino species. The main bound of the number comes from the relativistic degrees of freedom at the recombination and BBN. Both CMB and the abundance of primordial elements depends very sensitively on the relativistic energy density

$w_{\rm eff}$ at the recombination and BBN. It is possible to write $\omega_{\rm eff}$ as a sum

$$\omega_{\rm rel} = \omega_\gamma + N_{\rm eff} \cdot \omega_\nu, \tag{3.24}$$

where ω_γ is the energy density of photons, ω_ν is the energy density of one active neutrino species and $N_{\rm eff}$ is the effective number of neutrino species. Also we know from the last chapter that the density of radiation domination epoch is

$$\rho = \frac{\pi^2}{30} T_\gamma^4 \left[2 + 2 \times \frac{7}{8} N_{\rm eff} \left(\frac{T_\nu}{T_\gamma} \right)^4 \right], \tag{3.25}$$

where T_γ and T_ν are the photon and neutrino temperatures respectively.

From BBN the value of $N_{\rm eff}$

$$N_{\rm eff} = 3.1^{-1.2}_{+1.4}, \tag{3.26}$$

see e.g. [43]. Figure 3.3 presents some measurements of the He mass fraction from BBN which is sensitive to $N_{\rm eff}$. However, we should be careful comparing $N_{\rm eff}$ at the times of BBN and at times of CMB. For example, some unknown (but relevant) systematics can affect current astrophysical determinations of primordial elements (e.g. [43]). BBN at the energy $\sim$MeV and the recombination at the energy $\sim$eV may have different unknown physical "background" (for example, some decaying exotic particles etc). Thus the energy density of relativistic species may easily change between the time of BBN and the recombination. On the other hand BBN itself has strong restrictions for exotic content.

The combined value of $N_{\rm eff}$ from WMAP and other experiments in the linear regime is

$$1.1 < N_{\rm eff} < 4.8 \text{ (95\% C.L.)} \tag{3.27}$$

with a best-fit value of 2.6. Together with the data from smaller scales (the Lyman-α forest) the value is

$$2.2 < N_{\rm eff} < 5.8 \text{ (95\% C.L.)} \tag{3.28}$$

with 3.8 as the best fit. The upper shift appears due to the reason that the Lyman-α data has some inconsistencies with that inferred from CMB. For example, for longer discussion see [45].

Also, it is possible to predict directly from CMB and LSS measurements the total mass of the neutrino mass states

$$M_\nu = \sum_{i=1,2,\ldots N_\nu} m_{\nu i}, \tag{3.29}$$

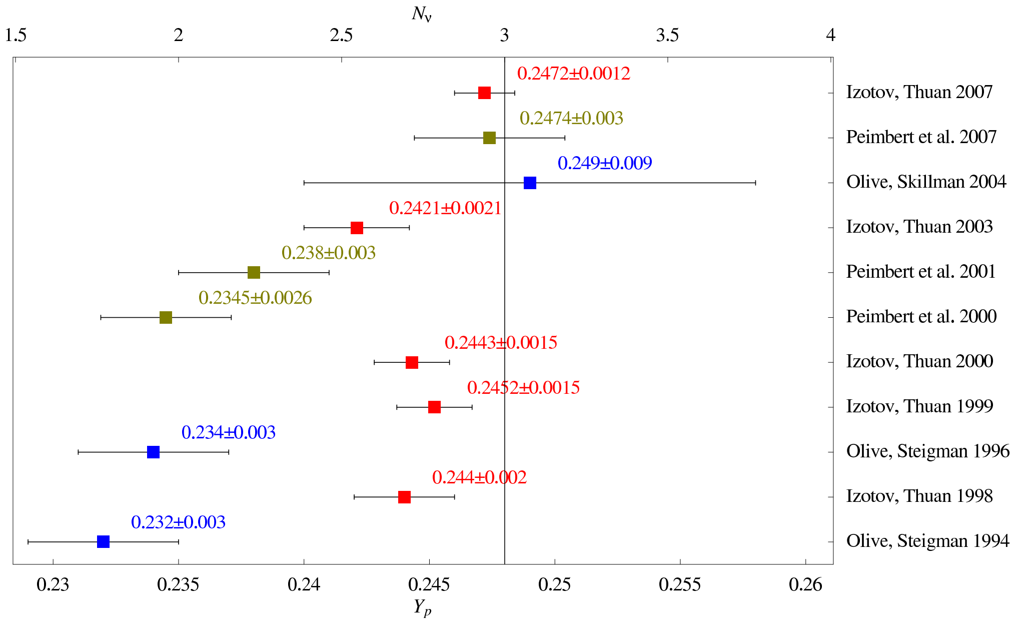

Figure 3.3: Recent measurements of the He^4 mass fraction Y_p. The upper axis shows the corresponding number of neutrinos at BBN. The later measurements of Y_p have relaxed around $N \simeq 3$. The figure is adapted from [44].

where $m_{\nu i}$ is the mass of a neutrino mass state and N_ν is the total number of the mass states. Hypothetically, if the mass of weakly interactive neutrinos is directly measured more precisely than 0.1 eV it is possible to predict the number of neutrino types (the standard cosmological model is assumed) [46, 47].

3.3.2 Neutrino mass bounds

Three possible hierarchies of the neutrino mass are allowed from the oscillation measurements:

1. *Normal hierarchy*, $m_1 < m_2 \ll m_3$. From the oscillation data, $\Delta m_{23}^2 \equiv m_3^2 - m_2^2 > 0$ and $m_3 \simeq \sqrt{m_{23}^2} \simeq 0.03 - 0.07$ eV and the solar neutrino oscillation involves the two lighter levels. The mass of the lightest neutrino is unconstrained in this case. If we set $m_1 \ll m_2$

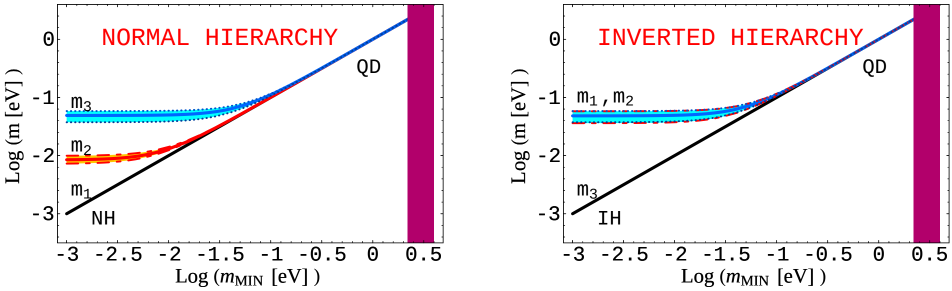

Figure 3.4: Three neutrino masses as a function of the lightest mass for the normal (left plot) and inverted (right plot) hierarchy. We see that at 0.1 eV of the lightest mass the mass states degenerate. The figure is adapted from [33].

then the value of $m_2 \simeq 0.008$ eV.

2. *Inverted hierarchy*, $m_1 \simeq m_2 \gg m_3$ with $m_1 \simeq m_2\sqrt{m_{23}^2} \simeq 0.03-0.07$ eV. In this case, solar pair oscillation takes place between the heavier levels and $m_{23}^2 \equiv m_3^2 - m_2^2 < 0$. Thus we have no information about m_3 except that its value is much less than the other two neutrino masses.

3. *Degenerate neutrinos* $m_1 \simeq m_2 \simeq m_3$.

However, the oscillation data cannot give the absolute mass bounds. Figure 3.4 shows the behavior of the absolute masses as a function of the lightest mass. In the present tritium β-decay, neutrinoless double β-decay and cosmology can give the best bounds of neurtino mass.

At the moment, the strongest upper bound on the neutrino mass scale comes from cosmology [20, 46]. The cosmological mass limits are based on the implications of neutrino masses for clustering of matter, in particular the fact that neutrinos can free-stream out of density perturbations and impede structure formation on small scales if they are a significant fraction of the dark matter. At the moment the upper bound combined from most cosmological observations is

$$M_\nu = \sum_i m_{\nu i} < 1.43 \text{ eV}, \tag{3.30}$$

16

where i counts the mass states of neutrinos [46–48]. Some authors have proposed that the new *weak lensing* data can improve the mass bound as $\Delta m_\nu \sim 0.03$ eV and the number of neutrinos N_ν as $\Delta N_\nu \sim 0.08$ [49].

The cosmological neutrino mass limits involve several assumptions. Naturally, the ΛCDM is assumed: the Friedmann-Robertson-Walker metrics of the Universe, general relativity describes the dynamics of the Universe, the primordial power spectrum of density perturbations is a scale-free power-law and dark energy is a cosmological constant. Second, the upper limit depends strongly on the combination of the cosmological data sets used for analysis.

The direct upper bound for the mass of electron neutrino comes from tritium β-decay experiments Mainz [50] and Troitsk [51]. It is presently

$$m_\beta \leq 2.2 \text{ eV}. \tag{3.31}$$

The KATRIN experiment [52] proposes the sensitivity down to

$$m_\beta \geq 0.2 \text{ eV}. \tag{3.32}$$

If the result is positive it clearly implies degenerate spectrum. On the other hand a negative result would be a very useful constraint, especially when it is combined with cosmological data.

The β-decay studies are sensitive to neutrino masses regardless of whether the neutrinos are Dirac or Majorana particles. An additional sensitive probe of the neutrino masses is a study of neutrinoless double beta decay, a nuclear process

$$2X^n_m \to 2Y^n_{m+1} + 2e^- + 0\bar{\nu}_e. \tag{3.33}$$

The decay rate is potentially measurable only if neutrino is a Majorana fermion. Also, $m_{\rm ee} = \sum_i U_i^2 m_{{\rm e}i}$ should be large enough [53, 54] and/or there should exist any new lepton number violating interactions [55, 56]. The present best upper bounds on double β-decay lifetimes come from the Heidelberg-Moscow [57] and the IGEX [58] experiments. The combined upper limit [59] is

$$m_{\beta\beta} \leq 0.9 \text{ eV}. \tag{3.34}$$

However, if $m_{\beta\beta}$ is very small and there are new lepton number violating interactions then neutrinoless double beta decay will measure the strength of the new interactions rather than neutrino mass. For example, doubly charged Higgs fields or R-parity violating interactions can strongly influence the value of $m_{\beta\beta}$. Thus, we must be very careful to interpret a nonzero signal in double β-decay experiments. The positive results do not automatically mean that a direct measurement of neutrino mass has been made. To distinguish between the neutrino mass effect or a reflection of new interactions we have to supplement double β-decay results with collider searches for these new interactions. For example, LHC and double beta experiments play complementary roles in the case. We will touch upon the topic in some of the next chapters.

3.4 Cold dark matter

By definition dark matter is a component of gravitational matter that does not emit or reflect electromagnetic radiation. A main candidate of dark matter is a weakly interacting particle or particles. We can separate dark matter into two components, cold dark matter (CDM) and hot dark matter (HDM). Also, we can define a component between them, warm dark matter (WDM). Thus CDM is an unrelativistic component of dark matter and HDM is a relativistic component of dark matter. HDM can redistribute freely and it forms a quite homogeneous background for CDM. In the early Universe, after the end of radiation domination epoche, the CDM rich perturbations were the seeds of the density perturbations that began to grow. Thus, the spatial distribution of CDM correlates strongy with the spatial distribution of galaxies and superclusters of galaxies. On the contrary, HDM sweeps away dense regions.

Thus we assume the existence of dark matter from the gravitational effects of visible matter and from the distribution of fluctuations of CMB. Alternatively, there is some effort to modify the theory of General Relativity or the Newtonian dynamics (e.g. the MOND models [60]), but as dark matter plays different roles in the different spacial and time scales the modified theories are rather complicated and unpopular. The CMB measurement of WMAP3 shows that CDM involves 23% from the total density of the Universe [20].

The most popular solution of the dark matter problem supposes that it is composed of some weakly interactive particles. Alternatively, dwarf and neutron stars or black holes are suggested as a candidate of CDM, but it needs a rather strong review of star evolution theory. The heavy object should behave as a small gravitational lens. Searches for such gravitational lenses have shown that there is not enough of that kind of heavy objects to form a significant component of CDM. So, weakly interactive particles remain the main candidate for dark matter. For example, light neutrinos would be a candidate for HDM. CDM needs the existence of at least one species of *weakly interactive massive particle*, WIMP.

Unfortunately, the Standard Model does not give any candidate for CDM. The extensions of the Standard Model give many candidates. However, at the present stage there is no clear evidence for them in terrestrial particle physics experiments. LHC and other future collider experiments can provide some candidates for CDM (and rule out other). Also, there are numerous experiments which are searching for CDM particles directly from the Galactic background.

Cosmological observations do not give any direct mass or cross-section bound for the candidate of CDM. We can develop some bounds from particle and statistical physics. The upper mass bound comes from the *unitarity condition*. The condition is valid only in the case of thermal relics. For example, massive particles produced from some possible phase transitions in the early Universe can easily pass the condition. However, the unitarity condition is based on the existence of a maximum annihilation cross section $\sigma_{\max}$ for a particle with the mass m. From $\sigma_{\max}$ we can set the upper bound for mass [61]. Nowadays, using the WMAP3 constraint on $\Omega_{\rm DM}h^2$ the upper bound of the mass is

$$m_{\rm DM} < 34 \text{ TeV}. \tag{3.35}$$

Also, we notice here that the unitarity condition is not valid in the case of a composite object.

We do not introduce all possible candidates for WIMP here. Let us just mention that in some neutrino models the heavy neutrinos can be the candidates for WIMP. For example, a nice review of all the possible candidates in particle physics can be found in Ref. [62].

3.5 Muon anomalous magnetic moment

The magnetic moment $\vec{M}$ is given by

$$\vec{M} = g\frac{q}{2m}\vec{S}, \tag{3.36}$$

where g is the dimensionless parameter called *gyromagnetic ratio*, q is the charge, m is the mass and $\vec{S}$ is the spin of particle. In fact, we are interested in the measurement of g. The gyromagnetic ratio g has been a challenging characteristic of particles through the history of quantum physics. It is due to two main reasons.

First, it is possible to measure the ratio with high accuracy with a rather small experimental setup. Naturally, the word small should be evaluated carefully in the current context. It is smaller than high energy accelerators and universal detector experiments.

Second, the gyromagnetic ratio has been a very sensitive parameter for new physics to date. First of all, in semiclassical case the ratio should be 1. The Dirac equation in quantum field theory predicts that the ratio is 2 and, actually, it is very close to 2. Quantum loop effects cause a small calculable deviation from $g = 2$, it is usually parametrized by the *anomalous magnetic moment*

$$a = \frac{g-2}{2}. \tag{3.37}$$

Eq. (3.36) gives a hint which simplifies any g measurements significantly. There is no need to measure all the factors of the equation to calculate g

$$g = \frac{2m}{q} \cdot \frac{|\vec{M}|}{|\vec{S}|}. \tag{3.38}$$

The fractional values on the right side are directly measurable with no need for separation to the different terms. Even more, using cyclotron setup, one can combine the parameters to the spin precession frequency equation and to the cyclotron frequency equation. The frequency equations of a charged particle moving in uniform constant magnetic field are:

$$\omega_s = \frac{geB}{2mc} - (1-\gamma)\frac{eB}{mc\gamma}, \tag{3.39}$$

$$\omega_c = \frac{eB}{mc\gamma}. \tag{3.40}$$

Hence, the difference $\omega_a = \omega_s - \omega_c$ is the precession frequency of a

$$\omega_a = \omega_s - \omega_c = \frac{(g-2)}{2}\frac{eB}{mc} = a\frac{eB}{mc}. \tag{3.41}$$

However, the external electric field is not taken account, which has to be considered in the case of cyclotron setup. It is possible to show that in the case of the specially tuned experimental setup the term of electric field vanishes.

The Standard Model prediction for a_{SM} has three separated parts (see Figure 3.5),

$$a_{\mathrm{SM}} = a_{\mathrm{QED}} + a_{\mathrm{EW}} + a_{\mathrm{had}}. \tag{3.42}$$

17

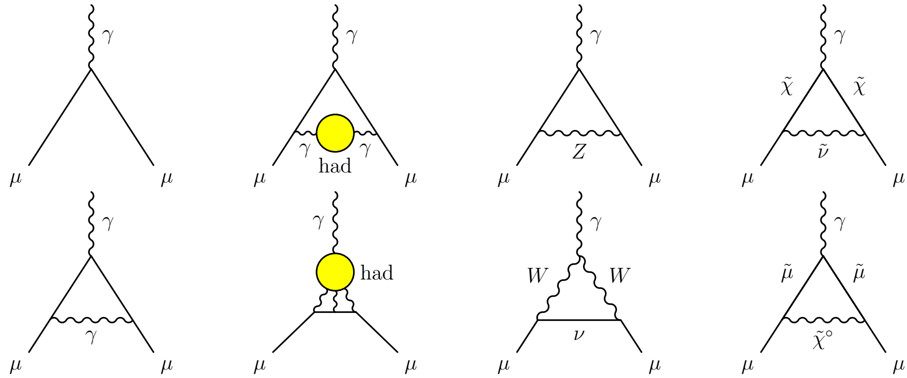

Figure 3.5: Representative Feynman diagrams contributing to a_μ. First column represents the lowest-order diagram (upper) and the first order QED correction (lower). The second column represents the lowest-order hadronic contribution (upper) and the hadronic light-by-light scattering (lower). The third column represents the weak interaction diagrams. Finally, the last column has the possible contributions beyond the Standard Model, the lowest-order SUSY. The figure is adapted from [63]

The QED part a_{QED} includes all photonic and leptonic loops. It has now been computed through 4 loops and estimated at the 5-loop level [11,64,65]. The loop contributions involving heavy $W^\pm$, Z and Higgs are collectively labeled as a_{EW}. The 2-loop contribution is important and the 3-loop leading logarithms are negligible [11]. The Higgs mass range is assumed to be $m_{\mathrm{H}} = 150^{+100}_{-40}$ GeV. Hadronic loop contributions a_{had} give rise to the main theoretical uncertainties for a_{SM}. The hadronic effects are not calculable from perturbation theory, but probably the lattice QCD or some other approaches propose a theoretical solution. Fortunately, the experimental cross-section $\sigma(e^+e \to \text{hadrons})$ data give a leading order hadronic vacuum polarization contribution [66]. In experimental case the errors are dominated by experimental systematic uncertainties and QED radiative corrections.

In summary, the best experimental value of a_{exp} is given by the Muon E821 Anomalous Magnetic Moment Measurement at BNL [67],

$$a_{\mathrm{exp}} = 11659208.0(6.3) \times 10^{-10}(0.54 \text{ ppm}). \tag{3.43}$$

The deviation between the experiment and theory is

$$\Delta a_{\mathrm{exp-SM}} \equiv a_{\mathrm{exp}} - a_{\mathrm{SM}} = (22.4 \pm 10 \text{ to } 26.1 \pm 9.4) \times 10^{-10}. \tag{3.44}$$

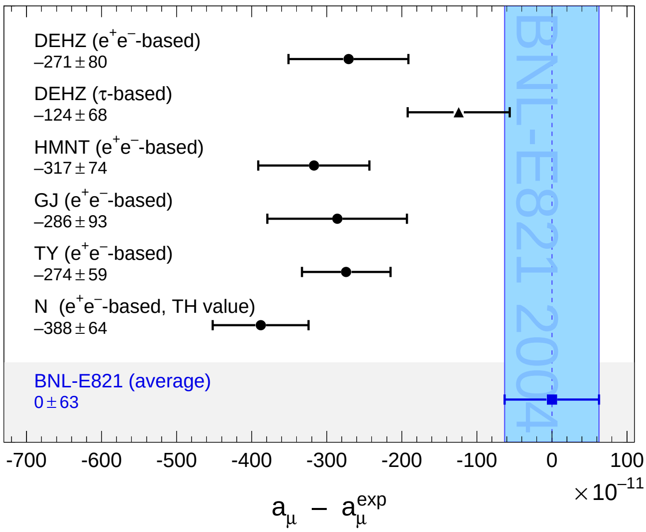

Figure 3.6: Comparison of the results of muon anomalous magnetic moment a_μ measurements ($a_{\rm exp}$) and calculations ($a_{\rm SM}$). a is in units of 10^{-11}. The Standard Model predictions are taken from the studies: DEHZ [66], HMNT [68], GJ [69], TY [70] and N [71]. The experimental value comes from Ref. [67]. The figure is adapted from [11].

It has a significance of 2.2 to 2.7 standard deviations. Figure 3.6 shows some theoretical predictions of $a_{\rm SM}$ compared to the experimental value of a.

Thus, at the present stage of experiment and theory we clearly need a theoretical explanation for the deviation $\Delta a_{\rm exp-SM}$. a is sensitive to effects beyond the standard model such as additional gauge bosons, new heavy particles, muon or gauge boson substructure, the existence of extra dimensions etc. So, the deviation $\Delta a_{\rm exp-SM}$ can be a clear hint of physics beyond the Standard Model.

Finally, for example, some last prediction of a and $\Delta a_{\rm exp-SM}$ together with the excellent summary figures can be found from Ref. [72].

Chapter 4

Neutrino physics beyond the Standard Model

4.1 Introduction: theories beyond the Standard Model

Before diving into the phenomenology of neutrinos we will briefly introduce some theoretical frameworks beyond the Standard Model. They are related to possible solutions to the neutrino mass problem. As it is impossible to give an exhaustive overview here, we will point out some of the most important properties in connection with neutrino physics. The reader is referred to some more detailed reviews. Below we will review, *Grand Unified Theories* (GUT) and *Sypersymmetry* (SUSY). We will end the section with a short list of some other directions.

4.1.1 Grand Unified Theories

The Standard Model Lagrangian has 19 free parameters. First, from esthetic point of view we would like to reduce the number of free parameters in any theory. Second, we would like to unite the lepton and quark sector of the Standard Model. Third, it would be excellent to fit the accidental symmetries to the new model as some new gauge symmetries. GUT is a framework, which tries to satisfy all these conditions.

A possible solution for the Standard Model is to suppose that the known gauge symmetry of the model, $SU(3)_c \otimes SU(2)_L \otimes U(1)_Y$, is the result of a symmetry breaking of a "bigger" group with a representation(s), which is able to house all the fields of the Standard Model. Also, we can try to identify some new fields a GUT model predicts, for example the heavy neutrino fields and/or some CDM candidates. The bigger group should unite the three couplings of the Standard Model into one coupling.

The running of the Standard Model renormalization group equations (RGE) supports the unification of the couplings, but the idea of the unification is not only a theoretical dream. Precision measurements, mainly from the LEP experiments, support the idea of the unification. For example, Figure 4.1 shows two different cases of the unification. The first one is based only the Standard Model running of the couplings. The second panel involves new SUSY particles to "correct" the RGE running.

Let us give a brief introduction of GUT which is summarized from [11, 73–76]. For example, Georgi-Glashow $SU(5)$ is the simplest group which is able to fit the symmetry groups of the Standard Model. Quarks and leptons are divided into two irreducible representations, $\mathbf{10} = \{Q, u, e\}$ and $\bar{\mathbf{5}} = \{d, L\}$. Three low energy gauge couplings are determined by two independent parameters, α_G and M_G.

To break the electroweak symmetry $SU(2)_L \otimes U(1)_Y \to U(1)_Q$ at the weak scale and give mass to quarks and leptons, we need Higgs doublets. In addition, 3 states of color triplet Higgs scalar are needed. In summary, it is possible to fit the Higgses into $\mathbf{5_H}$ or $\bar{\mathbf{5}}_\mathbf{H}$. (As an excursion to the next subsection we notice here that in the case of SUSY GUT both Higgs multiplets $\mathbf{5_H}$ and $\bar{\mathbf{5}}_\mathbf{H}$ are required to cancel anomalies and give mass to both up and down quarks.)

The couplings of the color triplets violate baryon and lepton number which gives a chance to measure the effect experimentally. For the moment the observations have not seen any nucleon decay due to the GUT, pushing the mass of the color triplets to 10^{11} GeV.

However, in the case of $SU(5)$ two irreducible representations are needed to fit the quark and lepton sector. More complete unification can be done in the symmetry group $SO(10)$. Then we have just one universal gauge coupling α_G. Every family of quarks and leptons are fitted to the 16-dimensional spinor representation $\mathbf{16} = \{\mathbf{10} + \bar{\mathbf{5}} + \mathbf{1}\}$. The last singlet $\mathbf{1}$ is reserved for heavy neutrinos. The exact structure of the fields in the representation can be found for example in Ref. [11].

There are many possibilities to break $SO(10)$ to reach the Standard Model. For example, two popular paths are

$$SO(10) \to SU(5) \otimes U(1)_X \tag{4.1}$$

and

$$SO(10) \to SU(4)_c \otimes SU(2)_L \otimes SU(2)_R. \tag{4.2}$$

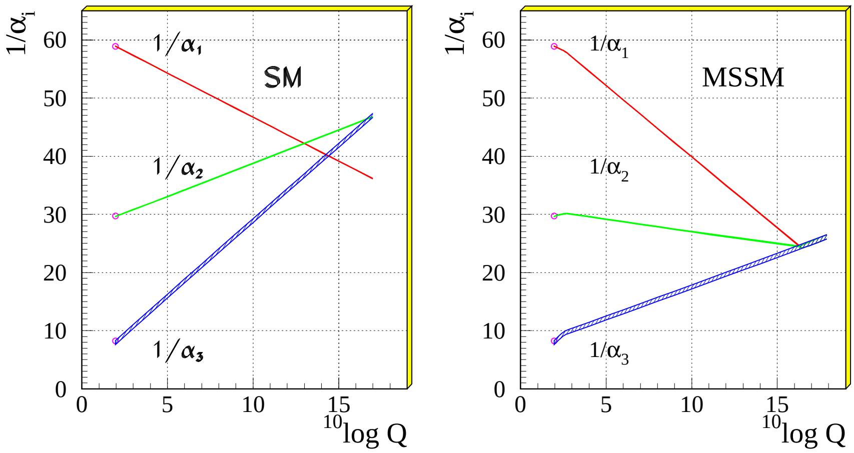

Figure 4.1: Gauge coupling unification with a non-SUSY GUT on the left side and a SUSY GUT (MSSM) on the right side. The parameter Q marks the energy scale. The extrapolations are based on the LEP data as of 1991. The difference comes from the inclusion of supersymmetric partners of Standard Model particles at scale of order 1 TeV. The present accurate measurements of the three low energy couplings show a need for GUT scale threshold corrections to fit the low energy data. The figure is adapted from [77].

In the first case, we obtain Georgi-Glashow $SU(5)$ if QED is given in terms of $SU(5)$ generators alone or the so-called *flipped* $SU(5)$ if QED is partly in $U(1)_X$. In the latter case, we have the *Pati-Salam symmetry*, where the QCD sector $SU(3)_c$ symmetry is supplemented by leptons as the fourth color, so we have $SU(4)_c$ [78]. In general, there are more possibilities for symmetry breaking available in $SO(10)$, which means more breaking scales and hence also more parameters. The need of gauge coplings unification significantly reduces possible breaking schemes. For example, in the case of breaking pattern $SO(10) \to SU(5) \to SU(3)_c \otimes SU(2)_L \otimes U(1)_Y$ with the highest breaking scale $\Lambda_{\rm GUT}$, the predictions from gauge coupling unification are preserved.

The Higgs multiplets in minimal $SO(10)$ are in the fundamental $\mathbf{10_H} = \{\mathbf{5_H}, \mathbf{\bar{5}_H}\}$ representation. Thus $SO(10)$ separates the gauge symmetry of quark and lepton multiplets from the Higgs multiplets. In principle, we have a chance to take one more step and unite the matter and Higgs sector. Also, in $SO(10)$ the generations are separated. An extension might be unification of the families.

In genereal, it is possible to choose a larger symmetry group than $SU(10)$, for example E_6 or $SU(6)$. A drawback of the larger symmetry groups is the larger number fields which must be removed from the low energy effective theory.

In summary, the GUTs are mainly proposed to answer the question how is it possible to have a universal gauge coupling g_{GUT} of a GUT from three unequal gauge couplings ($g_3 \neq g_2 \neq g_1$) of the Standard Model weak scale. The effective field theory (EFT) gives a solution for GUTs. The GUT symmetry is spontaneously broken at the scale Λ_{GUT} and all non-SM particles obtain masses of order M_{GUT}. When one calculates the Green functions with external energies $E \gg M_{\mathrm{GUT}}$ one can neglect the mass of all particles in the loop. Hence, all particles contribute to the renormalization group running of the universal GUT gauge coupling. For $E \ll M_{\mathrm{GUT}}$, one can consider an effective field theory including only the states with $m < E \ll M_{\mathrm{GUT}}$. The gauge symmetry of the EFT is the Standard model $SU(3)_c \otimes SU(2)_L \otimes U(1)_Y$ symmetry and we are able to renormalize three gauge couplings independently. Finally, the physical fields of the EFT include only the SM fields: 12 gauge bosons, 3 generations of quarks and leptons and one or more Higgs doublets.

On the experimental side the constraints from the large neutrino oscillation experiments (mainly by Super-Kamiokande) are sufficient to rule out minimal SUSY $SU(5)$, only nonminimal Higgs sectors in $SU(5)$ or $SO(10)$ theories still survive [79–81]. Also, the nonminimal models are pushed close to their theoretical limits. If SUSY GUTs are correct, nucleon decay should be seen shortly in some soon to start experiments [75, 79].

The described GUT ideas have many associations with the potential extensions of the neutrino sector in the Standard Model. For example, the GUT $SU(10)$ representations can accommodate the heavy neutrinos. We will deal with the connections between the neutrino sector and GUT in the next section.

4.1.2 Supersymmetry

SUSY for particle physics was proposed in 1973 by Julius Wess and Bruno Zumino [82]. On the theoretical side the supersymmetric algebra had been studied in the late 1960s by Golfand and Likhtman [83]. In particle physics an initial idea behind SUSY was to find connections between fermion and boson fields. The current subsection is referred from [73, 77, 81, 84].

Later it has been discovered that SUSY seems to be able to solve a wide set of problems in particle physics. Let us count a list of the proposed goals of SUSY (naturally, some of the items listed below more or less overlap):

- SUSY provides symmetry between fermion and boson fields.
- In the SUSY models all the ultraviolet divergences related to the generation of mass are automatically cancelled.
- In exact SUSY all field contributions to the vacuum energy vanish.
- SUSY GUT models can predict correct running of the couplings.
- SUSY provides a (the only) possibility to unite gravitation (spin-2 field) and the known spin-1 gauge fields into an united algebra (to be more correct, *superalgebra*) within relativistic quantum field theory.
- SUSY (with *R-parity*) is able to provide some candidates of cold dark matter.
- Finally, SUSY field(s) can be the source of the cosmological inflation.

Let us expand upon on some of the items below. First, we will give a short introduction to some of the main principles of SUSY. Then we will talk about the cancellation of the divergences and vacuum energy problem. Also, we will describe the connections between SUSY and GUT. We will finish with SUSY dark matter and inflation.

Fermion and boson (super)symmetry

Let us start with the first item above. We will mark the boson fields as b and the fermion fields as f below. We know that fermion fields anticommute, $\{f, f\} = 0$. Boson fields on the contrary, commute, $[b, b] = 0$. First, we propose a SUSY transformation between fermion and boson fields,

$$\delta b = \varepsilon \cdot f, \tag{4.3}$$

where ε is the infinitesimal transformation generator (from the Poincare group). From that formal transformation (4.3) we see that ε anticommutes,

$$\{\varepsilon, \varepsilon\} = 0, \tag{4.4}$$

which means automatically that all the generators of SUSY are anticommuting and therefore they are fermionic. Fermionic operator changes spin in units 1/2 and therefore it always changes the type of statistics,

$$\varepsilon : \text{Fermi-Dirac} \leftrightarrow \text{Bose-Einstein} \tag{4.5}$$

Also, the pure SUSY states exactly equal numbers of degrees of freedom for fermions and bosons in the model.

Naturally, the first idea would be that the well-known bosons and fermions of the Standard Model are superpartners. Unfortunately, if we do some bookkeeping the bosonic content has 28 and the fermionic content has 90 (or 96 with massive neutrinos) degrees of freedom in the Standard Model. In addition, the Higgs field can not be a superpartner of the fermion content, since it has nonzero vev. Thus we need to introduce the superpartners for all the fields in the Standard Model. It can be shown that due to the form of the superpotentials and chirality of the matter superfields at least two complex chiral Higgs multiplets are needed to give masses to up and down quarks.

Hierarchy problem and vacuum energy

Why are there wide mass gaps in Nature? This is a big unanswered question in physics. A subexample of the question is the wide gap between the 10^2 GeV Higgs scale and the 10^{16} GeV GUT scale. If we add some new fields above the Higgs scale as an extrapolation of the Standard Model it will start to spoil up our physics at the lower scale. It is done by the quadratic divergence of the Higgs radiative corrections from the heavy fields at the higher scale. For example, Figure 4.1.2 shows the Feynman diagram which is proportional to the mass squared of a (heavy) higher scale boson. A possibility to save the Higgs is to cancel the bosonic correction with a fermion correction.

SUSY is able to provide an excellent cancellation of all the quadratic divergences. The reason is clear, every fermion or boson has a bosonic or fermionic superpartner which cancels the divergences. Figure 4.1.2 shows the compensating Feynman diagrams.

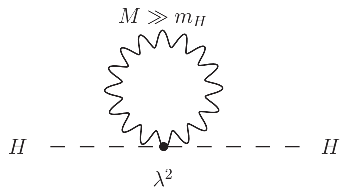

Figure 4.2: Radiative correction to the Higgs boson mass. The new fields between the electroweak and GUT scale as an extrapolation of the Standard Model spoil up our physics at the lower scale due to the quadratic divergence of the Higgs radiative corrections.

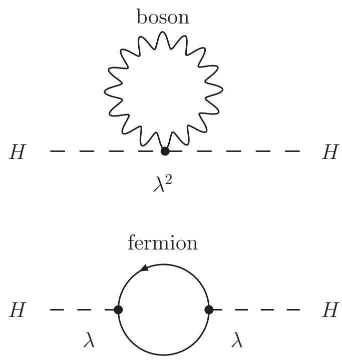

Figure 4.3: SUSY is able to provide excellent cancellation of all the quadratic divergences of the Higgs. Every fermion or boson has bosonic or fermionic superpartner which respectively cancels the divergences.

Naturally, the exact cancellation takes place only in the case of unbroken SUSY,

$$\sum_N m^2_{\text{fermion}} - \sum_N m^2_{\text{boson}} = 0, \tag{4.6}$$

where N is the order of the SUSY model. In the case of broken SUSY the cancellation mechanism works up to the scale of SUSY breaking,

$$\sum_N m^2_{\text{fermion}} - \sum_N m^2_{\text{boson}} = M^2_{\text{SUSY}}, \tag{4.7}$$

where M^2_{SUSY} is the scale of SUSY breaking. If we suppose the Higgs boson mass in the scale of 100 GeV and the Yukawa coupling is in the scale below 1 (but not very far from 1) then the SUSY breaking scale should we around

1 TeV,

$$gM_{\text{SUSY}} \propto M_H. \tag{4.8}$$

We mentioned above that in SUSY all the bosonic and fermionic field contributions cancel each other and the vacuum energy should be exactly zero. Unfortunately, in the case of SUSY breaking the value of the vacuum energy is unclear again. It would be natural to suppose that the vacuum energy is in the scale of the SUSY symmetry breaking, but as we can see from Nature, it is not true. If the SUSY breaking scale is $\Lambda_{\text{SUSY}} \simeq 1$ TeV then the big gap between the real vacuum energy Λ_{vac} from cosmology and from SUSY remains huge, $\Lambda_{\text{SUSY}}/\Lambda_{\text{vac}} \simeq 10^{43}$.

SUSY GUT

We know from experiments and theory that the couplings in the Standard Model are running in energy. Figure 4.1 shows the actual predictions from a simple GUT and a SUSY GUT. The present accurate measurements of three low energy couplings show a need for the GUT scale threshold corrections to fit the low energy data. The difference comes from the inclusion of supersymmetric partners of standard model particles at the scales of SUSY breaking, in order 1 TeV. We have to notice here that only a small set of SUSY model with tuned parameters can yield the unification target. Even a small change in the model can destroy the nice picture of unification. A possible solution to avoid the strong sensitivity is to shift all the scalars except the Standard Model Higgs up to a higher scale. It is done in *Split SUSY* models [85, 86].

Dark matter, inflation and dark energy from SUSY

In a simple SUSY model nothing prevents the decay of heavy SUSY particles into light Standard Model particles. To prevent the lightest SUSY particle against its decay, the *R-parity* is proposed. The R-parity is a discrete symmetry needed to leave at least one (lightest) SUSY particle stable. This particle is called the *lightest supersymmetric particle* or LSP for short. LSP can be a promising candidate of CDM. It should be heavy and it couples only very weakly with the Standard Model content. In the different SUSY models neutralino, gravitino or axino have been considered as candidates of LSP (e.g., see Ref. [87–89]).

The different SUSY models are proposed for the mechanism of cosmological inflation, for example, using the decay of some SUSY scalar fields. In general, it is rather problematic to get a sufficiently flat potential. The conventional point of view is to invoke a set of scalar fields and assume that they arise from a deeper theory behind the model [84].

Some SUSY related models are proposed to solve the puzzle of the cosmological constant. Naturally, in the case of the particle field models the solution of the cosmological constant should stand on the matter side of the Einstein equation. For example, it is possible to construct a time dependent vacuum energy $\Lambda(t)$ by the means of a scalar field (or a kind of mixture of scalar fields), which has not relaxed to the minimum of its potential. The *quintessence* represents a possible non-equilibrium approach to the positive cosmological constant. However, the models have to be built quite carefully as the cosmological observational data suggests w ($p = w\rho$) value very close to -1 [20, 84]. Typically, SUSY models for cosmological constant are rather fine tuned as the SUSY scale is much higher than the scale of cosmological constant.

The SUSY cosmology suffers from some general problems. For example, the cosmological gravitino overproduction problem and the moduli problems if the reheating is done at the GUT scale, see e.g. [90]. However, split SUSY models offer some solutions for the problem [85, 86].

4.1.3 Other directions

SUSY and GUT have been proposed to solve the set of more or less fundamental restrictions of the Standard Model. Naturally, nowadays the list of possible phenomenological and theoretical extensions of the Standard Model is much longer. The models with composite scalars and extended fermion content exist, e.g. *technicolor* and *little Higgs* models. There are also models with *extra dimensions* on a slightly different track of development. For example, the *Kaluza-Klein theory* is a subset of extra dimensional theories. Some additional Higgsless models have been proposed, for example, *top quark condensate*.

To lower the number of fundamental particles, the *preon* models have been proposed. This schema has some similarities with the QCD sector in the Standard Model. The Standard Model fundamentals are composed by more fundamental particles, so called preons, like quarks compose hadrons. Unfortunately, the preon models suffer due to some fundamental difficulties. The preon models represent a mass paradox: how could fermions be made of smaller particles that would have many orders of magnitude greater mass arising from their enormous momenta.

Two successful theories of the 20th century, quantum mechanics and general relativity, are yet to be unified. Several theories of quantum gravity have been proposed, quite apart from experiment and phenomenology. For example, *string theory*, *loop quantum gravity* etc. The mentioned theories lack real connections with experiment/observations. They have several mathematical problems that have trapped the models. The theory of superstrings has serious trouble due to huge number of possible (but different) vacua. No concrete idea has been proposed on how to overcome that. The theory of loop quantum gravity has many open questions in physical interpretations. For example, no clear path is known for how to interpret quantized space-time in the theory.

Unfortunately, it is impossible to describe all the possible paths of development here. In the current work we keep in mind only a subset (more-or-less) phenomenological tracks.

4.2 Neutrino masses beyond the Standard Model

4.2.1 Neutrino mass: Dirac or Majorana mass term?

In the Standard Model the fields transform under the gauge symmetries and the model is renormalizable. The gauge symmetries and renormalizability allow only definite forms of mass term in the Standard Model Lagrangian. An explicit fermion mass term would break the chiral $SU(2)$ symmetry. Thus the mass terms have to be generated dynamically by a scalar field via the Higgs mechanism. Due to the renormalizability the maximal mass dimension of a renormalizable term in the Lagrangian is four. The only allowed scalar potential form of the scalar field is the *Mexican hat potential*.

In the Standard Model the following Yukawa mass term of a fermion generation is presented,

$$\mathcal{L}_{\rm SM} \supset -\lambda_l \bar{L}_L H e_R - \lambda_d \bar{Q}_L H d_R - \lambda_u \bar{Q}_L \tilde{H} u_R - h.c., \tag{4.9}$$

where L_L and Q_L are the left-handed lepton and quark doublets and e_R, u_R and d_R are the right-handed lepton, up and down quark singlets. The Higgs doublets H and $\tilde{H}$ are defined in Section 2.2.

The mass term (4.9) is called the *Dirac mass term*. The term is composed of the left-handed and right-handed fields linked by the Higgs doublet. After the EWSB the Dirac mass term acquires the usual form

$$\mathcal{L}_D = -m_D \bar{\Psi}_L \Psi_R + h.c. = -m_D \bar{\Psi}\Psi, \tag{4.10}$$

where Ψ is a fermion field. The mass term for all the generations of the charged leptons is

$$\mathcal{L} \supset -m_{ij} \bar{e}_{Li} e_{Rj} + h.c., \tag{4.11}$$

20

where m_{ij} is the mass matrix of the charged leptons.

There is no mass term for neutrinos in the Lagrangian (4.9) as there are no right-handed neutrino fields in the Standard Model. In Chapter 3 we reviewed the clear experimental evidences that at least two neutrino species have to be massive. Thus we have to add the neutrino mass to the model. What is our prospect to embed the neutrino mass into the model?

Let us start from scratch. The lowest nontrivial representation of the Lorentz group allows to write the Lagrangian of a free spin 1/2 fermion in the form

$$\mathcal{L}_M = -i\rho^\dagger\sigma^\mu\partial_\mu\rho - i\frac{m}{2}\rho^T\sigma^2\rho + h.c., \tag{4.12}$$

where σ^i are the Pauli matrices with $i = 1, 2, 3$, $\sigma^0 = I$, ρ is 2-component spinor and the Greek indices denote Lorentz four-indices.

The mass term is not invariant under the transformation of $U(1)$ symmetry group,

$$\rho \to e^{i\alpha}\rho, \tag{4.13}$$

where α is any real number and $e^{i\alpha}$ is the fundamental representation of $U(1)$ symmetry group. Thus, only neutrino can be described by Eq. (4.12) in the fermion sector. The other particles of the Standard Model are charged by the electromagnetic $U(1)$ gauge. The simplest $U(1)$ invariant form of the Lagrangian is

$$\mathcal{L}_D = -i\sum_k \rho_k^\dagger\sigma^\mu\partial_\mu\rho_k - i\frac{m}{2}\sum_k \rho_k^T\sigma^2\rho_k + h.c., \tag{4.14}$$

where $k = 1, 2$. The symmetry $U(1)$ manifests itself as

$$\begin{pmatrix} \rho_1' \\ \rho_2' \end{pmatrix} = \begin{pmatrix} \cos\theta & \sin\theta \\ -\sin\theta & \cos\theta \end{pmatrix} \begin{pmatrix} \rho_1 \\ \rho_2 \end{pmatrix}. \tag{4.15}$$

Thus, in the case of $U(1)$ symmetry presented we need at least two 2-component spinor fields.

If we define two new 2-spinors as

$$\chi = \frac{1}{\sqrt{2}}(\rho_2 + i\rho_1), \tag{4.16}$$

$$\phi = \frac{1}{\sqrt{2}}(\rho_2 - i\rho_1), \tag{4.17}$$

we are able to fit the two fields into a 4-component Dirac spinor,

$$\Psi_D = \begin{pmatrix} \chi \\ i\sigma^2\phi^* \end{pmatrix}. \tag{4.18}$$

We can write down the *charge conjugation matrix* that flips the fields χ and ϕ in the Dirac spinor,

$$C\Psi_D = C\begin{pmatrix} \chi \\ \sigma^2\phi^* \end{pmatrix} = \begin{pmatrix} -\sigma^2\chi \\ \phi^* \end{pmatrix} = \begin{pmatrix} -\sigma^2 & 0 \\ 0 & \sigma^2 \end{pmatrix}\Psi_D = -\gamma^0\gamma^2\Psi_D, \tag{4.19}$$

and the charge conjugate spinor with the flipped components as

$$\Psi_D^c \equiv C\bar{\Psi}^T = \begin{pmatrix} \phi \\ i\sigma^2\chi^* \end{pmatrix}. \tag{4.20}$$

It is easy to show that if $\rho_1 \neq \rho_2$ then Eq. (4.14) and the definitions above present a Dirac mass term (4.10).

The 4-spinor is said to be a *Majorana* or *self-conjugate* spinor if

$$\Psi = C\bar{\Psi}^T, \tag{4.21}$$

which for 2-spinors means the condition $\phi = \chi$. The Dirac term reduces to the form of Eq. (4.12) which is called a *Majorana mass term.* A more familiar form of the Majorana mass is

$$\mathcal{L}_M \supset -\frac{m}{2}\Psi^T C\Psi - h.c., \tag{4.22}$$

which is written in 4-spinors now.

Thus, if the neutrino mass term is not restricted by a $U(1)$ it can be the Majorana mass term. Interestingly, non-abelian symmetry does not force a similar restriction on the mass term. The interactive particle fields under non-abelian symmetry are represented as multiplets. The non-interacting fields are represented as singlets and they do not communicate with multiplets: the gauge phases are compensated and the Lagrangian is covariant.

4.2.2 Sources of neutrino mass

In the Standard Model the Majorana mass (4.22) would correspond to the only possible gauge invariant term

$$\mathcal{L} \supset \lambda_{ij}\bar{L}_L^i H \bar{L}_L^j H \xrightarrow{\text{EWSB}} m_{ij}\nu_{Li}^T C\nu_{Lj}, \tag{4.23}$$

where ν_L is a left-handed neutrino field. However, as the dimension of the operator is $3/2 + 1 + 3/2 + 1 = 5$, one cannot introduce the term in the Standard Model Lagrangian as it is not renormalizable. The term above is the only possible gauge symmetric *dimension five effective operator* (for short, $d = 5$ operator below) presented in the Standard Model. It is a clear hint that we have to extend the Standard Model for the neutrino sector.

However, before jumping to a possible extension of the Standard Model let us carefully check all the known alternative mechanisms in the Standard Model to generate the neutrino mass. There are only two known mechanisms which we analyze below: (i) radiative mechanisms beyond the tree level perturbations and (ii) non-perturbative mechanisms.

(i) The Standard Model has the exact lepton symmetry L after EWSB, see e.g. Eq. (2.55). Therefore, it is impossible that the neutrino mass term can arise in perturbation level. Thus if we conserve L, neutrino remains massless in all orders of perturbation theory. However, let us remind that any Majorana mass term of the neutrinos violates L.

(ii) In the electroweak sector the only known nonperturbative effect is the weak instanton effect. Can the instanton break the lepton number symmetry and somehow generate neutrino mass? It is possible to show that the anomalies related to the instanton do not conserve the lepton number L, but they conserve the $B - L$ current, where B is the baryon number. Thus, due to exact $B - L$ conservation, neither the nonperturbative effects nor radiative higher order effects can not produce neutrino mass in the Standard Model. There is a "loophole" because of gravitation discussed later.

Now we are armed by the knowledge of the restrictions of the mass terms in the Standard Model. Let us think about a possible minimal extension of the Standard Model to incorporate the neutrino masses. The first idea would be to add right-handed neutrinos into the model and the well-known Dirac mass term generates the mass of neutrino. In that case we find that the Yukawa coupling in the Dirac mass term is unnaturally small. Figure 4.4 presents the mass gap between the neutrino sector and the rest of the fermions. The Yukawa coupling of neutrino is at least 10^{-6} times lower than the Yukawa coupling of electron and 10^{-11} times lower than the Yukawa of top quark. The problem is more or less esthetic as there is no known physical restriction to a very small Yukawa coupling. In addition, we can ask why there is only a Dirac mass term for neutrino if there is no restriction to have the Majorana term for uncharged neutrinos (forgetting the accidental L symmetry for a moment).

Another and more attractive path is to modify the Lagrangian with *effective operators* from an unknown theory from higher energy physics above

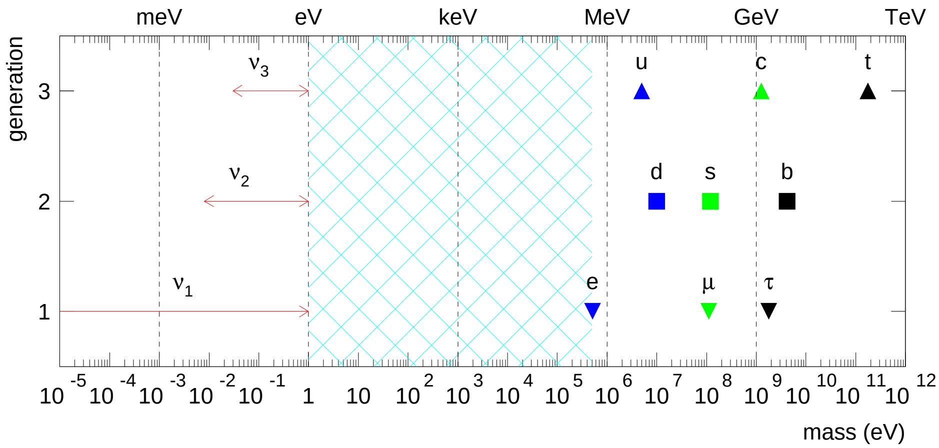

Figure 4.4: Masses of other fundamental fermions compared to neutrino masses. Normal hierarchy has been assumed for neutrino masses, $m_{\nu_1} < m_{\nu_2} < m_{\nu_3}$. A rather high upper bound $m_{\nu_i} < 1$ eV is used. The hatched region indicates the mass difference between the largest neutrino mass and the electron mass. The huge 10^6 times difference is a main puzzle in neutrino physics. The figure is adapted from [91].

the Standard Model. From the framework of effective theories we know that the low energy Lagrangian can have effective (nonrenormalizable) operators from the higher energy sector of theory [92, 93].

In the new effective theory the gauge group, the fermionic fields and the pattern of spontaneous symmetry breaking remain valid. The predictions of the Standard Model are modified by small effects that are proportional to powers of E/Λ_{NP}, where Λ_{NP} is the energy scale of new physics. Thus, if we take the limit $\Lambda_{\text{NP}} \to \infty$ we can integrate out all the effective (nonrenormalizable) terms.

The effective extension of the Standard Model Lagrangian can include a tower of *nonrenormalizable higher-dimensional operators*. The Lagrangian can be written as a series,

$$\mathcal{L}_{\text{eff}} = \mathcal{L}_{\text{SM}} + \frac{1}{\Lambda_{\text{NP}}}\mathcal{L}^{d=5} + \frac{1}{\Lambda_{\text{NP}}^2}\mathcal{L}^{d=6} + ... \qquad (4.24)$$

A general result of the effective theory is that the higher dimensional members are composed by the fields of the Standard Model and their coefficients

21

weighted by inverse powers of the high scale $\Lambda_{\rm NP}$. As it was mentioned, only one form of the gauge invariant $d = 5$ operator is possible in the Standard Model. The *dimension six operators* (for short, $d = 6$) are not so restricted and an effective model can include 81 different operators (without taking into account flavor indices). The observables, constructed from the $d = 6$ operators are important in order to distinguish between the different models experimentally, for example see Ref. [94, 95].

As mentioned only allowed effective $d = 5$ operator by the Standard Model gauges presents the Majorana mass term

$$\mathcal{L} \supset \lambda_{ij} \bar{L}^i_L H \bar{L}^j_L H \xrightarrow{\text{EWSB}} M_{ij} \nu^i_L \nu^j_L. \tag{4.25}$$

The term should be suppressed, thus the neutrino masses should be suppressed. The accidental symmetries L and $B - L$ are violated by the term (4.25). In particular, the numbers are violated by two units. If we reformulate the Standard Model as a low energy effective theory of a higher energy theory (e.g. at the GUT scale or the Planck scale) the suppressed term (4.25) fits excellently into the new model. The Standard Model is a valid approximation up to the scale $\Lambda_{\rm NP}$ of the new higher energy physics. All the effective terms are suppressed as

$$\mathcal{L} \supset \frac{\lambda_{ij}}{\Lambda_{\rm NP}} \bar{L}^i_L H \bar{L}^j_L H \xrightarrow{\text{EWSB}} \lambda_{ij} \frac{\upsilon^2}{\Lambda_{\rm NP}} \nu^i_L \nu^j_L, \tag{4.26}$$

and thus

$$M_{ij} = \lambda_{ij} \frac{\upsilon^2}{\Lambda_{\rm NP}}. \tag{4.27}$$

In conclusion, as the neutrino masses are very small it would be tantalizing to use an effective theory for the neutrino sector. For building the effective theory we should be looking for some higher scales in particle physics. In particle physics one can suppose two possible scales above the Standard Model: the Planck scale and the GUT scale.

Let us start with the Planck scale. The perturbative theory of gravity conserves $B - L$ based on general symmetry arguments. On the other hand, the nonperturbative effects clearly violate the global L, B and $B - L$ symmetries. For example, well-know gravitational instantons like *black holes* or *worm holes* do not respect L, B and $B - L$. We can drop many leptons into a black hole, but we do not have any guarantee that the black hole radiates back same amount of leptons in the Hawking black body radiation.

In the Standard Model, we can have effective gravitational terms (e.g. related to gravitational instantons) that violate L and B [96,97]. The terms are nonrenormalizable and they have general form of

$$\mathcal{L}_{\text{eff}} \supset \bar{L}_L H \bar{L}_L H. \tag{4.28}$$

However, in the effective Standard Model the terms are suppressed by the scale of gravitation, which means the Planck mass M_{Planck}. After EWSB the term (4.28) acquires the form

$$\mathcal{L}_{\text{eff}} \supset \frac{\upsilon_{\text{EW}}^2}{M_{\text{Planck}}} \nu_L \nu_L, \tag{4.29}$$

where υ is the electroweak vev. The ratio of the mass scales is at order $\upsilon_{\text{EW}}^2/M_{\text{Planck}} = (2 \times 10^2)^2/10^{19} \simeq 10^{-6}$ eV which should be many orders of magnitude higher especially in order to satisfy the experimental bonds of the atmospheric parameter Δm^2_{atm}.

The second well-known scale above the Standard Model is the GUT scale. In the GUT models $B - L$ is not violated. Thus perturbative nor nonperturbative effects alone cannot be the source of the neutrino mass. However, if we add some new (L violating) ingredients to the model it is easy to construct an effective mass term in the same form as Eq. (4.29) above

$$\mathcal{L}_{\text{eff}} \supset \frac{\upsilon_{\text{EW}}^2}{M_{\text{GUT}}} \nu_L \nu_L, \tag{4.30}$$

where the Planck mass scale are replaced by the GUT mass scale. If the typical GUT scale, $M_{\text{GUT}} \simeq 10^{15}$ GeV, then the ratio of the mass scales is at order $\upsilon_{\text{EW}}^2/M_{\text{GUT}} = (2 \times 10^2)^2/10^{15} \simeq 10^{-2}$ eV. It is in good accordance with the experimental neutrino masses.

From the arguments above the GUT seems to be a convenient source of neutrino mass. Also, in the case of $SO(10)$ unification the 16-dimensional spinor representation $\mathbf{16} = \{\mathbf{10} + \bar{\mathbf{5}} + \mathbf{1}\}$ reserves the last singlet $\mathbf{1}$ for an additional right-handed field, *heavy neutrinos* [11].

4.2.3 Different models of neutrino mass

An effective theory for the neutrino sector gives the most natural explanation for the smallness of neutrino mass. It also allows Majorana mass terms. However, in general we are interested to find a full theory beyond the effective theory. Below we give a very short list of some full scale theories. Naturally, there are many models proposed for the neutrino sector. For example, Ref. [11, 33] give some rather complete lists.

Let us summarize some extensions of the Standard Model for neutrino mass:

- We can add right-handed $U(1)_Y$ neutral singlet fields ν_R. Thus we are able to construct the mass terms $m_D\bar{\nu}_L\nu_R$, $m_N\nu_L^T\nu_L$ and $m_M\nu_R^T\nu_R$.
- We can include a scalar triplet $\Delta(1,3,1)$ [98–100]. We can write the Majorana mass term $m_\Delta\nu_L^T\nu_L$, where m_Δ is related to the vev of the triplet.
- We can include a vectorlike fermion $\vec{\Sigma}$ which is a triplet under $SU(2)$ to construct the mass term $m_\Sigma\bar{\Sigma}\nu_L$ [101].

The described models separately offer a rather minimal extension of the Standard Model. All the models can explain the tiny masses of neutrinos. Also, the models can be integrated into some more general framework beyond the Standard Model. For example, the first one can be embedded into the GUT framework, the second model can be associated with the Little Higgs framework etc.

Before a more detailed review of the three models above we will introduce some general properties of the mass matrix and mixing in the next subsection. After that we will review the mass matrix and mixing in the models presented above. Also, we will introduce the *see-saw mechanism*.

4.2.4 Mass matrix and mixing in the Standard Model

We know from experiment that the mass state of a fermion can be a linear combination of the flavor states of the fermion. We may generalize the Dirac mass term as

$$\mathcal{L}_D \supset (m_D)_{ij}(\bar{\psi_L})^i(\psi_R)^j + h.c. \tag{4.31}$$

In the Standard Model there are three generations of fermions and the mixing is done between the different generations. Thus, the mixing matrix $(m_D)_{ij}$ is a 3×3 matrix. However, in general models it does not have to be a square matrix.

For example, in the Standard Model the Cabibbo-Kobayashi-Maskawa (CKM) matrix is a mixing matrix which specifies the mismatch of quantum states of quarks when they propagate freely (Yukawa couplings) and when they take part in weak interaction. In the Dirac mass term it has the form

$$\mathcal{L}_{\mathrm{SM}} \supset -(G_d)_{ij}(\bar{q}_L)^i H(d_R)^j - (G_u)_{ij}(\bar{q}_L)^i\tilde{H}(u_R)^j - h.c., \tag{4.32}$$

where $i, j = 1, 2, 3$ count the generations, G_u and G_d are 3×3 matrices of the Yukawa couplings and q_L, u_R and d_R are the quark fields in the electroweak basis. The matrices can be diagonalized by unitary matrices,

$$M^2 = UGG^\dagger U^\dagger. \tag{4.33}$$

Now, using the quark term in the charged current,

$$\bar{u}_L^{(w)}\gamma_\mu d_L^{(w)} = \bar{u}_L^{(m)} U_u \gamma_\mu U_d^\dagger d_L^{(m)}, \tag{4.34}$$

where (w) marks the electroweak basis and (m) marks the mass basis, we can define the CKM matrix as

$$V = U_u U_d^\dagger. \tag{4.35}$$

In Chapter 3 we presented the MNS matrix in Eq. (3.16) which describes the similar mismatch in the neutrino sector as the CKM matrix in the quark sector. As neutrinos are strictly massless in the Standard Model the MNS matrix is a clear effect from new physics beyond the Standard Model.

In the Standard Model the mixing of the charged leptons is rather different form the quark sector. In the Yukawa sector of the charged leptons,

$$\mathcal{L}_Y \supset (m_e)_{ij}\bar{L}_{Li} e_{Lj} + h.c. \tag{4.36}$$

The mass matrix $(m_e)_{ij}$ can be diagonalized by the biunitary transformations,

$$(m_L)_{\text{diag}} = U_{eL}^\dagger m_e U_{lR} = \text{diag}(m_e, m_\mu, m_\tau), \tag{4.37}$$

which appears in the charged current as

$$\mathcal{L}_{\text{CC}} = \frac{\upsilon}{2}\bar{L}_L \gamma^\mu U_{eL}^\dagger \nu_L W_\nu^+ + h.c. \tag{4.38}$$

Neutrinos are strictly massless in the Standard Model. Thus there is no Yukawa mass terms for neutrinos which can restrict the redefinition of the neutrino fields to eliminate U_{eL},

$$\nu_L' = U_{eL}^\dagger \nu_L. \tag{4.39}$$

Also, the eliminated mixing guarantees the lepton number L conservation for the every generation separately,

$$L = L_e + L_\mu + L_\tau. \tag{4.40}$$

Naturally, if we extend the Standard Model Lagrangian with a Yukawa sector of neutrinos the redefinition of the neutrino fields in the charged current sector influences the Yukawa sector or vice versa. In the next subsection we will analyze the lepton mass matrix and mixing in the concrete neutrino related extensions of the Standard Model.

4.2.5 See-saw scenarios

Now, we will give a short overview of three different minimal models of the neutrino mass presented above: (i) right-handed singlet neutrinos, (ii) scalar triplet and (iii) heavy vector-like fermions. All the models have been extensively studied in neutrino physics. We will analyze the mass matrices and mixing in the models. In the context of our work we focus mostly on details of the models which are important for the futher story of leptogenesis in the next chapter. Also, we will present the effective operators only up to order $d = 5$.

Type I see-saw

Let us take a deeper look at the composition and the properties of mass matrix. As we deal with the neutrino sector here it is more clear to start with 2-spinors. We will add mass mixing into the Lagrangian (4.12). In principle, we are able to mix any arbitrary number of Majorana neutrinos, but for simplicity we assume here the mixing of two 2-spinors. Thus, the mass matrix is a 2×2 matrix. The Lagrangian is

$$\mathcal{L} = -\sum_i \rho_i^\dagger \sigma^\mu \partial_\mu \rho_i - \frac{1}{2}\sum_{i,j} M_{ij} \rho_i^T \sigma^2 \rho_j + h.c., \tag{4.41}$$

where $i, j = 1, 2$ and the mass matrix (M_{ij}) is

$$(M_{ij}) = \begin{pmatrix} m_1 & m_3 \\ m_3 & m_2 \end{pmatrix}. \tag{4.42}$$

From the Fermi-Dirac statistics the mass matrix M_{ij} has to be symmetric as we can interchange the fermion fields in the mass term. We can diagonalize the symmetric matrix using an orthogonal matrix. The eigenvalues of the 2×2 symmetric matrix are

$$m_\pm = \frac{1}{2}[(m_1 + m_2) \pm \sqrt{4m_3^2 + (m_1 - m_2)^2}]. \tag{4.43}$$

The diagonalized matrix has the form

$$M_{\text{diag}} = OMO^T = \begin{pmatrix} m_+ & 0 \\ 0 & m_- \end{pmatrix}, \tag{4.44}$$

where O is an orthogonal diagonalizing matrix.

It is educating to look at some specific cases. Below we will deal with neutrinos, so all spinor fields there are neutrino fields. Also, if any $U(1)$

symmetry arises it cannot be electromagnetic charge symmetry as neutrinos are electrically neutral.

(i) Dirac mass. Let us assume that $m_1 = m_2 = 0$ and $m_3 \neq 0$. Then the eigenvalues of the matrix are $\pm m_3$ and the Lagrangian (4.41) acquires the form of the Dirac mass term as in Eq. (4.14). Thus a pure Dirac neutrino can be thought of as a composition of two Majorana neutrinos with equal masses. The theory (see Eq. (4.14)) is invariant under a $U(1)$ symmetry. The opposite sign of the eigenvalues refers to the C transformation, $\Psi^c = C\Psi$, where the two 2-spinor fields of Dirac neutrino have opposite charge conjugation properties, $Q(\rho_1) = -Q(\rho_2)$. As mentioned above the charge here is not electromagnetic. For example, in the Standard Model it can be associated with the accidental lepton number symmetry.

(ii) Pseudo-Dirac mass. The case of $m_1 \sim m_2 \ll m_3$ is called *pseudo-Dirac*. The neutrino is Majorana, but there is only a slight departure from the Dirac case. The mass of neutrino is $\pm m + \delta$, where $\delta \ll m$. The 2-spinors are maximally mixed in this case. We remember from Section 3.3 that the atmospheric neutrino data support maximal mixing.

(iii) Majorana mass. In the case of $m_1 = 0$ and $m_3 \ll m_2$ the eigenvalues are

$$m_\nu \equiv m_- = \frac{1}{2}(m_2 - \sqrt{4m_3^2 + m_2^2}) \simeq -\frac{m_3^2}{m_2}, \tag{4.45}$$

$$M_\nu \equiv m_+ = \frac{1}{2}(m_2 + \sqrt{4m_3^2 + m_2^2}) \simeq m_2. \tag{4.46}$$

It is known as the *seesaw mechanism*. The source of the name is clear: if M_ν is getting bigger then m_ν is getting smaller and vice versa.

The last case needs a longer analysis as the conditions of the mass may seem artificial. First, why $m_3 \ll m_2$? In the Standard Model the field ν_1 belongs to a $SU(2)_L$ doublet as a weakly interacting left-handed neutrino field. The field ν_2 is a $SU(2)_L$ singlet as the weakly non-interacting right-handed neutrino field. Thus the only possible mass term which can include $m_3 \nu_1^T \sigma^2 \nu_2$ is

$$\mathcal{L}_{\text{SM}} \supset -\lambda_\nu \bar{L}_L \tilde{H} \nu_R + h.c., \tag{4.47}$$

where ν_1 belongs to L_L and ν_2 is noted as ν_R. λ_ν is limited by the weak scale since it is generated by the electroweak Yukawa, we can say it is protected by $SU(2)_L \otimes U(1)_Y$ gauge. On the other hand, the mass term $m_2 \nu_2^T \sigma^2 \nu_2$ is a pure Majorana mass term composed by the electorweak singlets. Thus it is unprotected by the gauge. It is rather natural to suppose that m_2 is limited by some higher scale, for example by the GUT scale. In summary, $m_3 \ll m_2$ as the electroweak scale at 10^2 GeV is much lower than a typical GUT scale, for example 10^{16} GeV.

The second statement, $m_1 = 0$, means that there is no mass term $m_L \nu_L^T \sigma^2 \nu_L$. In principle, there is a way to introduce that mass term, but then we need a scalar triplet or a triplet of vectorlike fermions. However, in a minimal model we do not like to mix different mechanisms of neutrino mass. Thus in the current type I see-saw $m_1 = 0$.

To generalize the case of two neutrinos to the three generations of the neutrino field follows from the mass terms,

$$\begin{aligned}\mathcal{L} &\supset -(\frac{1}{2}\nu_L^T C m_L \nu_L + \bar{\nu}_L m_D \nu_R + \frac{1}{2}\nu_R^T C M_R \nu_R + \bar{L}_L m_e e_R) + h.c.\\ &= -(\frac{1}{2} n_L^T C \mathcal{M}^* n_L + \bar{L}_L m_e e_R) + h.c.,\end{aligned} \tag{4.48}$$

where m_L, m_D and M_R are 3×3 matrices if we have the mixing of the three generations. The 6×6 matrix $\mathcal{M}$ can be presented as the block matrix:

$$(M_{ij}) = \begin{pmatrix} m_L & m_D \\ m_D & M_R \end{pmatrix}, \tag{4.49}$$

and $n_L = (\nu_L, (\nu_R)^c)$. In the case of neutrinos all the submatrices are not necessarily square $N \times N$ matrices but they can be $N \times M$, where $M \neq N$. The reason is that experiment gives us some freedom to choose the number of sterile and heavy neutrinos. The properties pointed out in the analysis of the two neutrino cases above remain valid for the case of $2N$ neutrinos.

Let us develop some exact forms of the mixing and mass matrix. As we discussed above in the charged current interaction, the charged lepton fields can be diagonalized in the weak basis. The relevant part of the Lagrangian is presented then as

$$\mathcal{L}_{\mathrm{CC}} = \frac{\upsilon}{2}\bar{L}_L \gamma^\mu \nu_L W_\nu^+ + h.c. \tag{4.50}$$

The charged current forces the left-handed fields to transform in the same way,

$$\bar{L}_L U^\dagger \gamma^\mu U \nu_L W_\nu^+ \to \bar{L}_L \gamma^\mu \nu_L W_\nu^+ \quad \Rightarrow \quad L_L \to U L_L, \quad \nu_L \to U \nu_L. \tag{4.51}$$

The right-handed fields are independent,

$$e_R \to V e_R, \quad \nu_R \to W \nu_R, \tag{4.52}$$

since the right-handed fields do not participate in the charged current.

One can diagonalize the matrix $\mathcal{M}$,

$$V^T \mathcal{M}^* V = \mathcal{D}. \tag{4.53}$$

where $\mathcal{D}$ is the diagonal matrix with the physical light and heavy Majorana neutrino masses on the diagonal:

$$\mathcal{D} = \mathrm{diag}(m_1, m_2, m_3, M_1, M_2, M_3), \tag{4.54}$$

where m is a mass of light neutrino and M is a mass of heavy neutrino. It is convenient to separate the "light" and "heavy" blocks in the V and $\mathcal{D}$ matrix:

$$V = \begin{pmatrix} A & B \\ C & D \end{pmatrix}; \quad \mathcal{D} = \begin{pmatrix} (m_i) & 0 \\ 0 & (M_i) \end{pmatrix}. \tag{4.55}$$

Now the equation (4.53) has the form

$$\begin{pmatrix} A^T & C^T \\ B^T & D^T \end{pmatrix} \begin{pmatrix} 0 & m_D \\ m_D^T & M_R \end{pmatrix} \begin{pmatrix} A & B \\ C & D \end{pmatrix} = \begin{pmatrix} (m_i) & 0 \\ 0 & (M_i) \end{pmatrix}. \tag{4.56}$$

The weak and mass eigenstates of light and heavy neutrinos are related as follows

$$\nu_{Li}^{(w)} = V_{i\alpha} \nu_{L\alpha}^{(m)} = (A\ B) \begin{pmatrix} \nu_{Li} \\ N_{Li} \end{pmatrix}, \tag{4.57}$$

where $i = 1, 2, 3$ and $\alpha = 1, 2...6$. Now the charged current of the leptons can be written as

$$\begin{aligned} \mathcal{L}_{\mathrm{CC}} &= -\frac{g}{\sqrt{2}} (\bar{L}_{Li} \gamma^\mu V_{i\alpha} \nu_{L\alpha}) W_\mu^+ + h.c. \\ &= -\frac{g}{\sqrt{2}} (\bar{L}_{Li} \gamma^\mu A_{ij} \nu_{Lj} + \bar{L}_{Li} \gamma^\mu B_{ij} N_{Lj}) W_\mu^+ + h.c. \end{aligned} \tag{4.58}$$

We do not expand the block matrix equations above here, but we summarize some important approximations. As $M_R \gg m_D$ one can derive approximations:

$$C^\dagger = -A^\dagger m_D M_R^{-1}, \tag{4.59}$$

which means that C is very suppressed and it is in the scale m_D/M_R. Also, we can derive the approximate mass values of light neutrino sector,

$$(m_i) = -A^\dagger m_D M_R^{-1} m_D^T A^*. \tag{4.60}$$

23

The matrix A is effectively the neutrino mixing matrix or Maki-Nakagawa-Sakata matrix, presented as U_{MNS} in Chapter 3. The matrix A has deviations from unitarity, but it is very suppressed, on the order of m_D^2/M_R^2.

There is correspondence between the present general case and the simplified case (4.42) above, $m_D \leftrightarrow m_3$ and $M_R \leftrightarrow m_2$. Using the approximation $M_R \gg m_D$ the generalized see-saw formula is in the form

$$m_{\text{eff}} \simeq -m_D M_R^{-1} m_D^T, \tag{4.61}$$

where m_D is the Dirac submatrix in the order of the electroweak scale and M_R is the submatrix of the right-handed neutrino fields in the order of the GUT scale.

If we develop a full scale theory of neutrinos we are interested in the connection between the low and high energy sector. For example, we can derive a relation between the submatrix B which connects the light and the submatrices of the heavy sector:

$$B = m_D D^* (M_i)^{-1}. \tag{4.62}$$

The equation shows that the connection is very suppressed and it is of the order of m_D/M_R.

Also, as it is described in Section 3.3 the mixing matrix has nine free parameters. Three parameters from 12 parameters (6 complex parameters) of the mixing matrix are absorbed by the phases of the complex neutrino fields. One can be interested to connect the mixing parameters and the neutrino mass observables. In general, the observables can be separated into two classes.

(i) The observables accessible to neutrino oscillation experiments: two mass differences (solar and atmospheric), three mixing angles and the CP phase.

(ii) The observables non-accessible to oscillation experiments: the lightest mass of three neutrinos and the two Majorana phases.

In conclusion, the type I see-saw is sometimes called as the most minimal see-saw mechanism. Only a set of right-handed neutrino fields added to the Standard Model Lagrangian. The leptonic Yukawa sector of the Lagrangian has two new terms

$$\mathcal{L}_Y \supset -\sum_{ij} \lambda_{ij}^e \bar{L}_L^i H e_R^j - \sum_{ij} \lambda_{ij}^N \bar{L}_L^i \tilde{H} N_R^j - \frac{1}{2} M_{ij}^N \bar{N}_R^i (N_R^c)^j + h.c., \tag{4.63}$$

where $i, j = 1, 2, 3$ are flavor indexes, N_R denotes the right-handed neutrino field, λ is the Yukawa coupling and M_{ij}^N is the mass matrix of right-handed neutrinos. The mass matrix M_{ij}^N corresponds to the scale of new physics, for example to the GUT scale.

After EWSB the $d = 5$ operator leads to the light neutrino mass in the flavor basis,

$$m_\nu = -\frac{v^2}{2} Y_N^T M_N^{-1} Y_N. \tag{4.64}$$

It is the same see-saw term that is presented in Eq. (4.61).

Type II see-saw

In the case of the type II see-saw the Standard Model content is extended only by the addition of a $SU(2)$ triplet of scalar fields with the hypercharge 2. It is usually denoted as

$$\vec{\Delta} \equiv (\Delta^1, \Delta^2, \Delta^3), \tag{4.65}$$

which has the physical eigenstates

$$(\Delta^{++}, \Delta^+, \Delta^0), \tag{4.66}$$

where the physical states are given by

$$\Delta^{++} = \frac{1}{\sqrt{2}}(\Delta^1 - i\Delta^2), \quad \Delta^+ = \Delta^3, \quad \Delta^0 = \frac{1}{\sqrt{2}}(\Delta^1 + i\Delta^2). \tag{4.67}$$

The minimal gauge invariant Lagrangian has the following Yukawa terms for the lepton and the Higgs sector

$$\begin{aligned} \mathcal{L}_Y \supset & [\bar{\tilde{L}}_L \lambda_\Delta (\vec{\sigma} \cdot \vec{\Delta}) L_L + \mu_\Delta \tilde{H}^\dagger (\vec{\sigma} \cdot \vec{\Delta})^\dagger H + h.c.] \\ & - [\vec{\Delta}^\dagger M_\Delta^2 \vec{\Delta} + \frac{1}{2}\lambda_2 (\vec{\Delta}^\dagger \cdot \vec{\Delta})^2 + \lambda_3 (H^\dagger H)(\vec{\Delta}^\dagger \vec{\Delta}) \\ & + \frac{\lambda_4}{2} (\vec{\Delta}^\dagger T^\alpha \vec{\Delta})^2 + \lambda_5 (\vec{\Delta}^\dagger T^\alpha \vec{\Delta}) H^\dagger \sigma^\alpha H], \end{aligned} \tag{4.68}$$

where $\alpha = 1, 2, 3$ is the $SU(2)$ index and repeated indices in a member mean summation.

From the Lagrangian above one $d = 4$ and one $d = 5$ operator emerges. The $d = 4$ operator is

$$\mathcal{L}^{d=4} = 2\frac{|\mu_\Delta|^2}{M_\Delta^2}(H^\dagger H)^2, \tag{4.69}$$

and the $d = 5$ operator leads to the mass term of the neutrino after EWSB,

$$m_\nu = -2\lambda_\Delta v^2 \frac{\mu_\Delta}{M_\Delta^2}. \tag{4.70}$$

It is a typical see-saw term. The term above has an important difference from the mass term (4.64) of the type I see-saw, it depends on the Yukawa coupling Y_Δ only linearly. In this case, the left and right hand side have the same number of parameters. It differs from the type I see-saw, where there are 9 unphysical parameters. It can shed some experimental light to the neutrino parameters in this case [95].

Type III see-saw

The last possibility considered, the type III see-saw, is the extension of the Standard Model with a $SU(2)$ triplet fermions with zero hypercharges. Let us note the triplet as

$$\vec{\Sigma} \equiv (\Sigma^1, \Sigma^2, \Sigma^3). \tag{4.71}$$

The eigenstates of electric charge are given by

$$\Sigma^\pm \equiv \frac{1}{\sqrt{2}}(\Sigma^1 \mp i\Sigma^2), \quad \Sigma^0 \equiv \Sigma^3. \tag{4.72}$$

The triplet $\vec{\Sigma}$ is an adjoint representation of the $SU(2)$ gauge group, thus the Majorana mass term is automatically gauge invariant. The Yukawa and mass terms in the Lagrangian are

$$\mathcal{L} \supset -\frac{1}{2}\bar{\vec{\Sigma}}_R M_\Sigma \vec{\Sigma}^c_R - \bar{\vec{\Sigma}}_R \lambda_\Sigma (\tilde{H}^\dagger \vec{\sigma} L_L) - h.c. \tag{4.73}$$

Three $\vec{\Sigma}$ components of $SU(2)$ have identical Majorana mass terms. After EWSB the terms induce Majorana neutrino masses for the left-handed neutrino fields of the Standard Model via the exchange of $\vec{\Sigma}$ fermions. Thus, the terms in the Lagrangian (4.73) generate a neutrino mass term

$$m_\nu = -\frac{v^2}{2}\lambda_\Sigma^T M_\Sigma^{-1} \lambda_\Sigma. \tag{4.74}$$

4.2.6 CP violation in and beyond the Standard Model

CP violation in the quark sector of the Standard Model

In the context of the current work we need to understand the mechanism of CP violation in the Standard Model and in the neutrino sector for the futher story of leptogenesis in the next chapter. We remember that CP (or P) violation is a necessary condition for baryogenesis (Subsec. 3.2, p. 48). The only source of the CP violation in the Standard Model is the CKM matrix via the Kobayashi-Masakawa (KM) mechanism.

Let us take a quick look at the KM mechanism in the Standard Model. First, it has shown that no model with just fermion and vector gauge fields cannot violate CP [102]. One possibility to violate CP in a model is to use scalar fields with complex couplings. For example, only the Higgs mechanism can be the source of CP violation in the Standard Model. The Yukawa couplings between the Higgs field and fermion fields are only complex couplings in the Standard Model. The vev of the Higgs can not be the source of the violation as one can absorb the phase in the Higgs field. Also, the Higgs self-interaction sector alone,

$$V = -\mu^2 H^\dagger H + \lambda (H^\dagger H)^2 + h.c., \tag{4.75}$$

can not be the source of the violation as the μ^2 and λ are real due to hermiticity constrains.

The necessary condition for CP invariance has a rather simple form [103],

$$\mathrm{tr}([H_u, H_d]^3) = 0, \tag{4.76}$$

where the Hermitian matrices H_u and H_d are defined as

$$H_u = m_u m_u^\dagger, \quad H_d = m_d m_d^\dagger, \tag{4.77}$$

and the matrices m_u and m_d are the mass matrices of the up and down type quarks in the Standard Model,

$$\begin{aligned} \mathcal{L}_{\mathrm{Y}}^{\mathrm{quark}} &\supset -\lambda_d \bar{Q}_L H d_R - \lambda_u \bar{Q}_L \tilde{H} u_R + h.c. \\ &\xrightarrow{\mathrm{EWSB}} -\bar{d}_L^{(m)} m_d d_R^{(m)} - \bar{u}_L^{(m)} m_u u_R^{(m)} + h.c. \end{aligned} \tag{4.78}$$

A great property of the condition (4.76) is that it is independent of the choice of basis. Also, it is possible to show that in the case of three generations the condition (4.76) reduces to a simpler form,

$$\mathrm{tr}([H_u, H_d]) = 0. \tag{4.79}$$

We are interested in the relations between the condition (4.76) and the quantities of the CKM matrix. First, we have to relate the quark fields in the Yukawa and the charged current terms. The Lagrangian of the charged current is

$$\mathcal{L}_{\mathrm{CC}}^{\mathrm{quark}} = \frac{g}{\sqrt{2}} W_\mu^+ \bar{u}_L^{(w)} \gamma^\mu d_L^{(w)} + h.c. \tag{4.80}$$

and the following unitary transformations relate the weak state (w) and mass state (m) as

$$u_L^{(w)} = U_L^u u_L^{(m)}, \quad u_R^{(w)} = U_R^u u_R^{(m)}, \tag{4.81}$$

$$d_L^{(w)} = U_L^d d_L^{(m)}, \quad d_R^{(w)} = U_R^d d_R^{(m)}. \tag{4.82}$$

The mass matrices are diagonalized by the unitary transformations U,

$$U_L^{u\dagger} m_u U_R^u = \mathrm{diag}(m_u, m_c, m_t), \tag{4.83}$$

$$U_L^{d\dagger} m_d U_R^d = \mathrm{diag}(m_d, m_s, m_b). \tag{4.84}$$

Now, the CKM matrix is defined by

$$\mathcal{L}_{\mathrm{CC}}^{\mathrm{quark}} = \frac{g}{\sqrt{2}} W_\mu^+ \bar{u}_L^{(m)} \gamma^\mu V_{\mathrm{CKM}} d_L^{(m)} + h.c., \tag{4.85}$$

where $V_{\mathrm{CKM}} = U_L^{u\dagger} U_L^d$. Also, we see that there is no similar matrix for the right-handed fields as they do not participate in the weak dynamics.

Finally, we are able to write down the condition (4.76) in the relation with the CKM matrix and quark masses [103],

$$\begin{aligned} \mathrm{tr}([H_u, H_d]^3) = 6i&(m_t^2 - m_c^2)(m_t^2 - m_u^2)(m_c^2 - m_u^2) \\ &\times (m_b^2 - m_s^2)(m_b^2 - m_d^2)(m_s^2 - m_d^2) \\ &\times \mathrm{Im}(V_{12}V_{23}V_{13}^* V_{22}^*), \end{aligned} \tag{4.86}$$

where V_{ij} denotes the entries of CKM matrix.

Let us make a quick analysis of the expression (4.86). From experiment we know that all the differences between the squared masses are nonzero. Thus, the nonzero value of the member $\mathrm{Im}(V_{12}V_{23}V_{13}^* V_{22}^*)$ is needed to guarantee CP violation in the Standard Model. Naturally, the CP symmetry is violated if V_{CKM} is a complex matrix, only then $\mathrm{Im}(V_{12}V_{23}V_{13}^* V_{22}^*) \neq 0$. Using the standard parametrization of V_{CKM} [11],

$$U = \begin{pmatrix} c_{12}c_{13} & s_{12}c_{13} & s_{13}e^{-i\delta} \\ -s_{12}c_{23} - c_{12}s_{23}s_{13}e^{i\delta} & c_{12}c_{23} - s_{12}s_{23}s_{13}e^{i\delta} & s_{23}c_{13} \\ s_{12}s_{23} - c_{12}c_{23}s_{13}e^{i\delta} & c_{12}s_{23} - s_{12}c_{23}s_{13}e^{i\delta} & c_{23}c_{13} \end{pmatrix}, \tag{4.87}$$

where $c_{ij} = \cos\theta_{ij}$, $s_{ij} = \sin\theta_{ij}$, and δ parametrizes the CP violation phase. The phase δ is not a rephasing invariant. If we like to give a rephasing invariant quantity then we can present V_{CKM} in the rephasing invariant terms. For example, a rephasing invariant form of V_{CKM} and a longer analysis is presented in [104].

CP violation in the lepton sector at low energy

In general, in the type I minimal see-saw the description of CP violation in the lepton sector is rather similar to the quark sector as it is presented above. However, some significant differences exist. The main difference come from the Majorana nature of neutrino. Let us present some basis invariant quantities for the lepton sector and let us try to relate them to physical observables in the neutrino mixing matrix. We will present here a short summary. For example, the longer study can be found in Ref. [105, 106].

First, let us start with the effective low energy theory ($M_R \gg m_D$) with only left-handed neutrinos. In the effective lepton mixing one can present an invariant expression for the CP violation which is rather analogous to the expression (4.86) in the quark sector,

$$\mathrm{tr}([h_{\mathrm{eff}}, h_l]^3) = 6i\Delta_{21}\Delta_{32}\Delta_{31}\mathrm{Im}[(h_{\mathrm{eff}})_{12}(h_{\mathrm{eff}})_{23}(h_{\mathrm{eff}})_{31}], \tag{4.88}$$

where $h_{\mathrm{eff}} = m_{\mathrm{eff}} m_{\mathrm{eff}}^\dagger$, $h_l = m_l m_l^\dagger$ and $\Delta_{\alpha\beta} = m_\alpha^2 - m_\beta^2$, where $\alpha, \beta = e, \mu, \tau$. Also, the charged mass matrix is taken to be real and diagonal. We remind from Eq. (4.61) that the effective mass matrix of neutrinos is defined in the type I see-saw as

$$m_{\mathrm{eff}} \simeq -m_D M_R^{-1} m_D^T. \tag{4.89}$$

The imaginary part in (4.88) can be fully expressed in the physical observables of the oscillation of neutrino,

$$\mathrm{Im}[(h_{\mathrm{eff}})_{12}(h_{\mathrm{eff}})_{23}(h_{\mathrm{eff}})_{31}] = -\Delta m_{21}^2 \Delta m_{31}^2 \Delta m_{32}^2 \times I, \tag{4.90}$$

where I is the imaginary part of an invariant quartet in the leptonic mixing matrix U_{MNS} and Δm_{ij} is the mass difference of neutrino masses in the mass basis. The imaginary part I is given by the mixing angles and phase of U_{MNS},

$$I = \frac{1}{8} \sin 2\theta_{12} \sin 2\theta_{23} \cos\theta_{13} \sin\delta. \tag{4.91}$$

In the quark sector I is of the order 10^{-5}. In the neutrino sector it can be larger, up to 10^{-2}.

The expression (4.88) does not count the Majorana phases which are unobservable in oscillation experiments. It is possible to show that the Majorana phases can be an additional source of CP violation in the effective low energy theory. For example, the exact relations are derived and presented in Ref. [106, 107].

CP violation in the lepton sector at high energy

We described CP violation in the low energy effective theory of neutrinos. Luckily, at low energy we have many physical observables available, for example the observables from the oscillation effects in vacuum and matter. However, we are interested in the CP violation of the full theory in general. For example, the CP violation of the heavy neutrinos can be the main source of the matter-antimatter asymmetry in the present Universe. A wide community of particle physicists has accepted the idea that baryogenesis appears through leptogenesis in the early Universe. A main reason is insufficient CP violation in the frames of the Standard Model. Alternatively, the neutrino mixing matrix can provide sufficient CP violation in the lepton sector. For example, leptogenesis can appear due to the effects of high energy neutrino sector in the type I see-saw. A variety of other models exists which relates leptogenesis to the type II see-saw or the so called *resonance effects*. Unfortunately, the parameters related to CP violation in the low and high energy sectors are rather independent. Only in some specific models can one derive stronger relations between low and high energy sector.

Let us take a quick at the type I see-saw model. We will not present here the invariant expressions needed to describe CP violation in the full theory. For example, CP violation of the full theory is the invariant described in the papers [106, 107]. We will give an example of the L violating decay of heavy neutrino which can be the main source of CP violation needed for leptogenesis in some models. Figure 4.5 presents some Feynman diagrams of the L violating process of the heavy neutrino N_k decay. The L asymmetry of the decay is parametrized as

$$\epsilon_\alpha \equiv \epsilon_{N_\alpha} = \frac{\sum_i \Delta\Gamma_i^\alpha}{\sum_i [\Gamma(N_\alpha \to l_i H^+) + \Gamma(N_\alpha \to \bar{l}_i H^-)]}, \tag{4.92}$$

where $\Delta\Gamma_i^\alpha = \Gamma(N_\alpha \to l_i H^+) - \Gamma(N_\alpha \to \bar{l}_i H^-)$, $\alpha = 1,2,3$ denotes the heavy neutrino species and $i = e, \mu, \tau$. Let us try to present the parameter just for the case $\alpha = 1$. In the next chapter of leptogenesis we show that in the case of $M_{N_3} \gg M_{N_2} \gg M_{N_1}$ only ϵ_1 (the decay of the lightest heavy neutrino) contributes to the final lepton asymmetry. From the diagrams in Figure 4.5 we can calculate

$$\Gamma(N_1 \to l H^+) \propto \sum_a |Y_{1a} + A \sum_{b,c} Y_{1b} Y_{cb}^* Y_{ca}|^2 \tag{4.93}$$

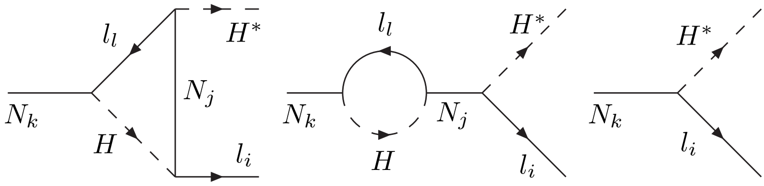

(a) (b) (c)

Figure 4.5: Feynman diagrams contributing to the asymmetry from the N_k decay.

and

$$\Gamma(N_1 \to \bar{l}H^-) \propto \sum_a |Y_{1a} + A\sum_{b,c} Y_{1b}Y^*_{cb}Y_{ca}|^2, \tag{4.94}$$

where A is the complex loop factor and Y denotes the matrix of the Yukawa couplings. Now we can present the parameter ϵ_1,

$$\epsilon_1 = \frac{1}{8\pi(YY^\dagger)_{11}} \sum_{a=2}^{3} \mathrm{Im}[(YY^\dagger)^2_{1a}]\mathrm{I}(\frac{M_a^2}{M_1^2}), \tag{4.95}$$

where the function $\mathrm{I}(x)$ is defined as

$$\mathrm{I}(x) = \sqrt{x}[(1+x)\mathrm{ln}(\frac{x}{1+x}) + \frac{2-x}{1-x}. \tag{4.96}$$

If we apply the mentioned assumption $M_{N_3} \gg M_{N_2} \gg M_{N_1}$ then we can simplify the function $\mathrm{I}(x)$ and the result is

$$\epsilon_1 = \frac{3}{16\pi(YY^\dagger)_{11}} \sum_{a=2}^{3} \mathrm{Im}[(YY^\dagger)^2_{1a}](\frac{M_1}{M_a}). \tag{4.97}$$

It is possible to show that by appling all the known experimental restrictions to the Y matrix we finally have only one free phase in the low energy sector and one mass and two phases at high energy. For example, see [106, 107] and the references presented there.

4.2.7 Running of the neutrino parameters

Nowadays we are able to measure particle processes up to the electroweak scale. We have presented the effective $d = 5$ operator in Eq. (4.26)

$$\mathcal{L} \supset \frac{\lambda_{ij}}{\Lambda}\bar{L}^i_L H \bar{L}^j_L H \xrightarrow{\text{EWSB}} \lambda_{ij}\frac{v^2}{\Lambda}\nu^i_L\nu^j_L. \tag{4.98}$$

25

The operator is defined at the scale Λ. On the other hand, in the present oscillation experiments we can measure the neutrino mixing below the weak scale. Also, all other conventional measurements can probe the parameters at the weak scale, for example in direct mass measurements or in double beta decay experiments. Thus, to understand the full theory of neutrinos one has to be able to run the neutrino parameters down from the scale Λ to the weak scale and back.

The renormalization of the neutrino parameters is rather complicated between the neutrino parameters measured at the low-energy neutrino experiments and any supposed mass matrix at the high-energy seesaw scale Λ. The main reason is that the renormalization depends on the unknown parameters in the seesaw model. The running based on the *renormalization group equations* (RGEs) has been studied extensively during some last years [108–110]. We can expect the neutrino mass matrix to be close to being bimaximal or diagonal at scale Λ, where Λ is typically fixed as the GUT scale, Λ_{GUT}. The observed low-energy neutrino mixing can be obtained starting from either the bimaximal [111–113] or from the diagonal [114–118] neutrino mass matrix at the GUT scale.

We will present here an example of the dependence of neutrino renormalization effects on all the seesaw parameters based on our study [119]. In this example we will pay special attention to obtaining the correct low-energy neutrino parameters as these parameters are reachable for experiment. The running of the effective neutrino mass matrix below the lightest singlet neutrino mass is generally well under control. The large renormalization effects can be expected only in the case of degenerate light neutrino masses. In the case of supersymmetric models, it can be expected for very large values of $\tan\beta$ [120–124]. However, understanding the renormalization effects above and between the heavy neutrino scales is much more complicated, since new non-trivial dependencies on the heavy neutrino Yukawa couplings Y_ν^{ij} are introduced [108–110, 125]. The flavor structure of the new contribution to the RGEs can be very different from that due to the effective neutrino mass matrix, thus some large effects are possible.

The couplings Y_ν^{ij} are largely unknown. Frequently, the *top-down* approach is realized in studies: the neutrino parameters are fixed at the GUT scale and then the parameters are run down to the electroweak scale. Finally, the low-energy neutrino parameters have to be compatible with experimental data from the neutrino experiments. In our example we will take a *bottom-up* approach. We will start from the known low-energy neutrino parameters and evaluate renormalization towards higher scales consistently in the framework of the MSSM seesaw model.

In our approach, every set of studied neutrino parameters is physical by construction. We will present nine high-energy parameters of seesaw using the orthogonal complex matrix R [126]. Then we will scan over the total set of seesaw parameters by generating the unknown parameters (including Dirac and Majorana phases) randomly. We will study the dependence of the renormalization effects on (i) the other observable low-energy and (ii) the high-energy parameters.

The superpotential of MSSM with singlet (right-handed) heavy neutrinos is given by

$$W = D^c Y_d Q H_1 + U^c Y_u Q H_2 + E^c Y_e L H_1 + N^c Y_\nu L H_2 + \frac{1}{2} N^c M N^c, \quad (4.99)$$

where the Yukawa matrices Y are general complex 3×3 matrices and the 3×3 heavy neutrino mass matrix M is symmetric. As it was presented above, the Yukawa matrices can be diagonalized by bi-unitary transformations $Y^D = U^\dagger Y V$, where V, U refer to the rotation of the left- and right-chiral fields. In the case of the symmetric matrix M, $U = V^*$. To explain the neutrino data naturally, the hierarchy in M should preferably be of the same order as the square of the hierarchy in Y_ν [127]. We therefore assume hierarchical heavy-neutrino masses: $M_1 \leq M_2 \leq M_3$.

Integrating out all the heavy singlet neutrinos, one gets the effective $d = 5$ operator

$$\mathcal{L} = -\frac{1}{2}\kappa L L H_2 H_2, \quad (4.100)$$

which after EWSB gives masses to the light neutrinos:

$$m_\nu(\mu) = \kappa(\mu) v^2 \sin^2\beta, \quad (4.101)$$

where μ is the renormalization scale, $v = 174$ GeV and $\tan\beta = v_2/v_1$ is the ratio of the vev's of the corresponding Higgs doublets. Above the heaviest neutrino mass scale, $\mu > M_3$, the light-neutrino mass matrix reads

$$m_\nu(\mu) = Y_\nu^T(\mu) M^{-1}(\mu) Y_\nu(\mu) v^2 \sin^2\beta. \quad (4.102)$$

Between the heavy-neutrino mass scales, $M_1 \leq M_2 \leq M_3$, there exist a series of effective theories with, in general, n active heavy neutrinos. The tree-level matching conditions between these theories at the neutrino thresholds are

$$\overset{(n)}{\kappa}_{gf}|_{M_n} = \overset{(n+1)}{\kappa}_{gf}|_{M_n} + \overset{(n+1)}{(Y_\nu)}_{ng} \overset{(n+1)}{M_n^{-1}} \overset{(n+1)}{(Y_\nu)}_{ng}|_{M_n}, \quad (4.103)$$

where (n) is the number of heavy neutrinos not integrated out. In general, the light-neutrino mass matrix can be written as

$$m_\nu = \left(\overset{(n)}{\kappa} + \overset{(n)}{Y_\nu^T}\overset{(n)}{M}{}^{-1}\overset{(n)}{Y_\nu}\right) v^2 \sin^2\beta. \tag{4.104}$$

Since m_ν and $Y_e^\dagger Y_e$ can be diagonalized with the unitary matrices V_ν and V_e, respectively, the mixing matrix observable in the low-energy experiments is

$$V_{MNS} = V_e^\dagger V_\nu. \tag{4.105}$$

While m_ν contains 9 physical parameters, Y_ν and M together contain 18 parameters. The missing 9 parameters crucially affect the physical observables. These include, for example, renormalization-induced lepton-number-violating processes [126,128–135] and electric dipole moments [132,136–140] in the supersymmetric seesaw model, as well as the renormalization of the light-neutrino parameters [108–110]. Therefore, to study the dependence of the renormalization of Eq. (4.104) on Y_ν, we parametrize Y_ν with the complex orthogonal matrix R [126]. In the basis in which M is diagonal, we write

$$\overset{(n)}{Y_\nu} = (\overset{(n)}{M}{}^D)^{\frac{1}{2}}\ \overset{(n)}{R}\,(m_\nu^D)^{\frac{1}{2}}\ V_\nu^\dagger\ (v\sin\beta)^{-1}, \tag{4.106}$$

where the matrix R is parametrized in terms of three *complex* angles θ_{12}^R, θ_{13}^R and θ_{23}^R:

$$R = \begin{pmatrix} c_{12}^R c_{13}^R & s_{12}^R c_{13}^R & s_{13}^R \\ -c_{23}^R s_{12}^R - s_{23}^R s_{13}^R c_{12}^R & c_{23}^R c_{12}^R - s_{23}^R s_{13}^R s_{12}^R & s_{23}^R c_{13}^R \\ s_{23}^R s_{12}^R - c_{23}^R s_{13}^R c_{12}^R & -s_{23}^R c_{12}^R - c_{23}^R s_{13}^R s_{12}^R & c_{23}^R c_{13}^R \end{pmatrix}, \tag{4.107}$$

where $s_{ij}^R \equiv \sin\theta_{ij}^R$ and $c_{ij}^R \equiv \cos\theta_{ij}^R$. Since Y_ν and M are renormalized, obviously also $\overset{(n)}{R}$, which consists of n rows, runs with energy. The RGEs for Y_ν and M can be found in [130, 131], and the RGEs for R were calculated in [141]. Using these, $\overset{(n)}{R}$ has to be evaluated at every heavy neutrino threshold when the matching is performed.

The scale dependence of the effective/combined quantities in Eq. (4.104) is characterized by the differential equation [108–110, 142–145]

$$\begin{aligned} 16\pi^2 \frac{d\overset{(n)}{X}}{dt} &= Y_e^\dagger Y_e + (\overset{(n)}{Y_\nu^\dagger}\overset{(n)}{Y_\nu})^T \overset{(n)}{X} + \overset{(n)}{X}(Y_e^\dagger Y_e + \overset{(n)}{Y_\nu^\dagger}\overset{(n)}{Y_\nu})^T \\ &\quad + (2\mathrm{Tr}(\overset{(n)}{Y_\nu^\dagger}\overset{(n)}{Y_\nu} + 3Y_u^\dagger Y_u) - 6/5g_1^2 - 6g_2^2)\overset{(n)}{X}, \end{aligned} \tag{4.108}$$

where $X = \kappa, Y_\nu^T M^{-1} Y_\nu$. Notice that below the M_1 scale $\overset{(n)}{Y}_\nu = 0$. Therefore one expects large renormalization effects to occur above the heavy-neutrino thresholds for two reasons. First, the Yukawa couplings Y_ν can be large. Second, the flavour structure of $Y_\nu^\dagger Y_\nu$ can be very different from the flavour structure of $Y_e^\dagger Y_e$ and κ. Both those effects can be traced back to the values of R via Eq. (4.106). Approximate analytical solutions to Eq. (4.108) have been derived in [108–110], which allow one to understand the generic behavior of the renormalization effects. However, due to enhancement/suppression factors and possible cancellations, the exact numerical solutions may differ considerably from those estimates.

Our study shows that the significant running effects can occur only when some of the light-neutrino masses have comparable contributions from more than one heavy neutrino N_i, and the light-neutrino mass scale is at least moderately degenerate. For example, for a normal hierarchy of neutrino masses, the complementarity relation between neutrino and quark mixing angles [146–150],

$$\theta_C + \theta_{12} = \frac{\pi}{4}, \tag{4.109}$$

where θ_C is the Cabibbo angle in the quark sector and θ_{12} is the neutrino mixing parameter, evolves very little between the GUT scale and the electroweak scale. Also, an example of running is given in Figure 4.6.

However, the other oscillation angles θ_{13} and θ_{23} run slightly more than θ_{12} and also beyond the expected measurement errors. In certain cases, we observe level crossing in the light-neutrino mass eigenstates that is accompanied by jumps in the oscillation angles. The running of the CP-violating oscillation phase δ is strong for random R but insignificant for $R = 1$.

26

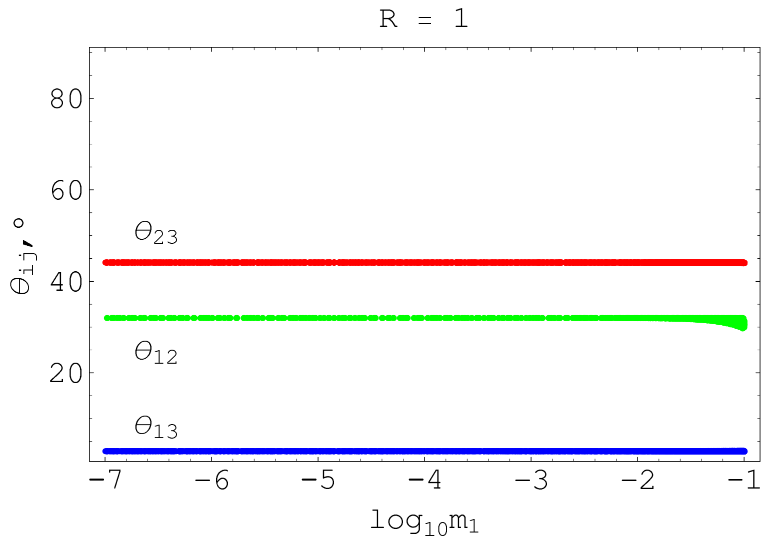

Figure 4.6: Neutrino mixing angles at the GUT scale Λ_{GUT} as functions of the lightest neutrino mass at $m_1(M_Z)$ for $R(M_Z) = 1$ (left panel), where M_Z notes the weak scale, and randomly generated R (right panel).

Chapter 5

Leptogenesis

5.1 Introduction

We described the problem of the matter-antimatter asymmetry in the present Universe in Section 3.2. If there were full symmetry between the matter and antimatter sector in Nature, there would have been no matter left for the present Universe. Luckily for us, the asymmetry exists. The parameter of the asymmetry is defined by Eq. (3.2) in Section 3.2 and its value is combined from CMB and BBN data [20] is

$$2.6 \cdot 10^{-10} < \eta < 6.2 \cdot 10^{-10}. \tag{5.1}$$

In Section 3.2 we presented the Sakharov conditions which must be satisfied for successful generation of the asymmetry (baryogenesis):

- Violation of CP- or P-symmetry
- Violation of baryon number B,
- thermal non-equilibum in the cosmological history of the Universe.

Let us consider the Standard Model to describe the particle content of the early Universe and let us try to estimate the value of η. We start with the plasma of baryons B and other particles at temperatures of O(1 GeV), where the process $B + \bar{B} \leftrightarrow 2\gamma$ is in equilibrium. The Universe cools and the process $2\gamma \rightarrow B + \bar{B}$ becomes ineffective because of the Boltzmann factor. The direct estimation of η (e.g. [151]) gives the approximate value,

$$\eta \simeq 10^{-18}. \tag{5.2}$$

In the context of the Standard Model, the difference between observation and theory can be explained, but it needs a very late decay of a scalar field at temperature O(100 MeV) to produce baryon excess [152].

Another scenario is the *GUT baryogenesis*, where baryon asymmetry is produced at the GUT scale [153–156]. At the GUT scale the quark-lepton unification provides the required B violation. The Yukawa couplings contain the required CP phases. Also, the Yukawa couplings satisfy the out-of-equilibrium condition at the GUT scale. Thus all the Sakharov conditions are satisfied and the asymmetry can be produced. In the quark-lepton unification $B - L$ is a global symmetry in $SU(5)$ GUTs. It becomes a local symmetry in $SO(10)$ or E_6 GUTs. Thus, L and/or B asymmetry generated at the GUT scale conserves $B - L$ and only $B + L$ asymmetry can be generated in the GUT models.

On the other hand, $SU(2)_L$ of the Standard Model has a global anomaly, where the baryon number B and the lepton number L are violated [157]. They are violated equal equally, thus their difference $B - L$ is still conserved. The anomalous sphaleron mediated $B + L$ violating process is heavily suppressed at zero temperature. This process can become fast at higher temperature [158]. The GUT scale 10^{16} GeV is sufficiently high for sphalerons to wash out any primordial $B + L$ asymmetry between $T_{\mathrm{EW}} \simeq 10^2$ GeV $< T < T_{\mathrm{sph}} \simeq 10^{12}$ GeV. However, if there is any $B - L$ asymmetry the sphalerons partially transfer the $B - L$ asymmetry to a B asymmetry. In summary, direct GUT-baryogenesis at the GUT temperature fails to explain the matter-antimatter asymmetry in the present Universe. If we can provide a mechanism to generate L asymmetry, it can be partially transferred to B asymmetry at a high enough temperature by sphalerons.

In the present work we will focus on a third class of theories for generation of matter-antimatter asymmetry, the *leptogenesis* [31]. The central idea of the leptogenesis is to use L violation required for the neutrino masses. The L violation processes generate a lepton asymmetry at some intermediate symmetry breaking scale between the GUT and EW scale. The sphaleron effects described above convert the generated lepton asymmetry to a baryon asymmetry before the EW phase transition.

In our view, leptogenesis proposes a most compelling mechanism for generating the observed baryon asymmetry in the Universe. Leptogenesis is strongly supported by the neutrino sector beyond the Standard Model. There is a link between leptogenesis and neutrino parameters, some already measured and some to be measured in the future.

5.2 Equilibrium physics in the early Universe

After the Big Bang, the early Universe was very hot and dense. The CMB measurements have shown to a very high accuracy that the spectrum of CMB is very close to the radiation spectrum of black body [20]. Thus, the Universe had to be very close to thermal equilibrium at least at the epoch of the last scattering, $z = 1100$. In addition, the distribution of elements from BBN is very homogeneous in the Universe. As we know BBN processes are very sensitive to thermodynamical conditions. Any spatial difference in the conditions influences the final spatial distribution of the elements. In conclusion, the early Universe is rather well described by thermodynamical quantities.

Let us describe thermodynamics in the early Universe. We will start with some assumptions. First, we can suppose that the early epochs of the Universe were radiation dominated. A particle is relativistic in the hot particle soup or *thermal bath* if the following condition is satisfied

$$m_i \ll T(t), \tag{5.3}$$

where m_i is the mass of the particle type i and $T(t)$ is the temperature of the bath. For example, all the known masses of the Standard Model particle are below O(100 GeV). If temperature is above O(100 GeV), all the Standard Model particles are relativistic. Naturally, if new physics beyond the Standard Model arises it can have particle masses above 100 GeV and their relativistic limit is at higher temperatures than 100 GeV.

In addition, thermal equilibrium is established by the rapid rate of particle interactions relative to the expansion rate of the Universe. Thus, we suppose the condition

$$\Gamma_i(t) \gg H(t), \tag{5.4}$$

where $\Gamma_i(t)$ is the interaction rate of the particle type i and $H(t)$ is the expansion rate measured by the Hubble expansion parameter. As we noted, both parameters in (5.4) have time dependence. Thus the relation (5.4) may not be valid through the course of the Universe. However, we suppose it is valid through some next calculations as it is a condition for equilibrium. Later we will consider the scenario $\Gamma_i(t) < H(t)$.

In equilibrium, we can compute thermodynamic quantities: density ρ, pressure p and the entropy density s. For a weakly interacting gas, where a gas particle has g internal degrees of freedom, the quantities are given by the phase space distribution function $f(\vec{p})$:

$$\rho = \frac{g_i}{(2\pi)^3} \int E_i f(\vec{p_i}) dp_i, \tag{5.5}$$

$$p = \frac{g_i}{(2\pi)^3} \int \frac{p_i^2}{3E_i} f(\vec{p_i}) dp_i, \tag{5.6}$$

$$n = \frac{g_i}{(2\pi)^3} \int f(\vec{p_i}) dp_i, \tag{5.7}$$

where $p = |\vec{p}|$, $E^2 = p^2 + m^2$ is the energy, n_i is the density of states and the index i denotes the different particle types. The phase space distribution is given by

$$f(p_i) = \frac{1}{\exp((E_i - \mu_i)/T) \pm 1}, \tag{5.8}$$

where the sign is $+1$ for the Fermi-Dirac distribution of fermions and it is -1 for the Bose-Einstein distribution of bosons, T is temperature and μ_i is *chemical potential*.

Typically, it is assumed that the chemical potentials are zero. For example, in the Standard Model a chemical potential is associated with baryon number. Since the baryon density relative to the photon density is known to be very small, order 10^{-10}, we may neglect these tiny chemical potentials in computation of total thermodynamic quantities. Using this approximation we can solve (5.5-5.7):

$$\rho = \left(\sum_b g_b + \frac{7}{8} \sum_f g_f \right) \frac{\pi^2}{30} T^4, \tag{5.9}$$

where $g_{b,f}$ is the number of degrees of freedom for boson (b) and fermion (f) species. We can define the function of effective number of degrees of freedom

$$N(T) \equiv \sum_b g_b + \frac{7}{8} \sum_f g_f, \tag{5.10}$$

which is a fractional number describing the relativistic plasma. The dependence of temperature takes into account new particle degrees of freedom due to (5.3) as temperature is raised.

The process where a particle species (together with its antiparticle) falls out from the inelastic interaction in thermal bath is called its *freeze out*. Below that freeze-out temperature, $N(T)$ loses the number of degrees of freedom connected to that particle species. In general, the value of

Temperature	New Particles	$4N(T)$
$T < m_e$	γ, ν	29
$m_e < T < m_\mu$	$e^\pm$	43
$m_\mu < T < m_\pi$	$\mu^\pm$	57
$m_\pi < T < T_{h\to q}$	π	69
$T_{h\to q} < T < m_s$	$\pi, u, \bar{u}, d, \bar{d}, g$	205
$m_s < T < m_c$	$s, \bar{s}$	247
$m_c < T < m_\tau$	$c, \bar{c}$	289
$m_\tau < T < m_b$	$\tau^\pm$	303
$m_b < T < m_{W,Z}$	$b, \bar{b}$	345
$m_{W,Z} < T < m_H$	$W^\pm, Z$	381
$m_H < T < m_t$	H	385
$m_t < T$	$t, \bar{t}$	427

Table 5.1: The number of degrees of freedom (function $N(T)$) in the case of the Standard Model. $T_{h\to q}$ corresponds to the confinement-deconfinement transition between quarks and hadrons.

$N(T)$ depends on the particle physics model. For the Standard Model we can calculate $N(T)$ up to temperatures of scale 100 GeV as we know the particles and their masses. Table 5.1 refers the values of $N(T)$ at different temperatures.

Naturally, at temperatures above Standard Model mass scales the exact form of $N(T)$ is unknown. Different GUT scenarios add different numbers of degrees of freedom. For example, $SU(5)$ adds 54 degrees of freedom for new gauge bosons and Higgses. Also, SUSY models double the number and add additional degrees of freedom via Higgs scalars. In conclusion, $N(T)$ depends strongly on our choice of the model.

Above we described how thermodynamics is able to predict some quantitative properties of the course of the Universe. However, in the case of non-equilibrium system reversible thermodynamics or statistical physics cannot work. Non-equilibrium thermodynamics or statistical physics is needed. In general, we need a theory to describe the kinetics of the Universe. The *Boltzmann equation* gives a good approximation for a non-equilibrium system.

5.3 Non-equilibrium physics in the early Universe

5.3.1 Overview

We considered the case of $\Gamma_X(t) \gg H(t)$ in thermal equilibrium. What will happen if it changes to $\Gamma_X(t) \ll H(t)$ or a particle mass gets bigger than the temperature of thermal bath, $T < m_X$, in the course of the cooling down of the Universe? In general, two extreme scenarios are possible for $T(t) < m_X$:

- $\Gamma_X(t) \gg H(t)$: the X particles can annihilate with the $\bar{X}$ antiparticles to lighter particles,
- $\Gamma_X(t) \ll H(t)$: a part of X particles and antiparticles cannot annihilate and the mixture of particles and antiparticles remains.

Also, it is possible that the X particle is not stable. For example, it has a half-life period shorter than the age of the Universe.

For example, as we know neutrino is a very weakly interacting particle, thus the condition $\Gamma_i(t) \ll H(t)$ is well established. Therefore, the Universe should be filled with the neutrino-antineutrino mixture, *cosmological neutrino background*, CνB. Also, CDM may originate from the same type of freeze-out process. An opposite example is electron-positron plasma. In the case of electromagnetic interaction, $\Gamma_i(t) \gg H(t)$. Thus, the electromagnetically interacting particles should annihilate during the decoupling of the plasma. In order to describe this type of processes we have to compose the system of the Boltzmann equations and solve it. In the next subsections we will descibe the kinetic theory and Boltzmann equations and how to compose the equation system for leptogenesis. We will give some general results for leptogenesis.

5.3.2 Kinetic theory and Boltzmann equations

If we need to model a non-equilibrium system, kinetic theory based on statistical physics can help us. Kinetic theory is based on the *particle distribution function*. All physical quantities can in principle be calculated from this function. For example,

$$\int_x^{x+\Delta x} \int_k^{k+\Delta k} f(x,k) DC^3 DJ^3, \tag{5.11}$$

give as the number of particles in the volume $(x, x+\Delta x)$ and in the range of momenta $(k, k+\Delta k)$. In the same sense we are able to calculate all kinds of physical quantities of the system. Also, as we need a relativistic theory, f has to be a Lorentz invariant. f has to be a real number, hence it is a Lorentz scalar.

The Boltzmann equation determines the behavior of f. In general formalism, one can divide it into two operators,

$$L[f] = C[f], \tag{5.12}$$

where L is the Liouville operator which describes the evolution of a momentum and space-time element,

$$L[f] = k^{\mu}\delta_{\mu} f(x, k), \tag{5.13}$$

and C is the collision operator which describes the change of the distribution function due to interaction between the particles. Usually, one can only account for binary interactions. We suppose space-time inversion symmetry, so C has the form

$$C[f] = \int W(q, r|k, p)[f(x, q)f(x, r) - f(x, k)f(x, p)]dp^3 sq^3 dr^3, \tag{5.14}$$

where the function $W(q, r|k, p)$ describes the transition rate which is the probability per unit time and volume that two particles from the initial state with the momenta k and p are scattered into the final state with the momenta q and r.

However, in general the space-time inversion symmetry may not be present: then the condition

$$W(q, r|k, p) = W(k, p|q, r), \tag{5.15}$$

is not valid. For example, the case of CP-violation is an example of asymmetry of W.

In addition, the Boltzmann equation hides some simplifications which should be checked carefully case-by-case when one starts to model a thermal system. First, the distribution function f has to be slowly varying in the range of the interaction. Second, the interaction time of the particles has to be short compared to the mean time between the collisions. Third, the particles are assumed to move freely between the collisions. Forth, the interacting particles have to be uncorrelated. In the Universe all of the assumptions are more or less satisfied. However, in the quantum field theory at finite temperature there are corrections to the third assumption. Also, in very dense environment validity of the forth assumption has to be checked carefully.

In cosmology the Liouville operator has to take into account the curvature of spacetime. The covariant form of the operator is

$$L[f] = k^{\mu}\frac{\partial}{\partial x^{\mu}} - \Gamma^{\mu}_{\nu\lambda}k^{\nu}k^{\lambda}\frac{\partial}{\partial k^{\mu}}, \tag{5.16}$$

where $\Gamma^{\mu}_{\nu\lambda}$ are connection coefficients. In an isotropic and homogeneous Universe one is able to simplify the operator to the form

$$L[f] = \frac{\partial}{\partial t} - \frac{1}{R}\frac{\partial R}{\partial t}k\frac{\partial f}{\partial k}. \tag{5.17}$$

We have to take into account that the thermal bath of the early Universe was very hot and consisted of many different particle species. We have a system of Boltzmann equations, an equation per species. In addition, we should account for the inelastic processes in the bath. In conclusion, the final form of the Boltzmann equation is complicated and typically no analytical solution is known. Sometimes, using some simplifications, it is possible to construct semianalytic solutions. For majority of cases, numerical solutions are needed.

5.3.3 Boltzmann equations in the early Universe

In the early Universe we are able to make some simplifications in the Boltzmann equations. On the other hand, we have to take care of the curved space-time and high temperature effects in the early Universe. Let us present here main steps to develop the Boltzmann equations for the early Universe.

The Standard Model particles are in kinetic equilibrium due to rapid elastic scattering in the early hot Universe. Thus the Maxwell-Boltzmann distribution,

$$f(T) = \exp(-E/T), \tag{5.18}$$

describes the particle content well and we do not have to count the different statistics for bosons and fermions. In principle, it is possible to write down a set of the kinetic equations using the different statistics of bosons and fermions, but at this high temperature the effect is negligible.

All particle species are characterized by their total abundance and it can vary only in inelastic processes. Rapid inelastic processes guarantee *chemical equilibrium.* Then using Eq. (5.7) and Eq. (5.6) we can present equilibrium pressure $p^{\rm eq}$ and concentration $n^{\rm eq}$ as,

$$n^{\rm eq} = \frac{gT^3}{\pi^2}, \quad \rho^{\rm eq} = \frac{3gT^4}{\pi^2}, \tag{5.19}$$

where g is the effective number of degrees of freedom (see Table 5.1). Every right-handed neutrino adds two degrees of freedom to the plasma.

The Boltzmann equation for the evolution of the species n_N in the thermal bath of the early Universe is

$$\frac{\partial n_N}{\partial t} + 3Hn_N = -\sum_{a,i,j...}[Na... \leftrightarrow ij...], \tag{5.20}$$

where H is the Hubble parameter $H = \dot{a}/a = \sqrt{8\pi\rho/3M_{\rm Pl}^2}$ which is needed for the dilution from the expansion of the Universe. The brackets denote the term

$$\begin{aligned}[Na... \leftrightarrow ij...] \equiv\ & \frac{n_N n_a...}{n_N^{\rm eq} n_a^{\rm eq}...}\gamma^{\rm eq}(Na... \to ij...) \\ & - \frac{n_i n_j...}{n_i^{\rm eq} n_j^{\rm eq}...}\gamma^{\rm eq}(ij... \to Na...).\end{aligned} \tag{5.21}$$

$\gamma^{\rm eq}$ denotes the space-time density of scattering in thermal equilibrium of the various interactions in which the Nth particle species takes part,

$$\gamma^{\rm eq}(Na \to ij) \equiv \int d\vec{p}_N d\vec{p}_a f_N f_a \int d\vec{p}_i d\vec{p}_j (2\pi)^4 \delta^4(P_N + P_a - P_i - P_j)|A|^2, \tag{5.22}$$

where $d\vec{p}_X = d^3p_X/2E_X(2\pi)^3$ and $|A|^2$ is the squared transition amplitude summed over initial and final spins. If we neglect a small CP-violating effect then the inverse processes have the same reaction densities.

In the next step we have to neglect some small effects. We will neglect (i) the Pauli-blocking effect (the bath is away from the fermionic condensation), (ii) the stimulated emission factors (particles are free). Also we assume that $|A|^2$ does not depend on the relative motion of particles with respect to the plasma. Now, the scattering rates $\gamma^{\rm eq}$ can be simplified. The case of decay is now

$$\gamma^{\rm eq}(N \to ij...) = \gamma^{\rm eq}(ij... \to N) = n_N^{\rm eq}\frac{K_1(z)}{K_2(z)}\Gamma_N, \tag{5.23}$$

where K are the Bessel functions, $z = m_N/T$ and Γ_N is the decay width in the rest system of the decaying particle N. The Bessel function K arises from the thermal average of the time dilatation factor m_N/E.

The thermal rate $\gamma^{\rm eq}$ of a two-body scattering in Eq. (5.22) can be rewritten using a trick to multiply Eq. (5.22) by $1 = \int d^4P\delta^4(P - P_N - P_a)$,

$$\gamma^{\rm eq}(Na \to ij...) = \frac{1}{8\pi}\int \frac{d^4P}{(2\pi)^4}\ \tilde{\sigma}(Na \to ij...)\ e^{-P_0/T}, \tag{5.24}$$

where $\tilde{\sigma}$ is the *reduced cross section* defined as $\tilde{\sigma} \equiv 2s\lambda[1, m_N^2/s, m_a^2/s]\sigma$ and the λ function is $\lambda[a,b,c] \equiv (a-b-c)^2 - 4bc$. The total cross section σ is summed over all final and initial quantum numbers: spin, gauge multiplicity etc. If the total cross section σ depends only on the squared center of mass energy s and not on the thermal motion with respect to the plasma we can use the relation $d^4P = 2\pi\sqrt{P_0^2 - s}\; ds\; dP_0$ and we get

$$\gamma^{\mathrm{eq}}(Na \leftrightarrow ij...) = \frac{T}{64\pi^4} \int_{s_{\min}}^{\infty} ds \sqrt{s}\; \tilde{\sigma}(s)\; \mathrm{K}_1\left(\frac{\sqrt{s}}{T}\right), \tag{5.25}$$

where $s_{\min} = max[(m_N + m_a)^2, (m_i + m_j + ...)^2]$.

In the expanding Universe it is convenient to represent the thermodynamic parameters as the ratios to the entropy density s. The consentration n can represented by the *normalized consentration* $Y = n/s$. We know that during the adiabatic expansion of the Universe the term sR^3 is constant and $R \propto 1/T$. Also, it means that $H\; dt = d\ln R = d\ln z$. The Boltzmann equations of the normalized consentration are

$$zHs\frac{dY_N}{dz} = - \sum_{a,i,j...} [Na \leftrightarrow ij...]. \tag{5.26}$$

Now we have a framework of the needed approximations and thus we have the kinetics of the evolution of the early Universe. We are ready to describe leptogenesis.

5.4 Leptogenesis

5.4.1 Overview

We will present leptogenesis in the framework of the Standard Model (plus the heavy neutrinos) as an example.[1] Below we typically speak about thermal Standard Model leptogenesis with non-degenerated masses of heavy Majorana neutrinos. Some SUSY Standard Model (MSSM) scenarios can be found in Ref. [159, 160]. For example, Ref. [161] with the references included presents a model of leptogenesis within the type II see-saw. Also, resonant scenarios with degenerated masses are an interesting prospect [162–164].

In the following text we use the mass hierarchy $m_{N_{2,3}} \gg m_{N_1}$. In general, the processes (couplings, masses etc) are sensitive to temperature

[1] In the following text the Standard Model leptogenesis is talked about the framework of the Standard Model and the heavy Majorana neutrino singlets in the type I see-saw.

and thermal corrections are needed. However, we will mention just some of them and we will not present a thorough overview of the effects. For example, an excellent description of thermal effects are given by Ref. [159].

Let us present the general schema of the Standard Model leptogenesis. First, some specific decay and scattering processes of the heavy neutrinos generate L asymmetry. The ΔL can be calculated by the Boltzmann equations of non-equilibrium environment. The next step is to convert the lepton asymmetry ΔL to baryon asymmetry ΔB. As already mentioned, it can be done using the sphaleron effects which are able to convert ΔL to ΔB using the conservation $L-B$ of sphalerons. Finally, during the cooling down of the Universe sphalerons inactivate at some temperature and the baryon asymmetry gets frozen.

In the case of the hierarchical right-handed neutrinos, $m_{N_{2,3}} \gg m_{N_1}$ one has to study the evolution of the number density of N_1 only as N_1 alone determines the final amount of $B-L$ asymmetry $Y_{B-L} = n_{B-L}/s$, where s is entropy and n denotes concentration. We assume no pre-existing asymmetry. The relation between the abundance of N_1 and the production of $B-L$ asymmetry can be parameterised as

$$Y_{B-L} = -\epsilon_{N_1} \eta Y_{N_1}^{\text{eq}}(T \gg m_{N_1}), \tag{5.27}$$

where ϵ_{N_1} is the CP-asymmetry parameter in N_1 decays at zero temperature and

$$Y_{N_1}^{\text{eq}}(T \gg m_{N_1}) = \frac{135\zeta(3)}{(4\pi^4 g^*)}, \tag{5.28}$$

where g^* counts the effective number of spin-degrees of freedom in thermal equilibrium. Table 5.1 shows that $g^* = 106.75$ in the Standard Model with no right-handed neutrinos. η denotes the efficiency which summarises all effects of the number density of N_1 with respect to the equilibrium value, the out-of-equilibrium condition at the decay and the thermal corrections to ϵ_{N_1}. The function ζ parameterises the unknown contribution of $N_{2,3}$. It is possible to show that it is important only in the case of $m_{N_1} \gtrsim 10^{14}$ GeV.

In the *one-flavour approximation* it is defined as

$$\zeta = \max(1, m_{\text{atm}}/\tilde{m}_1), \tag{5.29}$$

where the parameter $\tilde{m}_1$ denotes

$$\tilde{m}_1 \equiv \frac{(\Lambda_\nu \Lambda_\nu^\dagger)_1 1}{m_{N_1}} \upsilon^2. \tag{5.30}$$

and $(\Lambda_\nu)_{ij}$ denotes the Yukawa couplings between the lepton doublets and the singlets of heavy neutrinos,

$$\mathcal{L} \supset \Lambda^\nu_{ij} L_i N_j H + h.c. \tag{5.31}$$

In that case the η depends only on two parameters, $\tilde{m}_1$ and m_{N_1}. In addition, if $m_{N_1} \ll 10^{14}$ GeV then η depends only on $\tilde{m}_1$.

In the next step, we have to take into consideration sphaleron transitions. The baryon asymmetry is related to the $B-L$ asymmetry through the sphaleron effects,

$$\frac{n_B}{s} = \frac{24 + 4n_H}{66 + 13n_H} \frac{n_{B-L}}{s}, \tag{5.32}$$

where n_H is the number of Higgs doublets. In the case of the Standard Model,

$$\frac{n_B}{s} = -1.38 \times 10^{-3} \epsilon_{N_1} \eta. \tag{5.33}$$

Let us assuming the ΛCDM cosmological model. From Section 3.2 and from Eq. (3.2) there we remember that the summarized BBN and WMAP measurements give

$$\frac{n_B}{n_\gamma} = (6.15 \pm 0.25) \times 10^{-10}, \; s = 7.04\, n_\gamma. \tag{5.34}$$

The parameter η can be obtained from (numerical) solution of Boltzmann equations. For simplicity one usually ignores flavour issues and solves the approximated Boltzmann equation for the total lepton asymmetry as we will describe in some next subsections. The following representation of leptogenesis is mainly based on Refs. [159–162, 165].

5.4.2 Relevant decay and scattering processes for leptogenesis

The processes involved in leptogenesis can be classified as the decay processes and the lepton number changing scattering processes [159]. In the case of $m_{N_{2,3}} \gg m_{N_1}$ the asymmetry generated by the heavy $N_{1,2}$ is rapidly washed out by the lighter heavy neutrino. Thus the relevant processes are (see Figure 5.1):

- The decay of heavy neutrinos, $N \to HL$ (γ_D) (at very high temperature when the Higgs boson becomes heavier than N_1, also the process $H \to N_1 L$). The respecive reaction density is denoted in the brackets.

- The lepton number violating ($\Delta L = 2$) scatterings $LH \to \bar{L}\bar{H}$ and $LL \to \bar{H}\bar{H}$ (γ_N).
- The $\Delta L = 1$ scattering involving the top quark: $N_1\bar{L} \to Q_3 U_3$ (γ_{S_s}), $LQ_3 \to N_1 U_3$ and $LU_3 \to N_1 Q_3$ (γ_{S_t}) and their inverse reactions (the reaction density of the inverse reactions differs only up to small CP-violating corrections).
- The $\Delta L = 1$ scattering involving $SU(2)_L \otimes U(1)_Y$ gauge bosons A: $N_1\bar{L} \to HA$ (γ_{A_s}), $LH \to N_1 A$, $\bar{L}A \to N_1 H$ (γ_{A_t}).

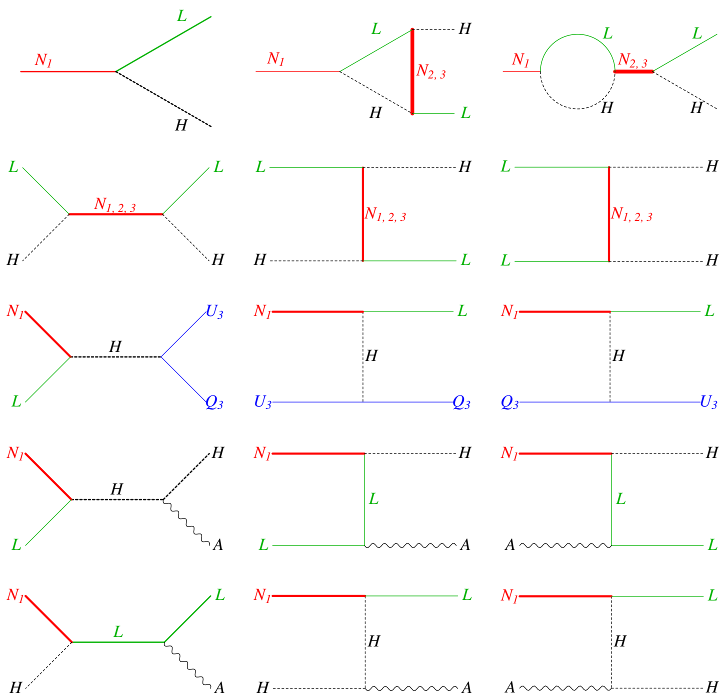

Figure 5.1: Feynman diagrams contributing to the thermal leptogenesis.

In the case of $m_{N_{2,3}} \gg m_{N_1}$, thermal corrections to N_1 propagation can be neglected since N_1 has no gauge interactions in the Standard Model and the Yukawa coupling is small in the temperature interval. The temperature corrections of the particle masses in the Standard Model are known [166–168]. Also, we have to include thermal corrections to the dispersion relations $\omega(k)$ of lepton doublets, third-generation quarks and the Higgs boson. Figure 5.2 presents the temperature dependence of the reaction densities for the fixed masses of the light and heavy neutrino, $\tilde{m}_1 = r\ |\Delta m| \cong 0.06$ eV and $m_{N_1} = 10^{10}$ GeV.

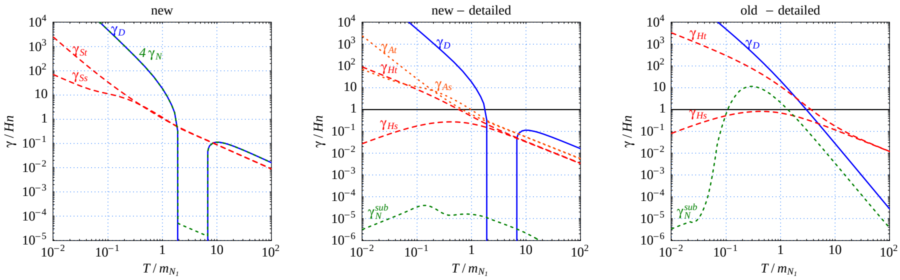

Figure 5.2: The Standard Model reaction densities for $\tilde{m}_1 \equiv (Y_\nu Y_\nu^\dagger)_{11}$, $v^2/m_{N_1} = 0.06$ eV and $m_{N_1} = 10^{10}$ GeV. The blue line denotes decays (γ_D), the red long-dashed lines the $\Delta L = 1$ scattering ($\gamma_{Ss,t} = \gamma_{Hs,t} + \gamma_{As,t}$) and the green dashed lines the $\Delta L = 2$ scattering (γ_N). The figure is adapted from [159].

.

5.4.3 The Boltzmann equations for leptogenesis and the solutions

Above we listed the relevant processes for leptogenesis. The sphaleron effects are negligible during the non-equilibrium phase of the decay and scattering processes. Using the brackets notation defined in Eq. (5.21), we define some short notations:

$$\Delta L = 1: \qquad D = [N_1 \leftrightarrow LH], \qquad S_s = H_s + A_s, S_t = H_t + A_t, \tag{5.35}$$

$$\Delta L = 2: \qquad N_s = [LH \leftrightarrow \bar{L}\bar{H}], \qquad N_t = [LL \leftrightarrow \bar{H}\bar{H}], \tag{5.36}$$

where we have used the notation

$$H_s = [LN_1 \leftrightarrow Q_3 U_3], \quad 2H_t = [N_1 \bar{U}_3 \leftrightarrow Q_3 \bar{L}] + [N_1 \bar{Q}_3 \leftrightarrow U_3 \bar{L}], \tag{5.37}$$

$$A_s = [LN_1 \leftrightarrow \bar{H} A], \qquad 2A_t = [N_1 H \leftrightarrow A\bar{L}] + [N_1 A \leftrightarrow \bar{H}\bar{L}]. \tag{5.38}$$

As mentioned, the decay and scattering quantities above depend on thermal effects and running of couplings (see Ref. [159] and the included references accordingly).

Now we assume that N_1, L and $\bar{L}$ fall out from thermal equilibrium. While the normalised concentrations $Y_H = Y_H^{\mathrm{eq}}$, $Y_{Q_3} = Y_{Q_3}^{\mathrm{eq}}$, and $Y_{U_3} = Y_{U_3}^{\mathrm{eq}}$ stay in thermal equilibrium. The Boltzmann equations are

$$zHsY'_{N_1} = -D - \bar{D} - S_s - \overline{S_s} - S_t - \overline{S_t}, \tag{5.39}$$

$$zHsY'_L = D - N_s - N_t - S_s + \overline{S_t}, \tag{5.40}$$

$$zHsY'_{\bar{L}} = \bar{D} + N_s - \overline{N_t} - \overline{S_s} + S_t. \tag{5.41}$$

Now we are able to write the decay rates in terms of the CP-conserving total decay rate γ_D and of the CP-asymmetry $\epsilon_{N_1} \ll 1$:

$$\gamma^{\mathrm{eq}}(N_1 \to LH) = \gamma^{\mathrm{eq}}(\bar{L}\bar{H} \to N_1) = \frac{(1+\epsilon_{N_1})}{2}\gamma_D, \tag{5.42}$$

$$\gamma^{\mathrm{eq}}(N_1 \to \bar{L}\bar{H}) = \gamma^{\mathrm{eq}}(LH \to N_1) = \frac{(1-\epsilon_{N_1})}{2}\gamma_D, \tag{5.43}$$

from the equations we can express D and $\bar{D}$,

$$D = \frac{\gamma_D}{2}\left[\frac{Y_{N_1}}{Y_{N_1}^{\mathrm{eq}}}(1+\epsilon_{N_1}) - \frac{Y_L}{Y_L^{\mathrm{eq}}}(1-\epsilon_{N_1})\right], \tag{5.44}$$

$$\bar{D} = \frac{\gamma_D}{2}\left[\frac{Y_{N_1}}{Y_{N_1}^{\mathrm{eq}}}(1-\epsilon_{N_1}) - \frac{Y_{\bar{L}}}{Y_{\bar{L}}^{\mathrm{eq}}}(1+\epsilon_{N_1})\right]. \tag{5.45}$$

The equilibrium values $Y_{N_1}^{\mathrm{eq}}$, Y_L^{eq} and $Y_{\bar{L}}^{\mathrm{eq}}$ are equal at high temperature as they have equal number of fermionic (two) degrees of freedom.

The Boltzmann equations need some subtractions due to some on-shell propagators [159, 162, 169–173]. We will summarise the result in some figures. Figure 5.3 presents a case of the normalised reaction rate N_{N_1} and the $B-L$ asymmetry produced accordingly. The next figure, Figure 5.4, presents two different cases of the evolution: the left-side panel shows the corrected normalised concentrations (the full set of thermal effects and the subtracted on-shell scattering effects) and the right-side panel shows the concentrations without the corrections.

5.4.4 Sphaleron effects

The normalised concentration of lepton asymmetry Y_L has to be converted to baryon asymmetry. Let us denote the corresponding normalised concentration as Y_B. The question is in the effectiveness of conversation process: we have to include sphaleronic scatterings to convert the lepton asymmetry into a baryon asymmetry.

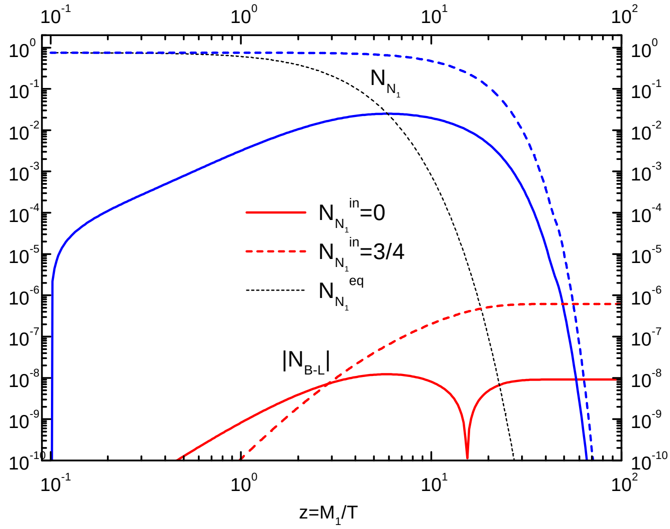

Figure 5.3: Evolution of the N_1 abundance $B-L$ asymmetry for $\tilde{m} = 10^{-5}$ eV, $M_{N_1} = 10^{10}$ GeV, thermal effects are not included. The figure is adapted from [174].

It is possible to show that it can be done by the conversion of the Boltzmann equation for Y_L into a Boltzmann equation for Y_{B-L}. The concentration Y_{B-L} is not affected by sphalerons. Thus we only need to find the relation between Y_{B-L} and Y_L.

At higher temperatures, $T > 10^{10}$ GeV, the sphaleronic scatterings are expected to be negligibly slow with respect to the expansion rate $H(T)$ of the Universe,

$$\Gamma_{\text{sph}}(T) \ll H(T),\ T > 10^{10} \text{ GeV}, \tag{5.46}$$

which means a very simple relation,

$$Y_L = -Y_{B-L}. \tag{5.47}$$

At lower temperatures sphaleronic processes are in thermal equilibrium. If all the Standard Model Yukawa couplings are large, the relation becomes,

$$Y_L = -(63/79)Y_{B-L}. \tag{5.48}$$

If the Yukawa couplings are negligible then

$$Y_L = -(9/8)Y_{B-L}. \tag{5.49}$$

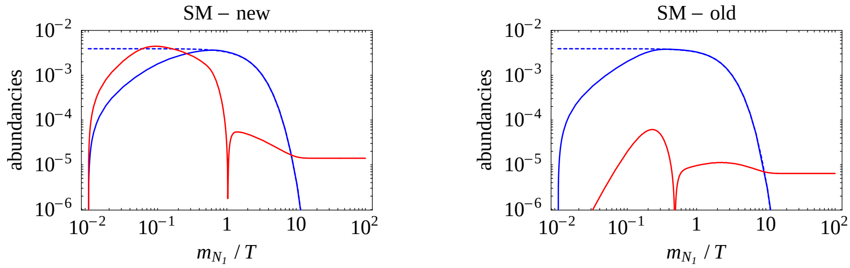

Figure 5.4: Evolution of the effective concentrations Y_{N_1} (blue curves) and $|Y_{B-L}/\epsilon_{N_1}|$ (red curves) with temperature in the Standard Model, the temperature effects are compared. The parameters are fixed as $m_{N_1} = 10^{10}$ GeV and $\tilde{m}_1(m_{N_1}) = 0.06$ eV. The dashed line shows the thermal abundance of Y_{N_1}. The left presentes a set of new effects (mostly thermal) included (in the means of Ref. [159]). The efficiency is $\eta = 0.0036$. The right plot presents the computations with no new effect included and on-shell scatterings incorrectly subtracted, $\eta = 0.0017$. The figure is adapted from [159].

In reality the situation is somewhere between the cases (5.48) and (5.49). Some couplings mediate equilibrium reactions and some others are negligible. Thus without making any approximations one cannot ignore flavour and the calculation can proceed as in Ref. [123]. To study the sharing of the lepton asymmetry between the three generations one has to consider the evolution of the full flavour density matrix.

Within acceptable accuracy (10%) one may approximate $Y_L \approx -Y_{B-L}$ and then solve the full set of Boltzmann equations (5.39) above, just replacing $-Y_{B-L} \to Y_L$.

5.4.5 Effects of inflaton and reheating

The Standard Model of cosmology presumes that the early Universe undergoes an inflation phase. Preferredly, the inflation is explained as an effect of a scalar *inflaton* field, ϕ. The inflation phase ends when the inflaton field decays. In the end of inflation phase, the Universe was very cold due to enormus expansion and a source of reheating needed. The source of reheating can be the decay of the inflaton. We are interested in how the reheating influences the Boltzmann equations for the final B asymmetry. One also should take reheating into account as it ifluences the kinetics of

N_1 decays.

Including these reheating effects, the Boltzmann equations become [159]:

$$HZz\frac{d\rho_\phi}{dz} = -3H\rho_\phi - \Gamma_\phi\rho_\phi, \tag{5.50}$$

$$sHZz\frac{dY_{N_1}}{dz} = 3sH(Z-1)Y_{N_1} - \left(\frac{Y_{N_1}}{Y_{N_1}^{\rm eq}} - 1\right)(\gamma_D + 2\gamma_{Ss} + 4\gamma_{St}), \tag{5.51}$$

$$\begin{aligned} sHZz\frac{dY_{B-L}}{dz} &= 3sH(Z-1)Y_{B-L} - \gamma_D\epsilon_{N_1}\left(\frac{Y_{N_1}}{Y_{N_1}^{\rm eq}} - 1\right) - \\ &- \frac{Y_{B-L}}{Y_L^{\rm eq}}\left(\frac{\gamma_D}{2} + 2\gamma_N^{\rm sub} + 2\gamma_{St} + \gamma_{Ss}\frac{Y_{N_1}}{Y_{N_1}^{\rm eq}}\right), \end{aligned} \tag{5.52}$$

where s and ρ_R are the entropy and energy density of the Standard Model particles, H is the Hubble constant at temperature T,

$$H = \sqrt{\frac{8\pi}{3M_{\rm Pl}^2}(\rho_R + \rho_{N_1} + \rho_\phi)}, \tag{5.53}$$

and Z takes into account reheating,

$$Z = 1 - \frac{\Gamma_\phi\rho_\phi}{4H\rho_R} - \frac{\gamma_D + 2\gamma_{Ss} + 4\gamma_{St}}{4H\rho_R}\frac{\rho_{N_1}^{\rm eq}}{n_{N_1}^{\rm eq}}\left(\frac{Y_{N_1}}{Y_{N_1}^{\rm eq}} - 1\right). \tag{5.54}$$

5.4.6 Summary of the type I leptogenesis

We presented a short overview of a version of leptogenesis mainly based on Refs. [159–162, 165]. The used neutrino model is based on the type I see-saw thus it is frequently noted as the type I leptogenesis. In general, leptogenesis has a number of different versions. However, we mainly focused on methodology needed to describe leptogenesis in general: kinetic theory, sphaleron effects, effects of inflaton and reheating.

Let us summarize some main conclusions for the type I leptogenesis in the case of the mass hierarchy $m_{N_{2,3}} \gg m_{N_1}$. First, Figure 5.4 describes the evolution of the N_1 and $B-L$ abundances at $\tilde{m}_1(m_{N_1}) = r|\Delta m_{\rm atm}| = 0.06$ eV and $m_{N_1} = 10^{10}$ GeV. It shows that leptogenesis depends only on the later stages of the evolution at relatively small temperatures, where the N_1 abundancy remains close to thermal equilibrium. Thus the final baryon asymmetry is only a weakly dependent on the initial abundancy of N_1 at higher temperatures.

Let us classify the result using three different cases (in following Ref. [159]), assuming no pre-existing $B-L$ asymmetry:

(1) The initial abundance of N_1 is zero, $Y_{N_1}=0$ at $T \gg m_{N_1}$. The scenario can be realised if the inflaton cannot decay into heavy neutrinos and the field is decaying mostly into the particles of the Standard Model.

(2) The initial abundance of N_1 is fully thermal, $Y_{N_1}=Y^{\rm eq}_{N_1}$ at $T \gg m_{N_1}$. This case needs extra interactions at $T \gg m_{N_1}$ to thermalize N_1. For example, an interaction can be mediated by a heavy Z' boson related to $SO(10)$ unification.

(3) The initial thermal bath is dominated by the abundancy of N_1, $\rho_{N_1} \gg \rho_R$ in the early Universe. For example, this case can be realised if an inflaton decays mostly into N_1.

In the introduction of leptogenesis we defined the efficiency parameter η that summarises all effects of the number density of N_1 with respect to the equilibrium value, the out-of-equilibrium condition at the decay and the thermal corrections to ϵ_{N_1}. As mentioned above, if $m_{N_1} \ll 10^{14}$ GeV the parameter η depends almost only on $\tilde{m}_1$. Figure 5.5 shows η as a function of $\tilde{m}_1$ for $m_{N_1}=10^{10}$ GeV. If $\tilde{m}_1 > 10^{-2}$ eV then the neutrino Yukawa couplings keep N_1 close to thermal equilibrium and η does not depend on the unknown initial N_1 abundancy. As we mentioned above, an pre-existing lepton asymmetry would be washed out similarly, if the Yukawa couplings of N_1 act on all flavours.

If $\tilde{m}_1$ is smaller the efficiency η depends on the initial N_1 abundancy ranging between the classification cases (1) and (2) above (the gray band in Figure 5.5). The maximal value of $\eta \sim g^*$ is reached at $\tilde{m}_1 \sim \tilde{m}_1^* \equiv 256\sqrt{g^*}v^2/3M_{\rm Pl} = 2.2\times 10^{-3}$ eV in case (3). The parameter η decreases at $\tilde{m}_1 \ll \tilde{m}_1^*$ because the particles H and L emitted in the N_1 decays have energy larger than the temperature T and split up in $\sim m_{N_1}/T^{N_1}_{\rm RH}$ particles correspondingly increasing the lepton asymmetry. It means that $\eta \sim g^*\sqrt{\tilde{m}_1^*/\tilde{m}_1}$.

If $\tilde{m}_1 \lesssim 10^{-6}$ eV, N_1 reheating starts to be significant even in case (1), giving $\eta < 1$. Even if N_1 initially has a thermal abundancy $\rho_{N_1}/\rho_R \sim g_{N_1}/g^* \ll 1$, its contribution to the total density of the Universe becomes non-negligible, $\rho_{N_1}/\rho_R \sim (g_{N_1}m_{N_1})/(g^*T)$, where it decays strongly out of equilibrium at $T \ll m_{N_1}$. This effect gives a suppression of η and for very small $\tilde{m}_1$ the case (1) and (3) give the same result.

31

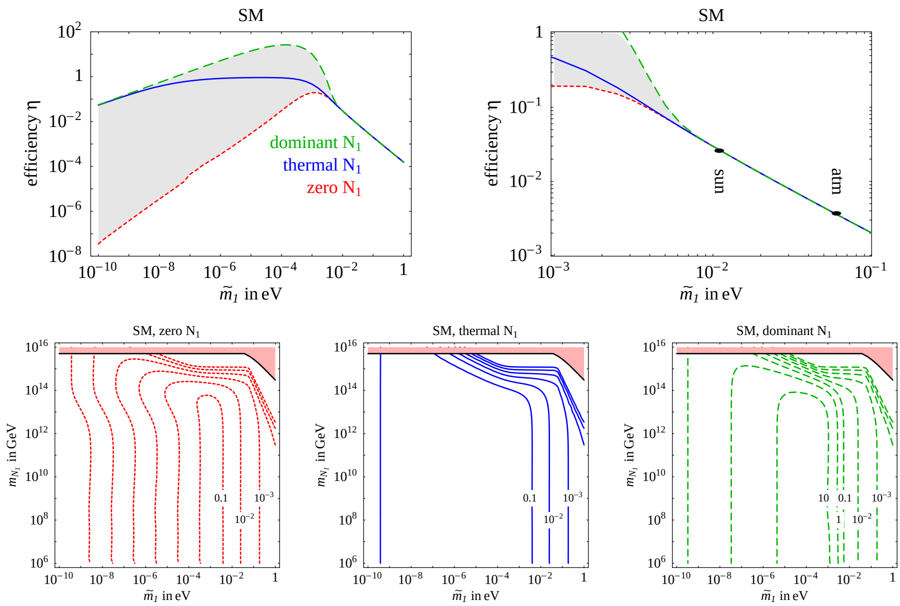

Figure 5.5: Efficiency η of leptogenesis in the Standard Model, assuming zero (dashed red line), thermal (continuous blue line) or dominant (long dashed green line) initial N_1 abundancy. In the upper plots η is a function of $\tilde{m}_1$ for $m_{N_1} = 10^{10}$ GeV renormalized at m_{N_1}. In the lower plots the contours of $\ln\eta(\tilde{m}_1, m_{N_1}) = -6, -5, \ldots, -1, 0, 1$. In the shaded regions the Yukawa couplings of neutrino are non-perturbative. The figure is adapted from [159].

The lower panel of Figure 5.5 presents the efficiency η of thermal leptogenesis computed in the cases (1), (2) and (3) as a function of $\tilde{m}_1$ and m_{N_1}. At $m_{N_1} \lesssim 10^{14}$ GeV non-resonant $\Delta L = 2$ scatterings strongly suppress η.

In conclusion, the given example of leptogenesis shows that the scenario of leptogenesis can produce the needed amount of baryon asymmetry. Also, the model represents some restrictions for the neutrino related parameters and the development scenarios of the early Universe. The example above introduced the Standard Model (plus type I see-saw neutrinos) leptogenesis with the condition $m_{N_{2,3}} \gg m_{N_1}$. The degenerate scenario $m_{N_1} \simeq m_{N_2}$ or even $m_{N_1} \simeq m_{N_2} \simeq m_{N_3}$ is also possible and exciting (e.g. [162, 163]). Also, the SUSY leptogenesis adds some new effects and restrictions on leptogenesis (see Ref. [159] and the included references). In next subsection we give a very short introduction to the model of leptogenesis based on the type II see-saw [161, 175, 176].

5.4.7 Alternative directions: type II leptogenesis

The most popular realizations of leptogenesis based on the type I seesaw mechanism. An alternative is leptogenesis based on the type II seesaw in which a $SU(2)_L$ triplet scalar Δ with non-zero hypercharge is exchanged as it was discussed in Subsection 4.2.5. In the supersymmetric scenario, the anomaly cancellation requires minimally a pair of triplets Δ, $\bar{\Delta}$ with opposite $U(1)_Y$ quantum numbers. However, only the triplet Δ couples to leptons.

The two leptogenesis scenarios differ:

- The type I seesaw has two sources of flavour structure: the Yukawa coupling matrix Y_N of the singlets N with the $SU(2)_L$ leptons and the mass matrix M_N of the states N, which combine to give $\mathcal{K}/M = Y_N^T M_N^{-1} Y_N$.
- The type II seesaw scenario has only one source of flavour: the symmetric Yukawa matrix Y_Δ of the triplet Δ couplings with the leptons, $\mathcal{K}/M = \lambda_2 Y_\Delta / M_\Delta$, where M_Δ is the triplet mass and λ_2 is a dimensionless "unflavoured" Higgs coupling.

As we see, in the type I see-saw the high-energy quantities, Y_N and M_N contain 18 parameters. Thus, they cannot be univocally related to the 9 low-energy neutrino parameters, which are encoded in the neutrino mass matrix m_ν. In the type II see-saw the high-energy quantity Y_Δ, which contains 9 parameters, can be matched directly to the flavour structure of the matrix m_ν [177–181]. Only the overall mass scale M_T/λ_2 is left undetermined.

The type II non-supersymmetric see-saw with one triplet Δ or the type II (minimal) supersymmetric seesaw with a pair $\Delta, \bar{\Delta}$ both contain sources of L and CP violation at high scale, but they cannot effectively induce leptogenesis [175, 182]. Successful leptogenesis has been achieved by adding one more vector-like $\Delta^{'}$, $\bar{\Delta}^{'}$ pair [175, 182], which means one additionl Yukawa matrix $Y_{\Delta^{'}}$. In such a case 9 additional flavour parameters will be included and the direct connection between the high-energy flavour structure and the low-energy one is lost.

Alternatively, it is possible to combine the hybrid type I plus type II model, which can be motivated by left-right and SO(10) models. In these models a single triplet couples to leptons [176, 183–188]. The successful leptogenesis can be obtained in agreement with neutrino data [176].

In summary, the minimal supersymmetric type II seesaw scenario with a single pair of triplets can generate successful leptogenesis through the L-violating decays of these states. The necessary CP-asymmetry for the observed baryon asymmetry arises from the interference between supersymmetric and soft-breaking terms and by a resonant-enhancement due to the "soft" mass splitting of the triplets Δ and $\bar{\Delta}$. In this case the mass of the triplet states should be in the range $(10^3 - 10^9)$ GeV depending on the size of the soft-supersymmetry breaking parameters. The detailed description of a version of type II leptogenesis is given in the included publication of the dissertant [161].

Chapter 6

Summary

This thesis links together a set of publications from the dissertant, which are devoted to neutrino physics in general. The work is focused on different neutrino related topics: neutrino physics in the context of cosmology and general particle physics, the mechanisms of neutrino mass generation and the properties of the different neutrino models and leptogenesis.

The thesis starts with a short description of particle physics and cosmology. Chapter 3 focused on experimental and observational effects beyond the Standard Model. The next chapter described some neutrino models beyond the Standard Model. The three mechanisms for neutrino mass were described: type I, II and II see-saw. In addition, CP-violation in the neutrino sector and the running of neutrino parameters were discussed. Chapter 5 introduced leptogenesis. The type I leptogenesis was presented as a most popular example of leptogenesis. Also, some short notes were made for the type II leptogenesis. The publications related to the thesis are summarized in the following separate chapter.

Chapter 7

Summary of the related publications

The thesis links the studies of three publications from the dissertant [119, 161, 189]. This work does not include the set of publication and technical notes from the dissertant, which are not directly related to neutrino physics. This excluded set of publications covers some experimental, detailed technical and computational topics in particle physics (and in related topics) [190–196]. A bunch of them are related to the dissertant's work with the CMS detector at the CERN LHC experiment [191–194].

7.1 Publication I

A. Hektor, M. Kadastik, M. Müntel, M. Raidal, and L. Rebane.
Testing neutrino masses in little Higgs models via discovery of doubly charged Higgs at LHC.
Nucl. Phys., **B787**, 198-210, 2007, [hep-ph/0705.1495].

In the paper we have investigated the possibility of direct tests of little Higgs models incorporating triplet Higgs neutrino mass mechanism at the CERN LHC experiments. We have performed Monte Carlo studies of Drell-Yan pair production of doubly charged Higgs boson Φ^{++} followed by its leptonic decays whose branching ratios are fixed from the neutrino oscillation data. We propose appropriate selection rules for the four-lepton signal, including reconstructed taus, which are optimized for the discovery of Φ^{++} with the lowest LHC luminosity phase. The Standard Model background can be effectively eliminated, thus an important aspect of our study is the correct statistical treatment of the LHC discovery potential. Adding detection efficiencies and measurement errors to the Monte Carlo analyses, Φ^{++} can be discovered up to the mass 250 GeV in the first year of LHC, and 700 GeV mass is reachable for the integrated luminosity $L = 30$ fb^{-1} of LHC.

7.2 Publication II

J. Ellis, A. Hektor, M. Kadastik, K. Kannike, and M. Raidal.
Running of Low-Energy Neutrino Masses, Mixing Angles and CP Violation.
Phys. Lett., **B631**, 32-41, 2005, [hep-ph/0506122].

We calculate the running of low-energy neutrino parameters from the bottom up. We use the parametrization of the unknown seesaw parameters in terms of the dominance matrix R. We find significant running only if the R matrix is non-trivial and the light-neutrino masses are moderately degenerate. In the case of the very hierarchical light-neutrino masses, the quark-lepton complementarity relation $\theta_c + \theta_{12} = \pi/4$ is rather stable, but $\theta_{13,23}$ may run beyond their likely future experimental errors. The running of the oscillation phase δ is enhanced by the smallness of θ_{13}, and jumps in the mixing angles occur in cases where the light-neutrino mass eigenstates cross.

7.3 Publication III

G. D'Ambrosio, T. Hambye, A. Hektor, M. Raidal, and A. Rossi.
Leptogenesis in the minimal supersymmetric triplet seesaw model.
Phys. Lett. B, **604**, 3-4, 199–206, 2004, [hep-ph/0407312].

In the (supersymmetric) triplet (type II) seesaw model, in which a single $SU(2)_L$-triplet couples to leptons, the high-energy neutrino flavour structure can be directly determined from the low-energy neutrino data. We show that even with such a minimal triplet content, leptogenesis can be naturally accommodated thanks to the resonant interference between superpotential and soft supersymmetry breaking terms. A set of bondaries for the neutrino parameters are shown.

Bibliography

[1] E. P. Wigner, Annals Math. **40**, 149 (1939).

[2] S. L. Glashow, Nucl. Phys. **22**, 579 (1961).

[3] A. Salam and J. C. Ward, Phys. Lett. **13**, 168 (1964).

[4] S. Weinberg, Phys. Rev. Lett. **19**, 1264 (1967).

[5] M. Gell-Mann, Phys. Lett. **8**, 214 (1964).

[6] D. J. Gross and F. Wilczek, Phys. Rev. Lett. **30**, 1343 (1973).

[7] H. D. Politzer, Phys. Rev. Lett. **30**, 1346 (1973).

[8] H. Fritzsch, M. Gell-Mann, and H. Leutwyler, Phys. Lett. **B47**, 365 (1973).

[9] S. R. Coleman and J. Mandula, Phys. Rev. **159**, 1251 (1967).

[10] R. Haag, J. T. Lopuszanski, and M. Sohnius, Nucl. Phys. **B88**, 257 (1975).

[11] W.-M. Yao *et al.*, Journal of Physics G **33**, 1+ (2006).

[12] G. L. Fogli and E. Lisi, Phys. Lett. **B228**, 389 (1989).

[13] M. Sher and Y. Yuan, Phys. Lett. **B285**, 336 (1992).

[14] L3, P. Achard *et al.*, (2005), hep-ex/0511049.

[15] CDF, C. Hays, (2005), hep-ex/0505064.

[16] OPAL, G. Abbiendi *et al.*, Eur. Phys. J. **C45**, 307 (2006), hep-ex/0508060.

[17] L3, P. Achard *et al.*, Phys. Lett. **B585**, 42 (2004), hep-ex/0402001.

[18] R. N. Mohapatra and A. Y. Smirnov, Ann. Rev. Nucl. Part. Sci. **56**, 569 (2006), hep-ph/0603118.

[19] E. Hubble, Proc. Nat. Acad. Sci. **15**, 168 (1929).

[20] D. N. Spergel *et al.*, (2006), astro-ph/0603449.

[21] R. A. Alpher, H. Bethe, and G. Gamow, Phys. Rev. **73**, 803 (1948).

[22] A. Kashlinsky, J. C. Mather, and S. Odenwald, (1999), astro-ph/9908304.

[23] WMAP, D. N. Spergel *et al.*, Astrophys. J. Suppl. **148**, 175 (2003), astro-ph/0302209.

[24] The SNLS, P. Astier *et al.*, Astron. Astrophys. **447**, 31 (2006), astro-ph/0510447.

[25] W. L. Freedman *et al.*, Astrophys. J. **553**, 47 (2001), astro-ph/0012376.

[26] M. Tegmark *et al.*, Phys. Rev. **D74**, 123507 (2006), astro-ph/0608632.

[27] G. 't Hooft, Nucl. Phys. **B79**, 276 (1974).

[28] A. H. Guth, Phys. Rev. **D23**, 347 (1981).

[29] A. D. Linde, Phys. Lett. **B108**, 389 (1982).

[30] A. Albrecht and P. J. Steinhardt, Phys. Rev. Lett. **48**, 1220 (1982).

[31] M. Fukugita and T. Yanagida, Phys. Lett. **B174**, 45 (1986).

[32] R. D. Peccei and H. R. Quinn, Phys. Rev. Lett. **38**, 1440 (1977).

[33] R. N. Mohapatra *et al.*, (2005), hep-ph/0510213.

[34] V. Van Elewyck, (2006), astro-ph/0610226.

[35] B. Eberle, DESY-THESIS-2005-024.

[36] L. Wolfenstein, Phys. Rev. **D17**, 2369 (1978).

[37] S. P. Mikheev and A. Y. Smirnov, Sov. J. Nucl. Phys. **42**, 913 (1985).

[38] The MiniBooNE, A. A. Aguilar-Arevalo *et al.*, Phys. Rev. Lett. **98**, 231801 (2007), arXiv:0704.1500 [hep-ex].

[39] O. Mena and S. J. Parke, Phys. Rev. **D69**, 117301 (2004), hep-ph/0312131.

[40] The ALEPH, DELPHI, L3, OPAL, SLD Collaborations, the LEP Electroweak Working Group, the SLD Electroweak and Heavy Flavour Groups, Phys. Rept. **427**, 257 (2006), hep-ex/0509008.

[41] LSND, A. Aguilar *et al.*, Phys. Rev. **D64**, 112007 (2001), hep-ex/0104049.

[42] MiniBooNE, I. Stancu, Nucl. Phys. Proc. Suppl. **155**, 164 (2006).

[43] G. Mangano, A. Melchiorri, O. Mena, G. Miele, and A. Slosar, JCAP **0703**, 006 (2007), astro-ph/0612150.

[44] A. Strumia and F. Vissani, (2006), hep-ph/0606054.

[45] J. Hamann, S. Hannestad, G. G. Raffelt, and Y. Y. Y. Wong, (2007), arXiv:0705.0440 [astro-ph].

[46] J. Lesgourgues and S. Pastor, Phys. Rept. **429**, 307 (2006), astro-ph/0603494.

[47] G. L. Fogli *et al.*, (2006), hep-ph/0608060.

[48] J. R. Kristiansen, O. Elgaroy, and H. Dahle, (2006), astro-ph/0611761.

[49] T. D. Kitching, A. F. Heavens, L. Verde, P. Serra, and A. Melchiorri, (2008), arXiv:0801.4565 [astro-ph].

[50] C. Kraus *et al.*, Eur. Phys. J. **C40**, 447 (2005), hep-ex/0412056.

[51] V. M. Lobashev *et al.*, Phys. Lett. **B460**, 227 (1999).

[52] KATRIN, A. Osipowicz *et al.*, (2001), hep-ex/0109033.

[53] S. M. Bilenky and S. T. Petcov, Rev. Mod. Phys. **59**, 671 (1987).

[54] A. Morales and J. Morales, Nucl. Phys. Proc. Suppl. **114**, 141 (2003), hep-ph/0211332.

[55] R. N. Mohapatra and J. D. Vergados, Phys. Rev. Lett. **47**, 1713 (1981).

[56] B. Brahmachari and E. Ma, Phys. Lett. **B536**, 259 (2002), hep-ph/0202262.

[57] H. V. Klapdor-Kleingrothaus *et al.*, Eur. Phys. J. **A12**, 147 (2001), hep-ph/0103062.

[58] IGEX, C. E. Aalseth *et al.*, Phys. Rev. **D65**, 092007 (2002), hep-ex/0202026.

[59] G. L. Fogli *et al.*, Phys. Rev. **D70**, 113003 (2004), hep-ph/0408045.

[60] M. Milgrom, Astrophys. J. **270**, 365 (1983).

[61] K. Griest and M. Kamionkowski, Phys. Rev. Lett. **64**, 615 (1990).

[62] G. Bertone, D. Hooper, and J. Silk, Phys. Rept. **405**, 279 (2005), hep-ph/0404175.

[63] Z. Zhang, (2008), arXiv:0801.4905 [Unknown].

[64] T. Kinoshita and M. Nio, Phys. Rev. **D73**, 013003 (2006), hep-ph/0507249.

[65] A. L. Kataev, (2006), hep-ph/0602098.

[66] ALEPH, A. Heister *et al.*, Eur. Phys. J. **C35**, 457 (2004).

[67] Muon G-2, G. W. Bennett *et al.*, Phys. Rev. **D73**, 072003 (2006), hep-ex/0602035.

[68] K. Hagiwara, A. D. Martin, D. Nomura, and T. Teubner, Phys. Rev. **D69**, 093003 (2004), hep-ph/0312250.

[69] S. Ghozzi and F. Jegerlehner, Phys. Lett. **B583**, 222 (2004), hep-ph/0310181.

[70] J. F. de Troconiz and F. J. Yndurain, Phys. Rev. **D71**, 073008 (2005), hep-ph/0402285.

[71] S. Narison, Phys. Lett. **B568**, 231 (2003), hep-ph/0303004.

[72] K. Hagiwara, A. D. Martin, D. Nomura, and T. Teubner, (2006), hep-ph/0611102.

[73] A. Zee, Princeton, UK: Princeton Univ. Pr. (2003) 518 p.

[74] S. Raby, (2006), hep-ph/0608183.

[75] Particle Data Group, S. Eidelman *et al.*, Phys. Lett. **B592**, 1 (2004).

[76] S. Raby, Rept. Prog. Phys. **67**, 755 (2004), hep-ph/0401155.

[77] D. I. Kazakov, (2000), hep-ph/0012288.

[78] J. C. Pati and A. Salam, Phys. Rev. **D8**, 1240 (1973).

[79] H. Murayama and A. Pierce, Phys. Rev. **D65**, 055009 (2002), hep-ph/0108104.

[80] R. Dermisek and A. Mafi, Phys. Rev. **D65**, 055002 (2002), hep-ph/0108139.

[81] G. Altarelli, F. Feruglio, and I. Masina, JHEP **11**, 040 (2000), hep-ph/0007254.

[82] J. Wess and B. Zumino, Phys. Lett. **B49**, 52 (1974).

[83] Y. A. Golfand and E. P. Likhtman, JETP Lett. **13**, 323 (1971).

[84] A. B. Lahanas, N. E. Mavromatos, and D. V. Nanopoulos, Int. J. Mod. Phys. **D12**, 1529 (2003), hep-ph/0308251.

[85] N. Arkani-Hamed and S. Dimopoulos, JHEP **06**, 073 (2005), hep-th/0405159.

[86] G. F. Giudice and A. Romanino, Nucl. Phys. **B699**, 65 (2004), hep-ph/0406088.

[87] J. L. Feng, K. T. Matchev, and F. Wilczek, Phys. Lett. **B482**, 388 (2000), hep-ph/0004043.

[88] T. Moroi and L. Randall, Nucl. Phys. **B570**, 455 (2000), hep-ph/9906527.

[89] U. Chattopadhyay, A. Corsetti, and P. Nath, Phys. Rev. **D68**, 035005 (2003), hep-ph/0303201.

[90] T. Banks, D. B. Kaplan, and A. E. Nelson, Phys. Rev. **D49**, 779 (1994), hep-ph/9308292.

[91] A. de Gouvea, (2004), hep-ph/0411274.

[92] S. Weinberg, Physica **A96**, 327 (1979).

[93] J. Gasser and H. Leutwyler, Ann. Phys. **158**, 142 (1984).

[94] F. del Aguila, J. A. Aguilar-Saavedra, J. de Blas, and M. Zralek, (2007), arXiv:0710.2923 [hep-ph].

[95] A. Abada, C. Biggio, F. Bonnet, M. B. Gavela, and T. Hambye, (2007), arXiv:0707.4058 [hep-ph].

[96] R. Barbieri, J. R. Ellis, and M. K. Gaillard, Phys. Lett. **B90**, 249 (1980).

[97] E. K. Akhmedov, Z. G. Berezhiani, and G. Senjanovic, Phys. Rev. Lett. **69**, 3013 (1992), hep-ph/9205230.

[98] R. N. Mohapatra and R. E. Marshak, Phys. Rev. Lett. **44**, 1316 (1980).

[99] J. Schechter and J. W. F. Valle, Phys. Rev. **D22**, 2227 (1980).

[100] T. P. Cheng and L.-F. Li, Phys. Rev. **D22**, 2860 (1980).

[101] E. Ma, Phys. Rev. Lett. **81**, 1171 (1998), hep-ph/9805219.

[102] W. Grimus and M. N. Rebelo, Phys. Rept. **281**, 239 (1997), hep-ph/9506272.

[103] J. Bernabeu, G. C. Branco, and M. Gronau, Phys. Lett. **B169**, 243 (1986).

[104] G. C. Branco, L. Lavoura, and J. P. Silva, Oxford, UK: Clarendon (1999) 511 p.

[105] G. C. Branco, L. Lavoura, and M. N. Rebelo, Phys. Lett. **B180**, 264 (1986).

[106] G. C. Branco and M. N. Rebelo, (2007), arXiv:0711.2650 [hep-ph].

[107] G. C. Branco and M. N. Rebelo, New J. Phys. **7**, 86 (2005), hep-ph/0411196.

[108] S. Antusch, J. Kersten, M. Lindner, and M. Ratz, Phys. Lett. **B538**, 87 (2002), hep-ph/0203233.

[109] S. Antusch, J. Kersten, M. Lindner, M. Ratz, and M. A. Schmidt, JHEP **03**, 024 (2005), hep-ph/0501272.

[110] J.-w. Mei, Phys. Rev. **D71**, 073012 (2005), hep-ph/0502015.

[111] S. Antusch, J. Kersten, M. Lindner, and M. Ratz, Phys. Lett. **B544**, 1 (2002), hep-ph/0206078.

[112] T. Miura, T. Shindou, and E. Takasugi, Phys. Rev. **D68**, 093009 (2003), hep-ph/0308109.

[113] S. Antusch, P. Huber, J. Kersten, T. Schwetz, and W. Winter, Phys. Rev. **D70**, 097302 (2004), hep-ph/0404268.

[114] P. H. Chankowski, A. Ioannisian, S. Pokorski, and J. W. F. Valle, Phys. Rev. Lett. **86**, 3488 (2001), hep-ph/0011150.

[115] S. Antusch and M. Ratz, JHEP **11**, 010 (2002), hep-ph/0208136.

[116] R. N. Mohapatra, M. K. Parida, and G. Rajasekaran, Phys. Rev. **D69**, 053007 (2004), hep-ph/0301234.

[117] R. N. Mohapatra, M. K. Parida, and G. Rajasekaran, Phys. Rev. **D72**, 013002 (2005), hep-ph/0504236.

[118] C. Hagedorn, J. Kersten, and M. Lindner, Phys. Lett. **B597**, 63 (2004), hep-ph/0406103.

[119] J. R. Ellis, A. Hektor, M. Kadastik, K. Kannike, and M. Raidal, Phys. Lett. **B631**, 32 (2005), hep-ph/0506122.

[120] J. R. Ellis and S. Lola, Phys. Lett. **B458**, 310 (1999), hep-ph/9904279.

[121] J. A. Casas, J. R. Espinosa, A. Ibarra, and I. Navarro, Nucl. Phys. **B569**, 82 (2000), hep-ph/9905381.

[122] J. A. Casas, J. R. Espinosa, A. Ibarra, and I. Navarro, Nucl. Phys. **B573**, 652 (2000), hep-ph/9910420.

[123] R. Barbieri, G. G. Ross, and A. Strumia, JHEP **10**, 020 (1999), hep-ph/9906470.

[124] S. Antusch, J. Kersten, M. Lindner, and M. Ratz, Nucl. Phys. **B674**, 401 (2003), hep-ph/0305273.

[125] S. F. King and N. N. Singh, Nucl. Phys. **B591**, 3 (2000), hep-ph/0006229.

[126] J. A. Casas and A. Ibarra, Nucl. Phys. **B618**, 171 (2001), hep-ph/0103065.

[127] O. Vives, (2005), hep-ph/0504079.

[128] F. Borzumati and A. Masiero, Phys. Rev. Lett. **57**, 961 (1986).

[129] J. S. Hagelin, S. Kelley, and T. Tanaka, Nucl. Phys. **B415**, 293 (1994).

[130] J. Hisano, T. Moroi, K. Tobe, M. Yamaguchi, and T. Yanagida, Phys. Lett. **B357**, 579 (1995), hep-ph/9501407.

[131] J. Hisano, T. Moroi, K. Tobe, and M. Yamaguchi, Phys. Rev. **D53**, 2442 (1996), hep-ph/9510309.

[132] J. R. Ellis, J. Hisano, S. Lola, and M. Raidal, Nucl. Phys. **B621**, 208 (2002), hep-ph/0109125.

[133] J. R. Ellis and M. Raidal, Nucl. Phys. **B643**, 229 (2002), hep-ph/0206174.

[134] S. Pascoli, S. T. Petcov, and W. Rodejohann, Phys. Rev. **D68**, 093007 (2003), hep-ph/0302054.

[135] I. Masina and C. A. Savoy, Phys. Rev. **D71**, 093003 (2005), hep-ph/0501166.

[136] J. R. Ellis, J. Hisano, M. Raidal, and Y. Shimizu, Phys. Lett. **B528**, 86 (2002), hep-ph/0111324.

[137] I. Masina and C. A. Savoy, Nucl. Phys. **B661**, 365 (2003), hep-ph/0211283.

[138] I. Masina, Nucl. Phys. **B671**, 432 (2003), hep-ph/0304299.

[139] Y. Farzan and M. E. Peskin, Phys. Rev. **D70**, 095001 (2004), hep-ph/0405214.

[140] E. J. Chun, A. Masiero, A. Rossi, and S. K. Vempati, Phys. Lett. **B622**, 112 (2005), hep-ph/0502022.

[141] P. H. Chankowski, J. R. Ellis, S. Pokorski, M. Raidal, and K. Turzynski, Nucl. Phys. **B690**, 279 (2004), hep-ph/0403180.

[142] P. H. Chankowski and Z. Pluciennik, Phys. Lett. **B316**, 312 (1993), hep-ph/9306333.

[143] K. S. Babu, C. N. Leung, and J. T. Pantaleone, Phys. Lett. **B319**, 191 (1993), hep-ph/9309223.

[144] S. Antusch, M. Drees, J. Kersten, M. Lindner, and M. Ratz, Phys. Lett. **B519**, 238 (2001), hep-ph/0108005.

[145] S. Antusch, M. Drees, J. Kersten, M. Lindner, and M. Ratz, Phys. Lett. **B525**, 130 (2002), hep-ph/0110366.

[146] A. Y. Smirnov, (2004), hep-ph/0402264.

[147] W. Rodejohann, Phys. Rev. **D69**, 033005 (2004), hep-ph/0309249.

[148] M. Raidal, Phys. Rev. Lett. **93**, 161801 (2004), hep-ph/0404046.

[149] H. Minakata and A. Y. Smirnov, Phys. Rev. **D70**, 073009 (2004), hep-ph/0405088.

[150] P. H. Frampton and R. N. Mohapatra, JHEP **01**, 025 (2005), hep-ph/0407139.

[151] E. . Piran, T. and E. . Weinberg, S., SINGAPORE, SINGAPORE: WORLD SCIENTIFIC (1986) 220 P. (JERUSALEM WINTER SCHOOL FOR THEORETICAL PHYSICS, 1).

[152] I. Affleck and M. Dine, Nucl. Phys. **B249**, 361 (1985).

[153] M. Yoshimura, Phys. Rev. Lett. **41**, 281 (1978).

[154] S. Dimopoulos and L. Susskind, Phys. Rev. **D18**, 4500 (1978).

[155] D. Toussaint, S. B. Treiman, F. Wilczek, and A. Zee, Phys. Rev. **D19**, 1036 (1979).

[156] S. Weinberg, Phys. Rev. Lett. **42**, 850 (1979).

[157] G. 't Hooft, Phys. Rev. **D14**, 3432 (1976).

[158] V. A. Kuzmin, V. A. Rubakov, and M. E. Shaposhnikov, Phys. Lett. **B155**, 36 (1985).

[159] G. F. Giudice, A. Notari, M. Raidal, A. Riotto, and A. Strumia, Nucl. Phys. **B685**, 89 (2004), hep-ph/0310123.

[160] W. Buchmuller, R. D. Peccei, and T. Yanagida, (2005), hep-ph/0502169.

[161] G. D'Ambrosio, T. Hambye, A. Hektor, M. Raidal, and A. Rossi, Phys. Lett. **B604**, 199 (2004), hep-ph/0407312.

[162] A. Pilaftsis and T. E. J. Underwood, Nucl. Phys. **B692**, 303 (2004), hep-ph/0309342.

[163] A. Pilaftsis and T. E. J. Underwood, Phys. Rev. **D72**, 113001 (2005), hep-ph/0506107.

[164] T. Hambye, J. March-Russell, and S. M. West, JHEP **07**, 070 (2004), hep-ph/0403183.

[165] M.-C. Chen, (2007), hep-ph/0703087.

[166] D. Comelli and J. R. Espinosa, Phys. Rev. **D55**, 6253 (1997), hep-ph/9606438.

[167] P. Elmfors, K. Enqvist, and I. Vilja, Nucl. Phys. **B412**, 459 (1994), hep-ph/9307210.

[168] J. M. Cline, K. Kainulainen, and K. A. Olive, Phys. Rev. **D49**, 6394 (1994), hep-ph/9401208.

[169] M. A. Luty, Phys. Rev. **D45**, 455 (1992).

[170] M. Plumacher, Z. Phys. **C74**, 549 (1997), hep-ph/9604229.

[171] W. Buchmuller, P. Di Bari, and M. Plumacher, Phys. Lett. **B547**, 128 (2002), hep-ph/0209301.

[172] W. Buchmuller and M. Plumacher, Int. J. Mod. Phys. **A15**, 5047 (2000), hep-ph/0007176.

[173] W. Buchmuller, P. Di Bari, and M. Plumacher, Nucl. Phys. **B665**, 445 (2003), hep-ph/0302092.

[174] W. Buchmuller, P. Di Bari, and M. Plumacher, Nucl. Phys. **B643**, 367 (2002), hep-ph/0205349.

[175] T. Hambye, E. Ma, and U. Sarkar, Nucl. Phys. **B602**, 23 (2001), hep-ph/0011192.

[176] T. Hambye and G. Senjanovic, Phys. Lett. **B582**, 73 (2004), hep-ph/0307237.

[177] M. Magg and C. Wetterich, Phys. Lett. **B94**, 61 (1980).

[178] C. Wetterich, Nucl. Phys. **B187**, 343 (1981).

[179] G. Lazarides, Q. Shafi, and C. Wetterich, Nucl. Phys. **B181**, 287 (1981).

[180] R. N. Mohapatra and G. Senjanovic, Phys. Rev. **D23**, 165 (1981).

[181] A. Rossi, Phys. Rev. **D66**, 075003 (2002), hep-ph/0207006.

[182] E. Ma and U. Sarkar, Phys. Rev. Lett. **80**, 5716 (1998), hep-ph/9802445.

[183] P. J. O'Donnell and U. Sarkar, Phys. Rev. **D49**, 2118 (1994), hep-ph/9307279.

[184] G. Lazarides and Q. Shafi, Phys. Rev. **D58**, 071702 (1998), hep-ph/9803397.

[185] W. Rodejohann, Phys. Rev. **D70**, 073010 (2004), hep-ph/0403236.

[186] P.-h. Gu and X.-j. Bi, Phys. Rev. **D70**, 063511 (2004), hep-ph/0405092.

[187] S. Antusch and S. F. King, Phys. Lett. **B597**, 199 (2004), hep-ph/0405093.

[188] W.-l. Guo, Phys. Rev. **D70**, 053009 (2004), hep-ph/0406268.

[189] A. Hektor, M. Kadastik, M. Muntel, M. Raidal, and L. Rebane, Nucl. Phys. **B787**, 198 (2007), 0705.1495.

[190] A. Hektor, Y. Kajiyama, and K. Kannike, (2008), 0802.4015.

[191] F. del Aguila *et al.*, (2008), 0801.1800.

[192] CMS, G. L. Bayatian *et al.*, CERN-LHCC-2006-001.

[193] CMS, G. L. Bayatian *et al.*, J. Phys. **G34**, 995 (2007).

[194] B. C. Allanach *et al.*, (2006), hep-ph/0602198.

[195] A. Hektor, E. Kolbe, K. Langanke, and J. Toivanen, Phys. Rev. **C61**, 055803 (2000).

[196] A. Hektor, L. Anton, M. Kadastik, K. Skaburskas, and H. Teder, Proc. Estonian Acad. Sci. Phys. Math. **54**, 111 (2005), physics/0411024.

[197] P. Gu, X. Wang, and X. Zhang, Phys. Rev. **D68**, 087301 (2003), hep-ph/0307148.

[198] R. Fardon, A. E. Nelson, and N. Weiner, JCAP **0410**, 005 (2004), astro-ph/0309800.

[199] O. E. Bjaelde *et al.*, JCAP **0801**, 026 (2008), 0705.2018.

[200] A. E. Bernardini and O. Bertolami, (2007), 0712.1534.

Acknowledgements

I would thank my parents for driving me to the field of science and for continuous support in the early studies. This work was steadily, strongly and personally supported by my girlfrend Eva Roomets, thank you. Very special thanks to my supervisor Martti Raidal, for patient supervision and teaching during many-many years.

I am very thankful for critical reading and corrections of the manuscript of the thesis to my colleague Kristjan Kannike. My friend, Kati Aus, thank you, your corrections and stylistical suggestions were exceptionally helpful for the preparation of the manuscript. Very special thanks to my other colleagues in the National Institute of Chemical Physics and Biophyiscs: Mario Kadastik, Yuji Kajiyama, Ilja Livenson, Mait Müntel, Liis Rebane. You were very helpful in discussions and in many relaxing table football matches between the writing of the thesis. Also, I would like to thank Mirt Gramann and Gert Hütsi for valuable discussions and corrections in cosmology.

I would acknowledge my cosupervisor Jaak Kikas at the Tartu University. Very warm thanks to my earlier (MSc) supervisor Rein Saar, who guided me to particle physics.

My PhD work was financially supported by the Estonian Science Foundation (the grants hold by Martti Raidal), by the Estonian Government (the grant for the CMS experiment at CERN) and by the FP6 of the European Union (the BalticGrid project).

Summary in Estonian

Standardmudeli järgne neutriinofüüsika

Neutriino on osake, mille roll osakestefüüsikas tundus läbi mitmete aastakümnete olevat suhteliselt ebahuvitav. Neutriinot peeti massituks osakeseks, mis pealegi oli pea püüdmatu igasugustele detektoritele. Siiski, juba 60.-te aastate lõpus nähti esimesi märke neutriino “ebastandardsest” käitumisest. Homestake eksperiment, mis mõõtis Päikselt saabuvat neutriinode voogu, avastas olulise erinevuse ennustatud neutriinode arvu ja mõõdetud neutriinode arvu vahel. Kuhugi oli kadunud ligi pool ennustatud neutriinodest. Siiski, kulus veel 30 aastat enne kui täie kindlusega sai väita, et see puudujääk pole lihtsalt eksperimentaalne viga või ei seisne meie teadmatuses päikese-siseste protsesside seletamisel. Selgus, et neutriinodel on mass ja puudujääv osa elektronneutriinodest muundus müü- ja tauneutriinodeks. Sellist muundumist saavad läbi teha vaid massiga neutriinod.

Teisalt, osakestefüüsika standardmudel väidab üheselt, et neutriinod peavad olema massitud. Higgsi mehhanism, mis annab massid teistele fermionitele, ei saa anda massi neutriinodele, kuna eksperiment näitab, et puuduvad väikese massiga paremakäelised neutriinod. Seega, neutriinode mass sai esimeseks tõsiseks probleemiks standardmudelile. Loomulikult, standardmudelit saab laiendada ja sinna võib lisada erinevaid mehhanisme neutriinode massi tekitamiseks. Üks populaarsemaid mehhanisme on nn *esimest tüüpi kiige mehhanism*. Mudelisse lisatakse rasked paremakäelised neutriinode (elektronõrgad) singletid ja nende suur mass “surub” kergete neutriinode massi üliväikeseks. Matemaatiliselt väljendub see neutriinode massimaatriksi diagonaliseerimise lesandena. Teine võimalus on lisada mudelisse spetsiaalne kolmekomponendiline skalaar, triplet, mis annaks neutriinodele massi (teist tüüpi kiige mehhanism). Kolmas populaarne mudel on spetsiaalsete uute fermionite lisamine. Siiski, see võimalike mudelite nimekiri pole kaugeltki täielik. Hea ülevaade võimalikest mudelitest ja nende eksperimentaalsetest omadustest on esitatud näiteks ülevaates [33].

Tänapäeva osakestefüüsika ja kosmoloogia väidab, et neutriinodel oli ja võibolla ka on praegu väga oluline roll looduses. Esiteks, neutriinod võisid mängida kriitilist osa aine-antiaine asümmeetria loomises, seda läbi leptogeneesiks nimetatud protsessi (vt ülevaateid [159–162, 165]). Teiseks, neutriinodel näib olevat oluline roll raskete elementide tekitamisel supernoova plahvatustes, kuna nad saavad kallutada tasakaalu raskete elementide poole (vt näiteks [195] ja seal toodud viiteid). Võib olla, et kõik rauast raskemad elemendid on tekkinud suuremal või vähemal määral neutriinode "süül". Kolmandaks, ürgsed kosmoloogilised neutriinod mõjutasid oluliselt gaaside dünaamikat ja seega tähtede ning galaktikate teket varases Universumis. Lõpetuseks, ürgsetel neutriinodel võib olla oluline osa mängida tumeda energia moodustamisel [46, 197–200].

Käesolev doktoritöö seob ja juhatab sisse autori poolt doktoriõpingute perioodi jooksul avaldatud olulisemad publikatsioonid. Esimene publikatsioon käsitleb leptogeneesi alternatiivset stsenaariumi, kus leptogenees toimub läbi triplet skalaaride ja nende superpartnerite [161]. Teine publikatsioon on pühendatud väikese ja suure massiga neutiinode sektorite seoste uurimisele [119]. Kolmas publikatsioon käsitleb triplet-mudeli signatuuride avastatavust LHC eksperimendi juures [189].

Doktoritöö algab osakestefüüsika ja kosmoloogia standardmudelite tutvustamisega. Järgmises peatükis tutvustame mõningaid eksperimentaalseid tõendeid, et eksisteerivad füüsikalised nähtused, mida osakestefüüsika standardmudel ei suuda kirjeldada: aine-antiaine asümmeetria, neutriinode massid, külm tume aine, müüoni anomaalne magnetmoment. Neljandas peatükis kirjeldame täpsemalt võimalikke standardmudeli laiendusi neutriinofüüsikast lähtuvalt. Käsitleme kolme mudelit: I-, II- ja III-tüüpi kiige mudelid. Täpsustame ka, kuidas (kvantitatiivselt) annavad neutriino-mudelid aine-antiaine asümmeetria ja kuidas on omavahel seotud "kerge" ja "raske" neutriinode sektor. Viimases peatüks tutvustame leptogeneesi. Esitame lühisissejuhatuse varase Universumi termodünaamikasse ja kineetikasse. Seejrel kirjeldame ühte konkreetset leptogeneesi mudelit, mis baseerub I-tüüpi kiige mudelil. Lõpetuseks käsitleme lühidalt II-tüüpi kiige mudelil baseeruvat leptogeneesi. Töö lõpeb põgusa kokkuvõtte ja ülevaatega tööle lisatud teaduspublikatsioonidest.

PUBLICATIONS

I

A. Hektor, M. Kadastik, M. Müntel, M. Raidal, and L. Rebane.
Testing neutrino masses in little Higgs models via discovery of doubly charged Higgs at LHC.
Nucl. Phys., **B787**, 198-210, 2007, [hep-ph/0705.1495].

II

J. Ellis, A. Hektor, M. Kadastik, K. Kannike, and M. Raidal.
Running of Low-Energy Neutrino Masses, Mixing Angles and CP Violation.
Phys. Lett., **B631**, 32-41, 2005, [hep-ph/0506122].

IIII

G. D'Ambrosio, T. Hambye, A. Hektor, M. Raidal, and A. Rossi.
Leptogenesis in the minimal supersymmetric triplet seesaw model.
Phys. Lett. **B604**, 3-4, 199–206, 2004, [hep-ph/0407312].

CURRICULUM VITAE

Andi Hektor

Date and place of birth:	August 22, 1975, Voru, Estonia
Citizenship:	Estonian
Maritial status:	Single
Address:	National Institute of Chemical Physics and Biophysics Akadeemia tee 23, 12618 Tallinn, Estonia
Phone:	(+372) 639 8300
Fax:	(+372) 670 3662
E-mail:	andi.hektor@cerh.ch

Education

1990-1993:	C. R. Jacobson Gymnasium, Viljandi, Estonia
1998:	BSc in physics (theoretical physics), University of Tartu
2000:	MSc in physics (theoretical physics), University of Tartu

Employement

1997-2000:	Manager of IT systems, Department of Physics, University of Tartu
2000-2008:	PhD student, different scholarships, University of Tartu
2003-	Researcher, National Institute of Chemical Physics and Biophysic

Scientific work

Main fields of research:
neutrino physics, new physics at LHC, leptogenesis, cosmology

CURRICULUM VITAE in Estonian

Andi Hektor

Sünniaeg ja koht:	22. august 1975, Võru, Eesti
Kodakondsus:	Eesti
Perekonnaseis:	vallaline
Aadress:	Keemilise ja Bioloogilise Füüsika Instituut Akadeemia tee 23, 12618 Tallinn, Eesti
Telefon:	(+372) 639 8300
Faks:	(+372) 670 3662
E-mail:	andi.hektor@cern.ch

Haridus

1990-1993:	C. R. Jacobson Gümnaasium
1998:	BSc füüsikas (teoreetiline füüsika), Tartu Ülikool
2000:	MSc füüsikas (teoreetiline füüsika), Tartu Ülikool

Teenistuskäik

1997-2000:	arvutisüsteemide spetsialist, füüsikaosakond, Tartu Ülikool
2000-2002:	doktorant, Tartu Ülikool, erinevad stipendiumid
2003-	Keemilise ja Bioloogilise Füüsika Instituut, teadur

Teadustegevus

Peamised töösuunad: neutriinofüüsika, standardmudeli jrgne füüsika, CMS eksperiment (CERN LHC), leptogenees, kosmoloogia

DISSERTATIONES PHYSICAE UNIVERSITATIS TARTUENSIS

1. **Andrus Ausmees.** XUV-induced electron emission and electron-phonon interaction in alkali halides. Tartu, 1991.
2. **Heiki Sõnajalg.** Shaping and recalling of light pulses by optical elements based on spectral hole burning. Tartu, 1991.
3. **Sergei Savihhin.** Ultrafast dynamics of F-centers and bound excitons from picosecond spectroscopy data. Tartu, 1991.
4. **Ergo Nõmmiste.** Leelishalogeniidide röntgenelektronemissioon kiiritamisel footonitega energiaga 70–140 eV. Tartu, 1991.
5. **Margus Rätsep.** Spectral gratings and their relaxation in some low-temperature impurity-doped glasses and chrystals. Tartu, 1991.
6. **Tõnu Pullerits.** Primary energy transfer in photosynthesis. Model calculations. Tartu, 1991.
7. **Olev Saks.** Attoampri diapasoonis voolude mõõtmise füüsikalised alused. Tartu, 1991.
8. **Andres Virro.** AlGaAsSb/GaSb heterostructure injection lasers. Tartu, 1991.
9. **Hans Korge.** Investigation of negative point discharge in pure nitrogen at atmospheric pressure. Tartu, 1992.
10. **Jüri Maksimov.** Nonlinear generation of laser VUV radiation for high-resolution spectroscopy. Tartu, 1992.
11. **Mark Aizengendler.** Photostimulated transformation of aggregate defects and spectral hole burning in a neutron-irradiated sapphire. Tartu, 1992.
12. **Hele Siimon.** Atomic layer molecular beam epitaxy of A^2B^6 compounds described on the basis of kinetic equations model. Tartu, 1992.
13. **Tõnu Reinot.** The kinetics of polariton luminescence, energy transfer and relaxation in anthracene. Tartu, 1992.
14. **Toomas Rõõm.** Paramagnetic H^{2-} and F^+ centers in CaO crystals: spectra, relaxation and recombination luminescence. Tallinn, 1993.
15. **Erko Jalviste.** Laser spectroscopy of some jet-cooled organic molecules. Tartu, 1993.
16. **Alvo Aabloo.** Studies of crystalline celluloses using potential energy calculations. Tartu, 1994.
17. **Peeter Paris.** Initiation of corona pulses. Tartu, 1994.
18. **Павел Рубин.** Локальные дефектные состояния в CuO_2 плоскостях высокотемпературных сверхпроводников. Тарту, 1994.
19. **Olavi Ollikainen.** Applications of persistent spectral hole burning in ultrafast optical neural networks, time-resolved spectroscopy and holographic interferometry. Tartu, 1996.
20. **Ülo Mets.** Methodological aspects of fluorescence correlation spectroscopy. Tartu, 1996.

21. **Mikhail Danilkin.** Interaction of intrinsic and impurity defects in CaS:Eu luminophors. Tartu, 1997.
22. **Ирина Кудрявцева.** Создание и стабилизация дефектов в кристаллах KBr, KCl, RbCl при облучении ВУФ-радиацией. Тарту, 1997.
23. **Andres Osvet.** Photochromic properties of radiation-induced defects in diamond. Tartu, 1998.
24. **Jüri Örd.** Classical and quantum aspects of geodesic multiplication. Tartu, 1998.
25. **Priit Sarv.** High resolution solid-state NMR studies of zeolites. Tartu, 1998.
26. **Сергей Долгов.** Электронные возбуждения и дефектообразование в некоторых оксидах металлов. Тарту, 1998.
27. **Kaupo Kukli.** Atomic layer deposition of artificially structured dielectric materials. Tartu, 1999.
28. **Ivo Heinmaa.** Nuclear resonance studies of local structure in $RBa_2Cu_3O_{6+x}$ compounds. Tartu, 1999.
29. **Aleksander Shelkan.** Hole states in CuO_2 planes of high temperature superconducting materials. Tartu, 1999.
30. **Dmitri Nevedrov.** Nonlinear effects in quantum lattices. Tartu, 1999.
31. **Rein Ruus.** Collapse of 3d (4f) orbitals in 2p (3d) excited configurations and its effect on the x-ray and electron spectra. Tartu, 1999.
32. **Valter Zazubovich.** Local relaxation in incommensurate and glassy solids studied by Spectral Hole Burning. Tartu, 1999.
33. **Indrek Reimand.** Picosecond dynamics of optical excitations in GaAs and other excitonic systems. Tartu, 2000.
34. **Vladimir Babin.** Spectroscopy of exciton states in some halide macro- and nanocrystals. Tartu, 2001.
35. **Toomas Plank.** Positive corona at combined DC and AC voltage. Tartu, 2001.
36. **Kristjan Leiger.** Pressure-induced effects in inhomogeneous spectra of doped solids. Tartu, 2002.
37. **Helle Kaasik.** Nonperturbative theory of multiphonon vibrational relaxation and nonradiative transitions. Tartu, 2002.
38. **Tõnu Laas.** Propagation of waves in curved spacetimes. Tartu, 2002.
39. **Rünno Lõhmus.** Application of novel hybrid methods in SPM studies of nanostructural materials. Tartu, 2002.
40. **Kaido Reivelt.** Optical implementation of propagation-invariant pulsed free-space wave fields. Tartu, 2003.
41. **Heiki Kasemägi.** The effect of nanoparticle additives on lithium-ion mobility in a polymer electrolyte. Tartu, 2003.
42. **Villu Repän.** Low current mode of negative corona. Tartu, 2004.
43. **Алексей Котлов.** Оксианионные диэлектрические кристаллы: зонная структура и электронные возбуждения. Tartu, 2004.

44. **Jaak Talts.** Continuous non-invasive blood pressure measurement: comparative and methodological studies of the differential servo-oscillometric method. Tartu, 2004.
45. **Margus Saal.** Studies of pre-big bang and braneworld cosmology. Tartu, 2004.
46. **Eduard Gerškevitš.** Dose to bone marrow and leukaemia risk in external beam radiotherapy of prostate cancer. Tartu, 2005.
47. **Sergey Shchemelyov.** Sum-frequency generation and multiphoton ionization in xenon under excitation by conical laser beams. Tartu, 2006.
48. **Valter Kiisk.** Optical investigation of metal-oxide thin films. Tartu, 2006.
49. **Jaan Aarik.** Atomic layer deposition of titanium, zirconium and hafnium dioxides: growth mechanisms and properties of thin films. Tartu, 2007.
50. **Astrid Rekker.** Colored-noise-controlled anomalous transport and phase transitions in complex systems. Tartu, 2007.
51. **Andres Punning.** Electromechanical characterization of ionic polymer-metal composite sensing actuators. Tartu, 2007.
52. **Indrek Jõgi.** Conduction mechanisms in thin atomic layer deposited films containing TiO_2. Tartu, 2007.
53. **Aleksei Krasnikov.** Luminescence and defects creation processes in lead tungstate crystals. Tartu, 2007.
54. **Küllike Rägo.** Superconducting properties of MgB_2 in a scenario with intra- and interband pairing channels. Tartu, 2008.
55. **Els Heinsalu.** Normal and anomalously slow diffusion under external fields. Tartu, 2008.
56. **Kuno Kooser.** Soft x-ray induced radiative and nonradiative core-hole decay processes in thin films and solids. Tartu, 2008.
57. **Vadim Boltrushko.** Theory of vibronic transitions with strong nonlinear vibronic interaction in solids. Tartu, 2008.